NRC·CNRC

NRC Publications Archive
Archives des publications du CNRC

Improving the aerodynamic efficiency of heavy duty vehicles: wind tunnel test results of trailer-based drag-reduction technologies

McAuliffe, Brian R.

For the publisher's version, please access the DOI link below./ Pour consulter la version de l'éditeur, utilisez le lien DOI ci-dessous.

Publisher's version / Version de l'éditeur:
https://doi.org/10.4224/21275397
Laboratory Technical Report (National Research Council of Canada. Aerospace. Aerodynamics Laboratory); no. LTR-AL-2015-0272, 2015-07-22

NRC Publications Archive Record / Notice des Archives des publications du CNRC :
https://nrc-publications.canada.ca/eng/view/object/?id=2bb332d0-924d-445b-bf23-9658934e59e0
https://publications-cnrc.canada.ca/fra/voir/objet/?id=2bb332d0-924d-445b-bf23-9658934e59e0

Access and use of this website and the material on it are subject to the Terms and Conditions set forth at
https://nrc-publications.canada.ca/eng/copyright
READ THESE TERMS AND CONDITIONS CAREFULLY BEFORE USING THIS WEBSITE.

L'accès à ce site Web et l'utilisation de son contenu sont assujettis aux conditions présentées dans le site
https://publications-cnrc.canada.ca/fra/droits
LISEZ CES CONDITIONS ATTENTIVEMENT AVANT D'UTILISER CE SITE WEB.

Questions? Contact the NRC Publications Archive team at PublicationsArchive-ArchivesPublications@nrc-cnrc.gc.ca. If you wish to email the authors directly, please see the first page of the publication for their contact information.

Vous avez des questions? Nous pouvons vous aider. Pour communiquer directement avec un auteur, consultez la première page de la revue dans laquelle son article a été publié afin de trouver ses coordonnées. Si vous n'arrivez pas à les repérer, communiquez avec nous à PublicationsArchive-ArchivesPublications@nrc-cnrc.gc.ca.

National Research Council Canada | Conseil national de recherches Canada

Canada

NRC·CNRC

AERODYNAMICS LABORATORY

Improving the Aerodynamic Efficiency of Heavy Duty Vehicles: Wind Tunnel Test Results of Trailer-Based Drag-Reduction Technologies

Unclassified Unlimited

LTR-AL-2015-0272

July 22, 2015

Brian R. McAuliffe

National Research Council Canada | Conseil national de recherches Canada

Canada

AERODYNAMICS LABORATORY

Improving the Aerodynamic Efficiency of Heavy Duty Vehicles: Wind Tunnel Test Results of Trailer-Based Drag-Reduction Technologies

Report No.: LTR-AL-2015-0272

Date: July 22, 2015

Authors: Brian R. McAuliffe

Classification:	Unclassified	**Distribution:**	Unlimited
For:	ecoTECHNOLOGY for Vehicles Stewardship and Sustainable Transportation Programs Transport Canada		
Project #:	A1-004876		
Submitted by:	Dr. Steven J. Zan, **Director R&D Aerodynamics**		
Approved by:	Jerzy Komorowski, **General Manager, Aerospace Portfolio**		

Pages:	95	**Copy No:**	
Figures:	61	**Tables:**	14

This report may not be published wholly or in part without the written consent of the National Research Council Canada

Disclaimer

This report reflects the views of the authors only and does not reflect the views or policies of Transport Canada.

Neither Transport Canada, nor its employees, makes any warranty, express or implied, or assumes any legal liability or responsibility for the accuracy or completeness of any information contained in this report, or process described herein, and assumes no responsibility for anyone's use of the information. Transport Canada is not responsible for errors or omissions in this report and makes no representations as to the accuracy or completeness of the information.

Transport Canada does not endorse products or companies. Reference in this report to any specific commercial products, process, or service by trade name, trademark, manufacturer, or otherwise, does not constitute or imply its endorsement, recommendation, or favoring by Transport Canada and shall not be used for advertising or service endorsement purposes. Trade or company names appear in this report only because they are essential to the objectives of the report.

References and hyperlinks to external web sites do not constitute endorsement by Transport Canada of the linked web sites, or the information, products or services contained therein. Transport Canada does not exercise any editorial control over the information you may find at these locations.

Executive Summary

Through its ecoTECHNOLOGY for Vehicles program, Transport Canada commissioned the National Research Council Canada (NRC) to investigate the aerodynamic improvements possible with current and emerging drag reduction technologies for heavy-duty vehicles, with the intent of guiding future implementation and regulation of such technologies for Canada's transportation industry. A wind-tunnel test campaign was undertaken in the NRC 9 m Wind Tunnel to evaluate the aerodynamic performance of various drag reduction concepts, with an emphasis on those for trailers, using a 30% scale model of modern tractor-trailer combinations. Project stakeholders also include Environment Canada's Transportation Division.

A wind-tunnel approach was taken for the project because of its ability to provide a precise measure of the aerodynamic differences between vehicle configurations. Advancements in testing techniques developed for the project have improved the accuracy of the results, such that they reflect better the aerodynamic performance of a tractor-trailer combination under real-world conditions. These advancements consisted of a modular model that can represent various tractor configurations (sleeper-cab and day-cab with various roof-fairings for each) and trailer configurations (40 ft dry-van, 53 ft dry-van, 53 ft half-height dry-van, 53 ft flatbed with various cargo configurations, tandem 28 ft long-combination vehicle arrangement). The model has spinning wheels matched to an appropriate ground-effect simulation consisting of a boundary-layer suction system and a moving ground plane. Cooling drag is simulated with an engine compartment through which the flow-rate is proportional to that of a real vehicle. The 30% scale of the model is small enough to minimize wall-interference effects in the wind tunnel even with a 53 ft-equivalent trailer, yet is big enough to provide the aerodynamic performance of a full-scale vehicle through appropriate Reynolds-number scaling. In addition to the model, a new Road Turbulence System (RTS) has been introduced in the NRC 9 m Wind Tunnel that provides road-representative turbulence in the wind. All of these advances create the appropriate relative motions between the vehicle, the ground, and the wind such that this represents the most advanced wind-tunnel-simulation of a heavy-duty vehicle in the world.

The overall test program described herein included distinct sub-studies to address drag reduction techniques for various regions of the vehicle or for different vehicle types. For each vehicle configuration tested, the wind-tunnel drag-coefficient measurements were used to calculate a wind-averaged-drag-coefficient that represents a long-term average of the aerodynamic performance for typical North-American wind conditions, from which fuel savings and greenhouse-gas reductions have been estimated based on typical Canadian driving distances. The table on the next page summarizes the main findings of the study, with fuel savings and greenhouse-gas reduction estimates for some of the configurations tested.

Drag-Reduction Technique	**Fuel Saved**[†] **[l/tractor/year]**	**CO_2 Reduction**[†] **[kg/tractor/year]**
Tractor-Trailer Gap:		
reduce tractor-trailer gap by 12"	800 ± 200	2,100 ± 500
add trailer fairing for sleeper-cab w/ 36" gap	600 ± 200	1,600 ± 500
add trailer fairing for day-cab w/ 36" gap	1,600 ± 500	4,200 ± 1,300
Trailer Underbody:		
add side-skirts to tandem axle trailer	2,900 ± 800	7,700 ± 2,100
add extended side-skirts to tandem axle trailer	3,300 ± 900	8,700 ± 2,400
add side-skirts to tridem axle trailer	3,800 ± 1,100	10,000 ± 2,900
Trailer Base:		
add long or short 4-panel boat-tail to trailer base	1,900 ± 500	5,000 ± 1,300
add tapered-side 3-panel boat-tail to trailer base	1,600 ± 500	4,200 ± 1,300
Trailer Upper-Body:		
profile the trailer roof (top 6")	1,000 ± 300	2,600 ± 800
Combinations:		
48" to 36" gap, trailer fairing, side-skirts, boat-tail (sleeper)	6,700 ± 1,900	17,700 ± 5,000
48" to 36" gap, trailer fairing, extended skirts, boat-tail, profile roof (sleeper)	8,300 ± 2,300	21,900 ± 6,100
48" to 36" gap, trailer fairing, side-skirts, boat-tail (day-cab)	7,900 ± 2,200	20,900 ± 5,800
48" to 36" gap, trailer fairing, extended side-skirts, boat-tail (day-cab)	8,600 ± 2,400	22,700 ± 6,300
Flatbed Trailers:		
add side-skirts to flatbed with high irregular cargo	2,900 ± 800	7,700 ± 2,100
add side-skirts to flatbed with low irregular cargo	1,600 ± 400	4,200 ± 1,100
Long Combination Vehicles - LCVs:		
add trailer fairing to LCV trailer-trailer gap	1,400 ± 400	3,700 ± 1,100
reduce LCV trailer-trailer gap from 5 ft to 3 ft	1,900 ± 500	5,000 ± 1,300
add trailer fairing and reduce gap, and add full aero package to LCV	7,900 ± 2,200	20,900 ± 5,800
Tractor-Trailer Height Matching:		
remove full-height fairing from day-cab with low dry-van trailer	5,400 ± 1,500	14,300 ± 4,000
remove full-height fairing from day-cab with full-height dry-van trailer	-5,400 ± 1,500	-14,300 ± 4,000

[†] estimated for 125,000±35,000 km/tractor/year @ 100 km/hr

Reducing the aerodynamic drag associated with dry-van trailers was the primary focus of the current effort, and several regions of a tractor-trailer combination were targeted with different drag reduction technologies. For these efforts, the vehicle model represented a modern aero tractor with a 53 ft dry-van trailer. The drag-reduction techniques tested do not represent specific commercial products, although some were designed to achieve drag reduction in a similar manner to technologies on the market.

The gap between the tractor and trailer is a region in which air can circulate and pass through, and is a dominant source of drag for a tractor-trailer combination. Many modern tractors are outfitted with side-extenders that reduce the effective air-gap between the two bodies, and provide a reduction in fuel use, however operational restrictions may prevent the ability to achieve such savings. To better understand the sensitivity of vehicle drag to the gap width, measurements were performed for several gap widths and it was found that the wind-averaged-drag was reduced by 2.6% for every foot the gap was reduced (8.5% per metre). A one foot reduction in gap width, which may be operationally feasible for many vehicles on

the road, translates to a reduction in fuel consumption on the order of 800 litres per tractor per year, with CO_2 emissions reductions of 2,100 kg per tractor per year. An active fifth-wheel system can provide such benefits at highway speed without adversely affecting low-speed manoeuvering and operations. Another technique to reduce drag associated with the tractor-trailer gap is to introduce a device that prevents air from flowing through the gap region. Of the concepts tested, a large trailer fairing was found to provide the greatest benefit, with drag reductions on the order of 2% for the sleeper-cab tractor variant tested, and 5% for the day-cab variant, providing associated fuel savings of 600 litres and 1,600 litres per tractor per year, respectively. Reducing the gap width and adding a trailer fairing can provide fuel savings in excess of 2,000 litres per tractor per year and greenhouse-gas reductions in excess of 4,000 kg CO_2 per tractor per year.

As would be expected based on their prevalent use on North-American highways, side-skirts provide the greatest drag reductions of the trailer-underbody concepts tested. By redirecting the wind around the trailer, they prevent high-momentum air from being entrained in the underbody region and from impinging on the trailer bogie. Drag reductions of 10% were measured for different side-skirt arrangements with a tandem-axle trailer bogie, and extending the skirts over the trailer wheels provided an added benefit such that fuel savings exceeding 3,000 litres per tractor per year may be realized. An even greater reduction in drag was measured for side-skirts applied to a tridem-axle bogie arrangement, with fuel savings of nearly 4,000 litres per tractor per year and greenhouse-gas reductions of 10,000 kg CO_2 per tractor per year.

Recent federal regulatory amendments in Canada have opened up the possibility of applying aerodynamic fairings, commonly called boat-tails, to the aft end of dry-van trailers that are larger than previous regulations allowed. Several boat-tail concepts were tested to examine the influence of a lower panel, the sensitivity to length, and the relative potential for inflatable boat-tails. All showed similar results, with the greatest benefit realized from the four-panel configurations (6-7% drag reduction), providing an estimated fuel savings of 1,900 litres per tractor per year and greenhouse-gas reductions of 5,000 kg CO_2 per tractor per year. The short (2 ft full-scale) and long (4 ft full-scale) boat-tail concepts showed the same level of drag reduction. Removing the lower panel and reducing the surface area of the side panels showed only a small reduction in performance (5-6% drag reduction), providing further evidence to support the hypothesis that the manner in which the top panel guides the air downwards towards the ground is the dominant influence on boat-tail performance. Other studies have shown boat-tails to be as effective as side-skirts, reaching drag reductions of 10%. The vertical offset of the top panel tested here (3 inches full-scale), included to leave room for lights at the top edge of the trailer base, may be a reason why the boat-tail concepts tested here have not provided the same magnitude of drag reductions observed for other similar boat-tail concepts. This presents a clear challenge to developing effective boat-tails for real-world applications.

The intent of the current study was to evaluate ways of reducing the drag associated with dry-van trailers without changing cargo capacity. In an effort to modify the shape of the roof while minimizing any influence to the cargo volume, the top 6 inches of the trailer were modified in three ways: rounding the front edge, rounding the side edges, and tapering the aft edge. The aft taper provided the greatest benefit of the three, however the combined profiled roof provided a drag reduction of 3.5%, which translates to 1,000 litres per tractor per year in fuel savings and a reduction in greenhouse gas emissions of 2,600 kg CO_2.

Of the various technologies tested, some did not provide any measurable drag reductions and some showed increased drag. A partial plate seal applied to the front face of the trailer and paired to the sleeper-cab with a 36 inch tractor-trailer gap showed no significant reduction in wind-averaged drag. Removing the landing gear, smoothing the trailer underbody, and adding an underbody diffuser fairing all showed a small increase in wind-averaged drag. For these attempts, it was found that by reducing the resistance to flow in the underbody region, a greater flow-rate is introduced in this region which increases the drag of the trailer bogie. Roof mounted vortex generators also showed increased wind-averaged drag. These various poorly-performing concepts do not represent specific commercial products or concepts and the designs used have not been optimized. These test results should not be taken to mean such concepts will not work, only that they show much lower potential for fuel savings than the well-performing technologies and that they must be carefully optimized.

The best performing techniques for each region of the dry-van trailer were combined to examine the additive properties of the various technologies, and similar combinations were paired with both the day-cab and sleeper-cab variants. Significant drag reductions of up to 29% have been observed for some combinations. Fuel savings in excess of 8,000 litres per tractor per year are predicted for some combinations (greater than $10,000 per year at current diesel rates). Greater reductions were observed for the day-cab than the sleeper-cab tractor, and have been attributed to the sleeper-cab guiding the wind over the gap region in a smoother manner as a result of its length, thus receiving less gains from the gap devices. Of particular note, it was found that side-skirts and boat-tails have a mutually beneficial interaction that provides a reduction in drag from their combined use that is greater than the sum of their individual drag reductions. An additional 3% drag reduction was observed in the current study when the extended side-skirts and boat-tail were paired. This interaction has been identified as a possible source of discrepancy for performance claims reported in literature of side-skirts and boat-tails when tested in a combined manner as opposed to when tested individually.

In addition to the full-height 53 ft single dry-van trailer, the current project examined other trailer types including a 53 ft flatbed trailer with different cargo configurations, a tandem 28 ft dry-van trailer, and a 53 ft half-height dry-van trailer. This was done in an attempt to identify fuel savings measures for a greater proportion of tractor-trailer combinations found on the road. Different tractor roof configurations were also tested for some trailer configurations to examine the sensitivity to proper matching of the tractor with the trailer.

Side-skirts were beneficial for all the flatbed configurations tested, but the magnitude of the drag reductions varied (5% to 8%). A mid-height tractor roof was shown to benefit all of the flatbed cargo configurations, even for a set of large boxes with a maximum height the same as a full-height dry-van trailer.

For the tandem 28 ft trailer, which was used to represent a long combination vehicle (LCV), reducing the trailer-trailer gap from 5 ft to 3 ft was most beneficial, but adding a trailer fairing or full-plate seal in the trailer-trailer gap provided measurable drag reductions. The same magnitudes of drag reductions were not realized when the rest of the trailer regions were treated with side-skirts, a boat-tail at the base of the aft trailer, and a fairing on the front of the forward trailer. A 25% drag reduction was measured for the full aerodynamic treatment of the LCV configuration.

Aerodynamic matching of the tractor and trailer was examined by testing different tractor-roof configurations with various trailers. The most interesting finding was that the drag increase when adding a full-height roof fairing to a low-tractor/low-trailer configuration is as great as the drag increase when removing the fairing from a high-tractor/high-trailer. The improperly-paired configurations can result in an increased fuel use in excess of 5,000 litres per tractor per year and increased greenhouse-gas emissions in excess of 14,000 kg CO_2 per tractor per year.

The results presented in this study are intended to provide guidance to Canadian regulators and Canada's transportation industry on effective ways to reduce the fuel consumption and emissions, through aerodynamic means, from the transportation of goods on Canadian roadways. Descriptions of the way in which the technologies affect the flow-field around a heavy-duty vehicle should also be helpful in providing guidance to technology developers, and in particular to trailer manufacturers that have the opportunity to design high-efficiency trailers for the next generation of heavy-duty vehicles.

Table of Contents

Executive Summary vii
List of Figures xv
List of Tables xviii
Nomenclature xix

1. Introduction **1**
1.1 Background 1
1.2 Project Objectives and Outcomes 4
1.3 Requirements for the Wind Tunnel Test Program 4
1.4 Test Program 5
1.4.1 Test Commissioning 6
1.4.2 Tractor and Trailer Type 6
1.4.3 Dry-Van Trailer Drag Reduction 7
1.4.4 Aerodynamics of Flatbed Trailers 7
1.4.5 Drag Reduction Methods for Long Combination Vehicles 7
1.4.6 Aerodynamic Matching of Tractor and Trailer Height 8
1.5 Report Outline 8

2. Test Setup and Procedures **9**
2.1 Test Setup 9
2.1.1 Wind Tunnel 9
2.1.2 Model 10
2.1.3 Ground Simulation 12
2.1.4 Model Mounting 14
2.2 Road Turbulence System 14
2.3 Test Procedure 16
2.4 Data Reduction 17

2.5 Fuel-Savings and Greenhouse-Gas-Reduction Analysis 18

3. Drag Characteristics of Tractor-Trailer Combinations 21

3.1 Truck Configurations 21

3.2 Tractor Configurations 21

3.3 Trailer Configurations 23

3.4 Influence of Tractor and Trailer on Fuel Use and Greenhouse-Gas Emissions . . 25

4. Drag Reduction Methods for Dry-Van Trailer 27

4.1 Approach 27

4.2 Tractor-Trailer Gap Width 28

4.3 Tractor-Trailer Gap Devices 34

4.4 Trailer Underbody Devices 41

4.5 Trailer Base Devices 49

4.6 Trailer Upper-Body Shaping and Devices 53

4.7 Device Combinations and Interactions 56

4.8 Influence of Tractor Type on Dry-Van Trailer Drag Reduction 61

4.9 Summary of Dry-Van Trailer Drag-Reduction Results 64

5. Drag Reduction for Flatbed Trailers 67

6. Drag Reduction for Long Combination Vehicles 71

7. Aerodynamic Matching of Tractor and Trailer Height 77

8. Summary and Conclusions 83

References 89

A. Test Log 93

List of Figures

1.1 Relative merits of aerodynamic evaluation methods for ground vehicles 2
1.2 Project overview 3

2.1 30% scale tractor-trailer model in the NRC 9 m Wind Tunnel. 9
2.2 Tractor model internal structure 10
2.3 Trailer underbody structure and tandem-axle trailer bogie arrangement. 11
2.4 Trailer wheel sets in tandem axle configurations. 12
2.5 Model mounted with Ground Effect Simulation System (GESS). 13
2.6 Road Turbulence System (RTS) installed in the 25 m (82 ft) diameter settling chamber of the NRC 9 m Wind Tunnel. 15

3.1 Day-cab and sleeper-cab tractor configurations. 22
3.2 Comparison of the drag-coefficient performance of the sleeper and day-cab tractor variants with the 53 ft dry-van trailer. 22
3.3 Sample of trailer configurations with sleeper-cab tractor. 23
3.4 Comparison of the 53 ft dry-van, 40 ft dry-van, 53 ft flatbed (empty), and tandem 28 ft dry-van trailers with the sleeper-cab tractor. 24

4.1 Tractor-trailer gap-width configurations 28
4.2 Influence of tractor-trailer-gap width for the sleeper-cab tractor with the 53 ft dry-van trailer. 29
4.3 Influence of tractor-trailer-gap width for the day-cab tractor with the 53 ft dry-van trailer. 30
4.4 Sensitivity of wind-averaged drag coefficient to tractor-trailer-gap width for the sleeper-cab and day-cab tractors with the 53 ft dry-van trailer. 30
4.5 Influence of tractor-trailer-gap width on trailer front face pressures. 31
4.6 Influence of tractor-trailer-gap width on trailer bogie face pressures. 32
4.7 Tractor-trailer-gap drag-reduction configurations. 35
4.8 Tractor-trailer-gap ancillary units. 35
4.9 Influence of tractor-trailer-gap devices for the sleeper-cab tractor with the 53 ft dry-van trailer and a 36 inch gap. 36

4.10 Influence of tractor-trailer-gap devices for the day-cab tractor with the 53 ft dry-van trailer and a 36 inch gap. 37

4.11 Drag reductions measurements for the trailer fairing with different tractor and gap-width combinations. 37

4.12 Drag reductions measurements for the full plate seal with different tractor and gap-width combinations. 38

4.13 Drag reductions measurements for the refrigeration unit with different tractor and gap-width combinations. 39

4.14 Influence of tractor-trailer-gap devices on the trailer roof centreline pressure distribution for the sleeper-cab tractor with the 53 ft dry-van trailer and a 36 inch gap. 39

4.15 Trailer-underbody drag-reduction configurations. 42

4.16 Tridem-axle dry-van trailer configurations. 43

4.17 Influence of side-skirt configurations, bogie fairing, and belly box for the sleeper-cab tractor with the 53 ft dry-van trailer. 44

4.18 Influence of the side-skirts, bogie fairing, and belly box on the trailer centreline base-pressure distributions for the sleeper-cab tractor with the 53 ft dry-van trailer and a 36 inch gap. 44

4.19 Influence of the standard side-skirts, removing the landing gear, smoothing the trailer underbody, and installing the diffuser fairing for the sleeper-cab tractor with the 53 ft dry-van trailer. 46

4.20 Influence of the standard side-skirts, removing the landing gear, smoothing the trailer underbody, and installing the diffuser fairing on trailer bogie face pressures. 46

4.21 Influence of a tridem-axle arrangement and side-skirts for the day-cab tractor with the 53 ft dry-van trailer. 47

4.22 Trailer-base drag-reduction configurations 50

4.23 Influence of the boat-tails for the sleeper-cab tractor with the 53 ft dry-van trailer. 51

4.24 Influence of the boat-tails on the trailer centreline base-pressure distributions for the sleeper-cab tractor with the 53 ft dry-van trailer and a 36 inch gap. . . . 52

4.25 Trailer roof drag-reduction configurations. 54

4.26 Influence of the trailer roof modifications for the sleeper-cab tractor with the 53 ft dry-van trailer. 55

4.27 Truck configuration with standard side-skirts and long 4-panel boat-tail. 57

4.28 Truck configuration with trailer fairing, extended side-skirts, long 4-panel boat-tail, and profiled roof. 57

4.29 Influence of the drag-reduction combinations for the sleeper-cab tractor with the 53 ft dry-van trailer. . . . 58
4.30 Mutual benefits from interactions between drag-reduction combinations. . . . 58
4.31 Drag-reduction trends for the standard side-skirts with different reference truck configurations. . . . 59
4.32 Differences in base pressure distribution from the standard side-skirts for different reference truck configurations. . . . 59
4.33 Drag reduction measurements for tractor-trailer gap-width and gap-device combinations for the different tractor types. . . . 62
4.34 Drag reduction measurements for side-skirt, boat-tail, and trailer fairing combinations for the different tractor types. . . . 63

5.1 Test configurations for flatbed-trailer study. . . . 68
5.2 Flatbed underbody structure. . . . 68
5.3 Drag characteristics of the flatbed cargo configurations compared to a dry-van trailer configuration. . . . 69
5.4 Influence of side-skirts on the drag characteristics of the flatbed trailer configurations. . . . 70

6.1 A-train type connection between tandem 28 ft trailers. . . . 71
6.2 Test configurations and trailer-trailer-gap devices for long-combination vehicle study. . . . 72
6.3 Drag characteristics of the tandem 28 ft trailer configuration with trailer-trailer gap changes and gap devices. . . . 73
6.4 Influence of full-vehicle aerodynamic treatments to the tandem 28 ft trailers. . . . 74

7.1 Half-height 53 ft dry-van trailer model with tridem-axle arrangement, paired with the day-cab tractor without a roof fairing. . . . 77
7.2 Day-cab roof-fairing configurations with the full-height dry-van trailer. . . . 79
7.3 Drag characteristics of the day-cab roof-fairing configurations with the full-height dry-van trailer. . . . 79
7.4 Day-cab roof-fairing configurations with the half-height dry-van trailer. . . . 80
7.5 Drag characteristics of the day-cab roof-fairing configurations with the half-height dry-van trailer. . . . 80
7.6 Sleeper roof-fairing configurations with various trailers. . . . 81

7.7 Drag characteristics of the sleeper-cab roof-fairing configurations with the full-height-dry-van and flatbed trailers. 81

List of Tables

2.1 Comparison of RTS turbulence characteristics with the target on-road condition. 16

3.1 Fuel savings and greenhouse-gas reduction estimates for changes in tractor and trailer configurations. 25

4.1 Fuel savings and greenhouse-gas reduction estimates for changes in the tractor-trailer-gap width. 33

4.2 Fuel savings and greenhouse-gas reduction estimates for tractor-trailer-gap devices. 40

4.3 Fuel savings and greenhouse-gas reduction estimates for trailer underbody configurations. 48

4.4 Fuel savings and greenhouse-gas reduction estimates for trailer base configurations. 52

4.5 Fuel savings and greenhouse-gas reduction estimates for trailer upper-body configurations. 55

4.6 Fuel savings and greenhouse-gas reduction estimates for dry-van drag-reduction combinations. 61

4.7 Fuel savings and greenhouse-gas reduction comparisons for the different tractor types. 63

5.1 Fuel savings and greenhouse-gas reduction comparisons for the side-skirts applied to different flatbed-trailer configurations. 70

6.1 Fuel savings and greenhouse-gas reduction comparisons for the side-skirts applied to different flatbed-trailer configurations. 75

7.1 Fuel savings and greenhouse-gas reduction comparisons for different tractor- and trailer-height combinations. 82

8.1 Sample of fuel savings and greenhouse-gas reductions estimated for different drag-reduction techniques. 84

A.1 Run Log for test program. 94

Nomenclature

Symbols:

A	area [m^2]
C_D	drag-force coefficient $\left(= \frac{F_D}{1/2\rho U_{ref}^2 A}\right)$ [ ]
C_P	pressure coefficient $\left(= \frac{P - P_{ref}}{1/2\rho U_{ref}^2}\right)$ [ ]
F_D	drag force [N]
I	turbulence intensity [%]
L^x	longitudinally-correlated turbulence length scale [m]
P	pressure [Pa]
sfc	specific fuel consumption [l/Whr]
U	wind speed [m/s]
u	wind speed component in x direction [m/s]
v	wind speed component in y direction [m/s]
w	wind speed component in z direction [m/s]
WAC_D	wind-averaged drag coefficient [ ]
ΔWAC_D	difference in wind-averaged drag coefficient from reference value [ ]
ΔWAC_D^{int}	difference in wind-averaged drag coefficient from device interactions [ ]
x	longitudinal coordinate [m]
y	lateral coordinate [m]
z	vertical coordinate [m]
η	transmission efficiency [ ]
θ	terrestrial wind angle [°]
$\Delta\mu$	change in fuel consumption rate [l/100km]
ψ	vehicle-referenced wind angle, yaw angle [°]
ρ	air density [kg/m^3]

Subscripts:

avg	average value
g	ground value
ref	reference value

Superscripts:

$+$	positive yaw-angle range value
$-$	negative yaw-angle range value
$\pm$	total yaw-angle range value

Acronyms:

CAD	computer aided design
CFD	computational fluid dynamics
DEF	diesel exhaust fluid
EC	Environment Canada
EPA	Environmental Protection Agency
eTV	ecoTECHNOLOGY for Vehicles
GESS	Ground Effects Simulation System
GHG	greenhouse gas
HDV	heavy duty vehicle
LDV	light duty vehicle
NRC	National Research Council
NRCan	Natural Resources Canada
RTS	Road Turbulence System
SAE	Society of Automotive Engineers
SLA	stereo lithography apparatus
SLS	selective laser sintering
TAP	trailer aerodynamics package
TC	Transport Canada

1. Introduction

1.1 Background

Transport Canada, through its ecoTECHNOLOGY for Vehicles (eTV) program, undertakes testing and evaluation of new and emerging vehicle technologies. The program helps inform various stakeholders that are engaged in the development of regulations, codes, standards, and products for the next generation of advanced light-duty vehicles (LDVs) and heavy-duty vehicles (HDVs).

In a report prepared for Transport Canada in 2012 (Patten *et al.*, 2012), NRC identified that aerodynamic drag (resistance to motion due to movement through air) is the greatest component of resistance to motion for heavy vehicles operating under highway conditions, and is thus a prime contributor to greenhouse gas emissions and fuel consumption. In cold and windy Canadian climates, aerodynamic drag can be an even more significant contributor to these issues. Drag is also a dissipative loss that cannot be recovered by any means. Many drag-reduction technologies are currently on the market and many are being proposed for improving fuel efficiency and reducing emissions. Some evidence has shown that fuel savings on the order of 10%-20% from such technologies are achievable for long-haul dry-van-trailer combinations (National Academy of Sciences, 2010). However, the evaluation of such technologies is difficult and error prone, thus making many manufacturers' claims suspect.

Transport Canada, through its eTV program, and Environment Canada are interested in investigating aerodynamic performance of new and emerging drag reduction technologies for heavy vehicles, and in particular for tractor-trailer combinations. Through several decades of working in the fields of ground-vehicle aerodynamics and wind engineering, the National Research Council Canada (NRC) has the capabilities and expertise to evaluate properly the aerodynamic performance of drag reduction technologies for ground vehicles and report on their aerodynamic benefits, ease of use, and potential fuel savings. As such, Transport Canada commissioned NRC to undertake a multi-year project to evaluate the performance of current and emerging drag reduction technologies to guide Transport Canada and its stakeholders, including Environment Canada's Transportation Division, in reducing greenhouse-gas emissions and fuel consumption from heavy vehicles.

The use of scale-model testing in a wind tunnel provides the benefit of testing in a systematically-controlled and representative environment including relative vehicle/ground/wind motions and the turbulent winds near the ground. Figure 1.1 shows the relationship between the three primary methods for aerodynamic evaluations, those being track testing, wind-tunnel testing, and computational fluid dynamics (CFD), and identifies the benefits of each. Although aerodynamic experiments on a test track provide realistic wind and ground

Method	Physics	Boundary Conditions	Drag Measurements
Road/Track	accurate (reality)	accurate (reality)	approximate (poor repeatability)
Wind tunnel	can be accurate	approximate (simulation)	reliable (excellent repeatability)
CFD	approximate (simulation)	can be accurate	reliable (excellent repeatability)

Figure 1.1: Relative merits of aerodynamic evaluation methods for ground vehicles

conditions and represent the true environment, current experimental techniques and procedures are not conducive to repeatable or accurate aerodynamic performance assessments. This shortcoming is being addressed in a separate project under the eTV program that will provide enhanced techniques for track testing, thus complementing the current proposed work. The wind tunnel can provide reliable measurements and repeatable results in a simulated environment that can closely match the true on-road conditions, depending on the fidelity of the boundary conditions. CFD techniques can provide a simulation of the vehicle in its true environment, but modelling assumptions regarding turbulence in the boundary layers and wakes of the vehicle provide an approximation to the physics of the wind that generates drag on the vehicle. In addition, the wind tunnel can be more efficient than CFD when considering wind-averaged-drag evaluations that require results at numerous wind angles relative to the vehicle direction of motion. The wind-tunnel technologies the NRC has implemented in the current project provide a significantly improved simulation of the environment in which heavy vehicles operate, therefore improving the realism and accuracy of the wind-tunnel measurements and providing confidence in the final recommendations of the project. The NRC is confident these techniques provide the most accurate wind-tunnel simulation of drag-reduction technologies for HDVs in the world, and allow an accurate measure of the differences between these technologies.

The project consists of two phases. Phase 1, initiated in the first year of work (2012) has two parallel streams of work that focus on the design and development aspects of the project. Phase 2, initiated in 2014, consists of the test and evaluation part of the project. Figure 1.2 shows an overview of the project structure, including the two phases of the project, their streams, and their major project elements.

This report presents the results from the wind-tunnel test program of Phase 2. A separate report in progress (McAuliffe and Kirchhefer, 2015) provides detailed documentation of the wind-tunnel setup, procedures, and commissioning efforts.

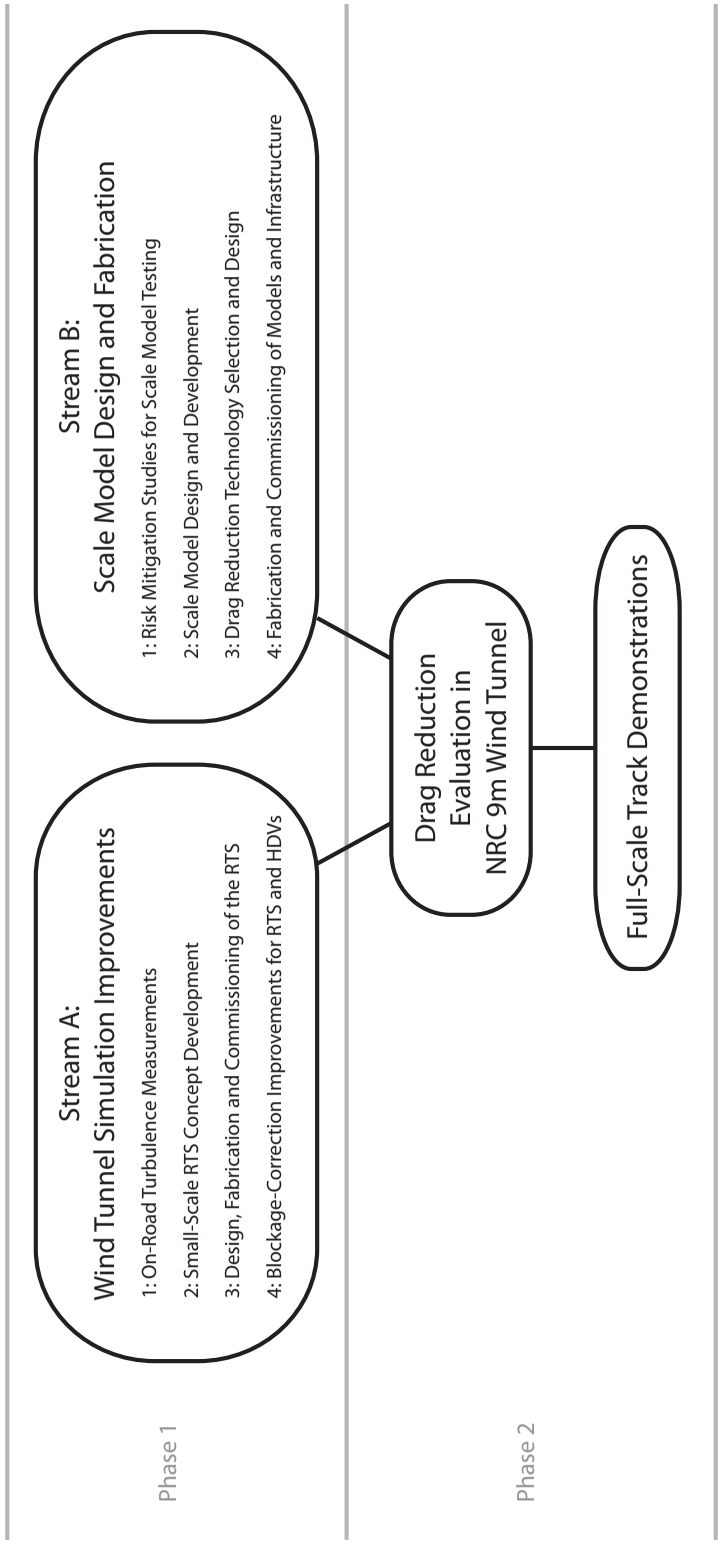


Figure 1.2: Project overview

1.2 Project Objectives and Outcomes

The primary objective of the project is to provide recommendations to HDV regulators, including Transport Canada (TC), Environment Canada (EC), Natural Resources Canada (NRCan), and the U.S. Environmental Protection Agency (EPA), on the most efficient means to reduce greenhouse gas emissions and fuel consumption of HDVs through aerodynamic drag-reduction technologies. The inconsistency of typical drag-reduction evaluations, combined with the inaccuracy associated with many of those techniques, requires a common objective basis upon which such evaluations must be performed. The NRC has performed a wind-tunnel test campaign that provides the consistency and realism required to ensure the most reliable predictions of drag reduction possible. To do so, it was important to simulate the effects of relative motion between the vehicle, the ground and the wind, and to simulate the turbulent wind characteristics near the ground encountered by heavy vehicles on the road. The performance of modern and emerging drag-reduction technologies have been evaluated using 30%-scale models of various heavy-vehicle combinations. These evaluations have been done in a manner that eliminates the largest uncertainties generally associated with wind-tunnel testing; those being the use of a representative vehicle with minimized wall-interference effects, the simulation of natural winds and the simulation of relative motions between the vehicle, the ground and the wind.

This project supports the following three eTV II program outcomes:

- Provide data to help support the development of future environmental (emissions) regulations: by providing test results on the efficiency gains offered by various HDV aerodynamic modifications/technologies.
- Provide data to help support the development of non-regulatory codes and standards: testing results will help industry optimize drag reduction technologies.
- Support energy efficiency programs: testing outcomes will help inform energy efficiency programs by providing data on various drag reduction technologies (for example, the Canadian Smartway Program).

1.3 Requirements for the Wind Tunnel Test Program

At the outset of the project, requirements were defined for the test program to ensure high-fidelity measurements of the drag performance of a heavy-duty vehicle:

1. The wind-tunnel simulation must correctly represent the aerodynamics of a full-scale HDV. This includes appropriate Reynolds-number scaling, and correct ground-effect simulation and wheel rotation.
2. The wind-tunnel simulation must provide wind characteristics in the test section representative of what HDVs experience on Canadian roads;
3. The model should be of an adequate size to minimize the influence of the walls on the flow around the vehicle.

4. The model must accommodate a variety of current and emerging drag-reduction technologies.

5. The model must represent various tractor and trailer configurations to demonstrate adequately the performance of drag reduction technologies for a variety of common vehicle types. This includes the two primary tractor types (day-cab and sleeper-cab), common trailer types (dry van, flatbed with and without cargo, etc.), and long-combination trailer configurations.

In addition to these technical requirements, the model was also to be designed to ensure confidence from the transportation industry for the future uptake of technologies. This has been partially addressed by testing technologies with the various tractor and trailer combinations. To further ensure confidence, the model must "look" like a real HDV. Its shape and details must represent those of a real HDV on the road.

To address the requirements listed above, two technology development projects were undertaken, as defined previously in Figure 1.2. The *Wind Tunnel Simulation Improvements* project tasks were directed towards improving both the realism of the wind environment and the accuracy of drag measurements. This encompasses the design of the new Road Turbulence System (RTS) for the NRC 9 m Wind Tunnel that provides road-representative flow conditions during the wind tunnel tests. The RTS is briefly described in Section 2.2 of this report, its development is described in previous progress reports (McAuliffe *et al.*, 2013a; and McAuliffe *et al.*, 2014a), and its commissioning is described in a separate report in progress (McAuliffe and Kirchhefer, 2015). The *Scale Model Design and Fabrication* project tasks consisted of selecting a concept and scale for wind tunnel model from which a detailed design was developed and built. The model is briefly described in Section 2.1.2, its development is described in previous progress reports (McAuliffe *et al.*, 2013b; and McAuliffe, 2014b), and its commissioning is described in a separate report in progress (McAuliffe and Kirchhefer, 2015).

1.4 Test Program

Through consultation with the Transport Canada - ecoTECHNOLOGY for Vehicle Program's Interdepartmental Heavy Duty Vehicle Steering Committee, an initial set of technology directions was selected for examination in the NRC 9 m Wind Tunnel test program, based on a survey of committee members. A detailed test plan, with specific technologies to test, was subsequently developed and approved by the Steering Committee.

The goal of the NRC 9 m Wind Tunnel investigation was to identify practical technologies and vehicle modifications that will best reduce HDV fuel consumption and GHG emissions through aerodynamic means. The technologies tested do not represent commercial products, although some were designed to achieve drag reduction in a similar manner to technologies on the market. Concepts to be tested have been designed by NRC, with guidance from commercial products and concepts in the open literature, to provide a measure of the performance potential of such classes of technologies. The practical implementation and operational use of such technologies has also be considered in their design.

The overall test plan includes distinct test programs to address the various regions of the vehicle or various vehicle types. Each major study is described in the following sections. Details of the technologies tested are described in their respective results sections of the report.

1.4.1 Test Commissioning

As part of the project development effort, commissioning of the new wind tunnel model and the Road Turbulence System (RTS) was performed. These efforts are described in a companion report (McAuliffe and Kirchhefer, 2015) and are summarized in Section 2. Commissioning tasks consisted of:

- RTS commissioning - Prior to installation of the 30% scale truck model, measurements were performed to characterize the flow-field in the presence of the RTS. This also included a comparison of drag measurements of the truck model in the turbulent-wind conditions compared to those measured in smooth flow conditions;
- Strut-tare measurements - Measurements were performed to characterize the wind loads experienced by the model mounting struts such that they could subsequently be subtracted from the truck-test measurements;
- Reynolds number sensitivity - Measurements performed during the commissioning phase of the project have demonstrated that the results, although not at full-scale Reynolds number conditions, are consistent with the performance of the vehicle at full-scale conditions;
- Ground-effect simulation - Measurements were performed to examine the influence of the moving ground plane and spinning wheels on the aerodynamic performance of the tractor-trailer combination;
- Model location influence - Based on model-scale selection requirements, the tractor-trailer model with a 53 ft equivalent trailer is longer than the length of the moving ground plane in the NRC 9 m Wind Tunnel. Measurements were performed with a shorter trailer to identify the extent of the model over which adequate ground simulation is most important; and
- Measurement repeatability - Throughout the test program, the model was returned to a standard configuration several times for characterization of the repeatability of the test procedures.

1.4.2 Tractor and Trailer Type

To give some context to the fuel savings potential of the various drag reduction technologies tested under the current project, a comparison of the drag performance of some of the various tractor-trailer combinations tested is provided (Section 3). The tractor and trailer variants used for the current test program are:

- Tractors: sleeper-cab and day-cab; and

- Trailers: 40 ft dry-van, 53 ft dry-van (tandem and tridem axle arrangements), half-height 53 ft dry-van, 53 ft flatbed with two cargo configurations, tandem 28 ft trailers (to represent a long combination vehicle).

1.4.3 Dry-Van Trailer Drag Reduction

A majority of the test program was dedicated towards evaluating the drag-reduction potential for a standard 53 ft dry-van trailer. Sub-studies were carried out to examine different regions of the tractor-trailer combination and to look at interactive influences:

- Tractor-trailer gap - Blocking the wind in the gap between the tractor and trailer has been demonstrated to provide reduced drag for combination vehicles. Changing the gap width and introducing devices in the gap have been examined (Sections 4.2 and 4.3);
- Trailer underbody - side-skirts and other devices have been examined to reduce the drag associated with the trailer underbody (Section 4.4);
- Trailer base - variants of a boat-tail concept have been examined for the rear of the trailer (Section 4.5);
- Trailer upper-body - shaping the roof and the use of roof mounted vortex generators have been examined (Section 4.6);
- Device combinations - combinations of the best performing techniques have been examined (Section 4.7); and
- Tractor influence - some drag-reduction configurations were examined with different tractor types to identify the influence of the tractor (Section 4.8).

1.4.4 Aerodynamics of Flatbed Trailers

The variability of cargo configurations for a flatbed trailer can make it difficult to approach a drag-reduction solution. The influence of side skirts on a flatbed configuration with an empty trailer and with two cargo configurations have been examined (Section 5).

1.4.5 Drag Reduction Methods for Long Combination Vehicles

With the prevalence of long combination vehicles appearing on some Canadian roads, such as tandem 53 ft trailers, the trailer-trailer gap provides an additional source of aerodynamic drag that can be treated to reduce fuel consumption and greenhouse-gas emissions. Due to the inability to test a tandem 53 ft trailer configuration because of its length, a tandem 28 ft configuration was tested to examine the influence of drag-reduction concepts for the trailer-trailer gap (Section 6). In addition, the drag reduction potential in the trailer-trailer gap was evaluated under the influence of aerodynamic treatments to the rest of the vehicle as well.

1.4.6 Aerodynamic Matching of Tractor and Trailer Height

The earliest drag-reduction technologies for trucks included roof and trailer fairings to minimize the effect of the tractor being shorter than the flat-faced trailer. Tractor roof fairings are generally designed for matching with a standard dry-van trailer, however many other trailer types with different heights are found on the roads. Questions are periodically posed in regards to the usefulness of full-height tractor fairings with lower trailers, and whether there may be sufficient fuel savings to pair a lower tractor with a lower trailer. To address this question, several tractor roof configurations were tested with various trailer configurations to identify the sensitivity of mismatching tractor and trailer heights (Section 7). The configurations tested include:

- Two sleeper-cab roofs with dry-van trailer;
- Three day-cab roofs with dry-van trailer;
- Two sleeper-cab roofs with half-height dry-van trailer;
- Three day-cab roofs with half-height dry-van trailer; and
- Two sleeper-cab roofs with three flatbed configurations.

1.5 Report Outline

This report documents the results of the various studies listed above, in the order described. To summarize, the basic outline of the report is as follows:

- Section 2: Brief description of the wind-tunnel setup and procedures;
- Section 3: Baseline drag characteristics of various tractor-trailer combinations tested;
- Section 4: Drag reduction methods for dry-van trailers including methods for the tractor-trailer gap; the trailer underbody, the trailer base and the trailer roof;
- Section 5: Drag reduction for flatbed trailers;
- Section 6: Drag reduction for long-combination vehicles;
- Section 7: Drag reduction through appropriate tractor-trailer matching; and
- Section 8: Summary of the main findings.

In addition, Appendix A provides the test log for the wind-tunnel test program that identifies the test runs performed, to which sub-study they belong, details of the model and test conditions, and the wind-averaged-drag-coefficient values calculated for each run (see Section 2.4 for explanation of data).

2. Test Setup and Procedures

2.1 Test Setup

2.1.1 Wind Tunnel

The test program was undertaken in the NRC 9 m Wind Tunnel located in Ottawa, Ontario, Canada. The wind tunnel is a horizontal closed circuit atmospheric facility with a large test section (9.1 m wide $\times$ 9.1 m high $\times$ 22.9 m long) that is suitable for testing tractor-trailer combinations up to full scale. It is powered by an air-cooled 6.7 MW DC motor that provides a maximum wind speed of approximately 55 m/s (200 km/h) in an empty test section. An external mechanical, pyramidal balance senses the six-components of aerodynamic forces and moments. The tractor-trailer model is shown in Figure 2.1 being installed in the test section of the wind tunnel. A turntable (blue circle in Figure 2.1) allows rotation of the model about a vertical axis to simulated the effect of cross winds.

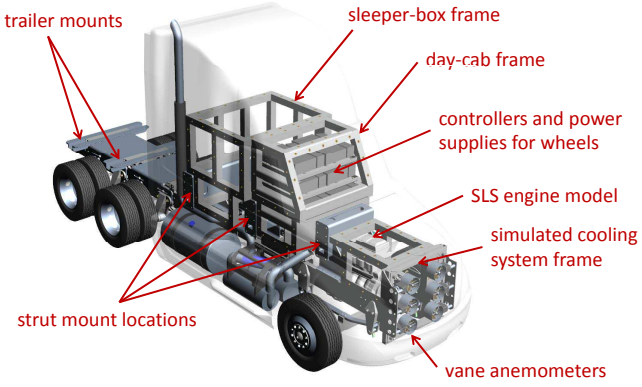


Figure 2.1: 30% scale tractor-trailer model in the NRC 9 m Wind Tunnel.

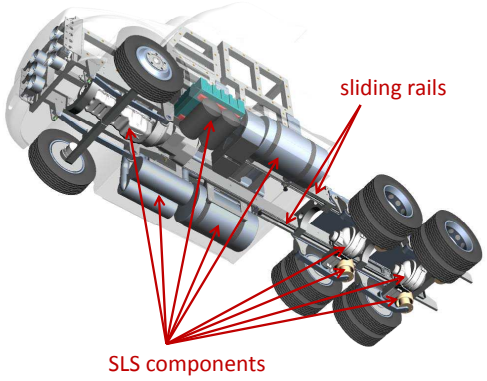
2.1.2 Model

A 30%-scale modular model of a tractor trailer combination was designed and built for the current test program. The model scale was selected based on a compromise of different requirements in an attempt to provide the most advanced wind-tunnel simulation of a heavy-duty vehicle in the world. The design and development efforts of the tractor-trailer model have been previously documented (McAuliffe *et al.*, 2013b; McAuliffe, 2014b). These efforts consisted of design studies to select the model scale, to develop an appropriate wheel-drive system, to design a low-interference model mounting system, to select a suitable material to represent the radiator and cooling system, and to develop a modular design concept to accommodate the various tractor and trailer configurations required.

The internal structure of the tractor model was designed to accommodate a variety of tractor types. Schematics of this structure, showing ancillary components, and a photograph of the day-cab variant of the structure are shown in Figure 2.2. Sliding rails are used to convert the model between a day-cab and sleeper-cab configuration. Underbody components such as the engine, the fuel tanks, the diesel exhaust fluid (DEF) tank, and the transfer casings were manufactured using a SLS (selective laser sintering) 3D printing approach.



(a) Top view of internal structure



(b) Bottom view of internal structure



(c) Day-cab configuration being installed in the wind tunnel

Figure 2.2: Tractor model internal structure



Figure 2.3: Trailer underbody structure and tandem-axle trailer bogie arrangement.

The tractor shape is based on CAD geometry provided by Navistar representing an International ProStar Short Sleeper. Under the agreement with Navistar to use the CAD geometry, the shapes of the tractor fairing, the A-pillars, and the bumper were modified from the original designs. Other details were modified for use with the 30% scale model, such as the removal of some gaps at the interfaces of various body panels. The external surfaces were manufactured using a 3D printing technique (SLA - stereo lithography apparatus) to produce lightweight components that mount to the internal structure.

A realistic engine bay and cooling pack were implemented in the model such that the cooling airflow through the engine bay would be adequately captured, and thus appropriate cooling drag would be experienced by the model. An appropriate level of resistance to flow through the engine bay was added to provide a cooling flow rate with an average wind speed, based on a set of six vane anemometers mounted behind the front grille, of approximately 19% of the freestream wind speed.

The structural frames of the trailer models were built using an extruded aluminum structure on which the external shell was installed. The trailer underbody was designed to be similar in structure to a real trailer, to provide a similar level of roughness and resistance for the airflow (shown in Figure 2.3. The rounded vertical edges on the front faces of the trailers (see Figure 2.2(c)) were machined from Renshape, an engineered material with similar characteristics to wood. The full front face and the roof of the 53 ft trailer model were fabricated entirely from Renshape. The trailer models consist of (full-scale equivalent dimensions):

- $1\times$ 40 ft dry-van trailer 118 inches high;
- $1\times$ 53 ft flatbed trailer;
- $1\times$ 53 ft dry-van trailer 118 inches high;
- $1\times$ 53 ft dry-van trailer 66 inches high; and
- $2\times$ 28 ft dry-van trailer 118 inches high.

The wheel-drive systems were designed with two motors per axle, one on each side. For the

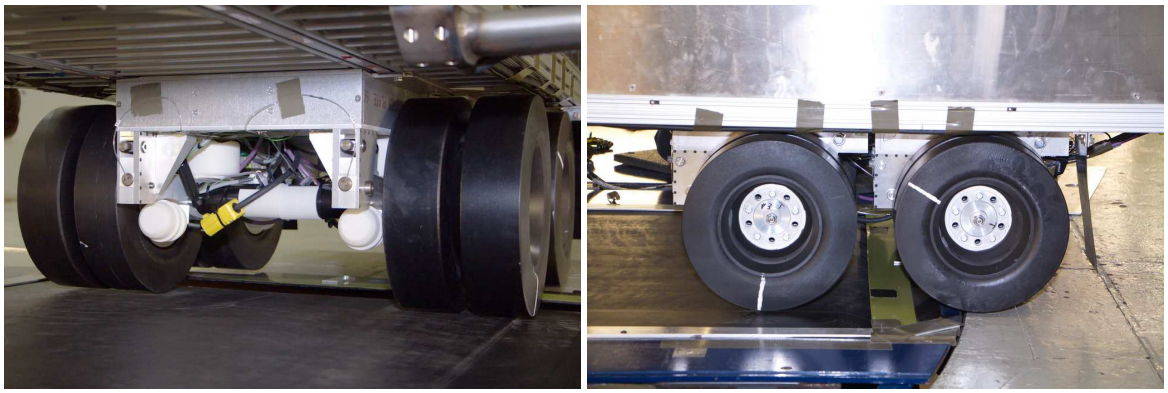


Figure 2.4: Trailer wheel sets in tandem axle configurations.

tractor, the motor controllers and power supplies were mounted in the tractor body, as identified in Figure 2.2(a). For the trailer wheels, each axle was a self-contained unit consisting of the motors, controllers, and power supplies, such that they could be positioned anywhere on the trailer underbody with minimal requirements for cable routing. The trailer was configured with up to four axles depending on the test requirements. A two-axle arrangement is shown in Figure 2.4. Each wheel was fabricated using an SLS 3D printing approach. Each wheel pair was assembled with a hub and balanced for use up to 3600 rpm prior to installation on the motors.

The drag-reduction devices, to be described in their respective sections of the report, were fabricated using a variety of techniques, from machined foam or Renshape, to milled aluminum sheets, to hand-assembled plywood structures, to welded sheet-metal structures.

In addition to the wind loads experienced by the model and measured by the underfloor balance, an onboard measurement system acquired data for other types of measurements, including:

- a set of six vane anemometers located behind the front grille to measure the speed of the wind entering the engine bay;
- the wheel speed and power requirements from each wheel motor to allow calculation of the aerodynamic resistive torque experienced by the wheels;
- three pressure scanners to measure the model surface pressure at up to 192 locations on the model (60 pressure taps on the tractor and the remainder on the trailer).

2.1.3 Ground Simulation

Adequately simulating the interaction of the vehicle with the wind in the near-ground region can be difficult in a wind tunnel due to the floor being stationary with respect to the vehicle (represents the road surface moving at the same speed as the vehicle). The truck model, which has spinning wheels, was designed for use with the Ground Effect Simulation System (GESS) of the NRC 9 m Wind Tunnel that includes a boundary layer suction system and mov-

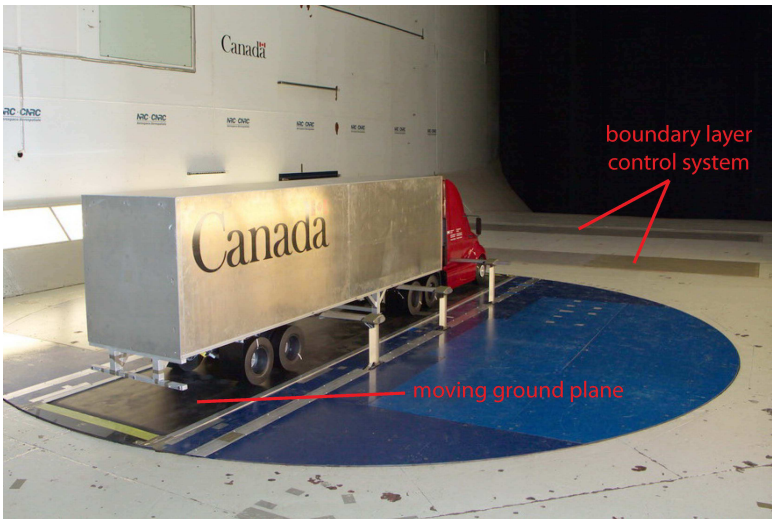


Figure 2.5: Model mounted with Ground Effect Simulation System (GESS).

ing ground plane to simulate the appropriate relative motions between the vehicle, the ground, and the air. The GESS systems are identified in Figure 2.5. The moving ground plane, which consists of a rolling belt system, is contained within the floor turntable and therefore is always moving in the "direction of motion" of the truck. To avoid mechanical fouling between the wheels and the ground plane, the wheels were raised approximately 5 mm from the surface.

As part of the commissioning tasks, measurements were performed for various levels of ground-effect simulation by combining conditions with the moving ground plane and wheels systematically turned on or off. These measurements, performed with the sleeper-cab tractor and 53 ft dry-van trailer and presented in McAuliffe and Kirchhefer (2015), show that the moving ground plane and the spinning wheels contribute to approximately 1% and 5% of the vehicle drag, respectively. This means that measurements using fixed-floor and stationary model wheels will under-predict the vehicle drag by approximately 6%.

As previously noted, when using the 53 ft trailer model, the tractor-trailer is longer than the exposed moving ground plane. In order to identify the most appropriate manner in which to mount the longer models, whether to overhang the front or the back over the fixed floor, tests were performed with the 40 ft equivalent trailer model that allowed full ground simulation under the entire model. This model was tested in three locations: 1) fully over the belt, 2) with the front overhanging the fixed floor, and 3) with the back overhanging the fixed floor. No significant change in the measured drag coefficients was found when overhanging the front of the model over the fixed floor, but a 3% increase in drag was found when overhanging the back of the model. The differences have been attributed to changes in the structure of the wake behind the vehicle, as identified by surface pressure measurements. It was therefore decided that the majority of testing with the 53 ft trailer would be performed with the front of the model overhanging the fixed floor. It was anticipated that changes to the tractor-trailer gap would be most sensitive to changes in the ground simulation under the tractor, and therefore the tests concerning the tractor-trailer gap were performed with the back of the model overhanging the fixed floor.

2.1.4 Model Mounting

As seen in Figures 2.1 and 2.5, the model is supported over the moving ground plane using a series of six struts (three on each side). The shape of the struts was defined based on a preliminary design study in which it was found that this horizontal outrigger approach provided a low and consistent aerodynamic interaction with the flow surrounding the model such that the interaction is within 2% of the measured drag of the vehicle (McAuliffe, 2014b). This interaction represents the manner in which the flow-field is modified in the presence of the struts and how it influences the wind loads experienced by the model.

In addition to the aerodynamic interaction effect, the wind loads experienced by the unshielded struts are themselves a component of the measured wind loads. As part of the model commissioning process, these strut loads were measured for several truck configurations and strut locations. These measurements were performed with the struts attached to the underfloor balance and the truck model securely mounted to the top of the turntable, without any contact between the two. These direct measurements of the strut loads, which are on the order of 5-6% of the truck drag, were characterized and subsequently subtracted from the test program measurements when the truck model was connected to the struts. The strut interaction effects were also quantified based on the earlier design study and subtracted from the wind tunnel measurements.

2.2 Road Turbulence System

At the outset of the current project it was recognized that simulating the winds that vehicles experience on the road may be just as important as simulating the appropriate aerodynamic ground effects. Many wind tunnels provide smooth, aeronautical-quality winds that are not representative of the ground-level winds experienced by vehicles on the road. Wind engineers recognized long ago that buildings and bridges can behave drastically different in smooth flow conditions than they do in the turbulent and gusty terrestrial winds that are experienced at ground level, and have developed means of simulating these appropriate turbulent winds in a wind tunnel.

Watkins and Cooper (2007) provide a review concerning the effects of turbulence on the aerodynamic performance of road vehicles. They discuss that drag reductions for commercial vehicles have been shown to be smaller in turbulent flows than smooth flows, implying that it may be more difficult to reduce the drag of heavy duty vehicles in flow conditions representative of the turbulent terrestrial winds experienced on the road. The measurements they described are a combination of road-to-wind-tunnel comparisons and comparisons between different turbulence conditions in a wind tunnel, all with older-style vehicles that have poor aerodynamic performance compared to today's commercial vehicles. The measurements also suffer from high uncertainties in the road measurements, or were performed at smaller scales than are generally accepted today (Wood, 2012a). As part of the development work of the project, measurements performed in a smaller wind tunnel for a 5% scale tractor-trailer model, demonstrated the sensitivity of a streamlined modern tractor shape to turbulence (McAuliffe

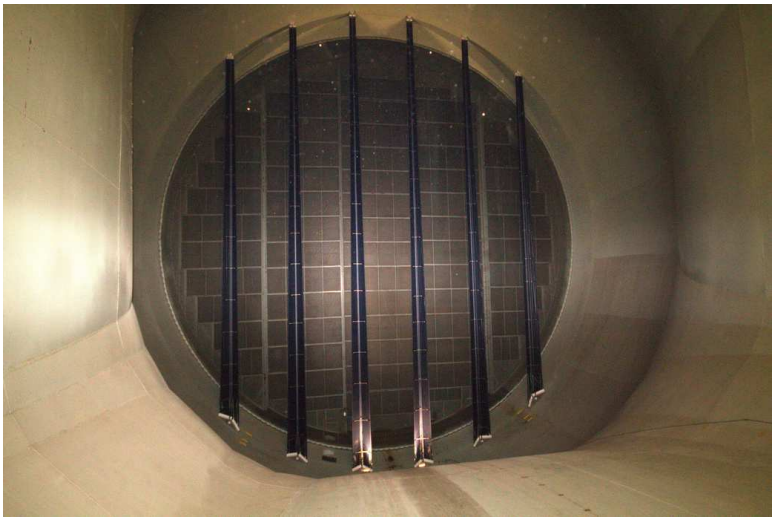


Figure 2.6: Road Turbulence System (RTS) installed in the 25 m (82 ft) diameter settling chamber of the NRC 9 m Wind Tunnel.

et al., 2014a). As such, a requirement for the current drag-reduction effort was to replicate road-representative turbulence conditions in the wind tunnel.

The development of a turbulence-generation system for ground vehicle testing was undertaken in parallel with the development of the 30% tractor-trailer model. To identify the wind characteristics of interest, a road-test campaign was first developed to measure the transient wind conditions experienced by vehicles on the road in a number of terrain, traffic, and wind conditions. The measurements and the selection of a target condition for the wind tunnel simulation have been summarized in an SAE technical paper (McAuliffe *et al.*, 2014c). Subsequently, development efforts were undertaken in smaller wind tunnels to identify a concept and ensure that it can be scaled to the NRC 9 m Wind Tunnel (McAuliffe *et al.*, 2013a; McAuliffe *et al.*, 2014a). At the outset of the current test campaign, the new NRC Road Turbulence System (RTS) was installed and commissioned for the NRC 9 m Wind Tunnel. A photograph of the RTS installed in the settling chamber of the wind tunnel is shown in Figure 2.6.

The target turbulence condition identified from the road-turbulence measurements represents a condition with moderate terrain roughness, moderate traffic density, and moderate wind strength (conditions defined by McAuliffe *et al.*, 2014c). The RTS was designed to match the wind spectra (energy distributions with frequency) as best as possible. These measurements and analyses are presented in detail by McAuliffe and Kirchhefer (2015). The wind spectra can be characterized by two parameters that represent the magnitude of turbulence energy in the wind, with respect to the mean wind speed, and the distribution of turbulence energy with frequency. These parameters, known as the turbulence intensity and the turbulence length scale, have been calculated for the wind-speed component in each coordinate direction (u-longitudinal, v-lateral, w-vertical) and are compared in Table 2.1 with those of the target road-turbulence measurements. Note that in comparing the turbulence length scales, the values in Table 2.1 for the RTS have been scaled to represent the appropriate values for the 30% truck model in relation to a full-scale truck on the road. The RTS turbulence characteristics are

Table 2.1: Comparison of RTS turbulence characteristics with the target on-road condition (M-M-M: Moderate Terrain, Moderate Traffic, Moderate Winds).

Component	Turbulence Intensity, I		Turbulence Length Scale, L^x	
	Road	RTS	Road	RTS†
u	4.0 %	3.6 %	4.7 m	1.0 m
v	3.5 %	5.0 %	1.9 m	2.6 m
w	3.1 %	4.4 %	0.6 m	1.3 m

† full-scale equivalent

similar to the road measurements. In the turbulence spectra that define these values, the high-frequency/small-scale turbulence shows a very good match to the on-road measurements. In the low-frequency/large-scale part of the turbulence spectra, the longitudinal component shows slightly lower energy than on the road, whereas the lateral and vertical components show higher energy. Despite these differences, the turbulence generated by the RTS provides a good representation of the turbulence characteristics measured on the road. This is also reflected in spatial correlation measurements of the turbulence, again documented in greater detail by McAuliffe and Kirchhefer (2015). Differences in the tractor-trailer drag characteristics with the RTS compared to tests is smooth flow are also reported by McAuliffe and Kirchhefer (2015), which indicate the drag measurements are approximately 2% lower with the RTS than in smooth flow, and that the smooth-flow results over-predicted the drag reductions measured for two common drag-reduction technologies.

2.3 Test Procedure

The measurements presented in this report have been performed in accordance with the SAE International recommended practice for wind-tunnel testing of trucks and buses (*SAE Wind Tunnel Test Procedure for Trucks and Busses*, 2012).

Measurements were performed at a wind speed of 50 m/s (180 km/hr), which is the highest speed attainable with the moving ground plane in the NRC 9 m Wind Tunnel. This wind speed provides a width-based Reynolds number for the 30% truck model of approximately 2.6×10^6. This is approximately 54% of that achieved by a full-scale vehicle traveling at 100 km/h ($Re = 4.8\times10^6$). Data by Wood (2012a) and Leuschen (2013) suggest that the aerodynamics of a tractor-trailer combination show a small sensitivity to Reynolds number between about 2×10^6 and 4-5×10^6, above which the drag coefficient (see Section 2.4) is not influenced by Reynolds number effects. Additional analysis presented by McAuliffe and Kirchhefer (2015) show that at the test condition of $Re = 2.6\times10^6$ the only region of the 30% scale truck model that appears to be sensitive to Reynolds number is the tractor underbody. It is therefore expected that Reynolds number effects will not influence the trailer technologies being tested in the current project. Although full-scale Reynolds number conditions have not been achieved in the current study, the data of Wood and Leuschen suggest that the drag coefficients mea-

sured here are within 1% of the full-scale Reynolds-number values.

For each vehicle configuration, measurements were performed at various yaw angles (turntable positions) to allow the calculation of a wind-averaged-drag coefficient. The largest yaw sweep used was 0°, -15°, -12°, -9°, -6°, -3°, -1°, 0°, 1°, 3°, 6°, 9°, 12°, 15°, 0°. For time and cost constraints, many yaw sweeps consisted of a maximum angle range of $\pm 12°$or $\pm 9°$, and for some configurations only negative-range yaw sweeps were performed.

2.4 Data Reduction

The drag coefficient is defined as

$$C_D = \frac{F_D}{1/2\rho U^2 A} \tag{2.1}$$

where F_D is the measured drag force, ρ is the air density, U is the wind speed, and A is the vehicle reference area (taken here as vehicle height $\times$ vehicle width, 0.962 m^2). To ensure all measurements presented in this report can be compared directly to one another, this value for the vehicle reference area has been used for all truck configurations tested, even those with smaller frontal areas.

The wind-tunnel drag-coefficient measurements have been corrected for the following influences, according to standard wind-tunnel practice:

- Blockage effects: Confinement of the air around the model in the closed-wall test section of the wind tunnel causes a local speed-up of the air in the vicinity of the model. At 30% scale, the wind-speed increase is on the order of 1%. The Thom-Heriot method (described in SAE SP-1176, 1996) has been used to correct the wind speed, and its influence on the drag coefficient and pressure coefficients.
- Strut loads: The wind loads measured by the under-floor balance system also measure the wind loads experienced by the struts that support the tractor-trailer model over the rolling road, as described previously in Section 2.1.4. The strut wind loads and their aerodynamic interactions have been subtracted from the model+strut measurements to provide the wind loads experienced by the model in the absence of the struts.
- Wheel aerodynamic resistance: The overall aerodynamic resistance to the motion of a ground vehicle includes not only the drag force of the vehicle in-line with the direction of motion, but also the aerodynamic torque experienced by the wheels. The engine must overcome the resistance to both aerodynamic resistance sources. The aerodynamic torque experienced by the wheels has been measured through the wheel motors, converted to an equivalent force measurement, and added to the linear drag measurement to obtain a vehicle drag coefficient representative of the aerodynamic resistance to motion on the road.

To provide a single representative measure of the aerodynamic performance of a ground vehicle with which the different configurations can be compared, a wind-averaged-drag coefficient (WAC_D) can be defined that, for a given ground speed (U_g), accounts for an equal probability

of experiencing terrestrial winds from all directions. The WAC_D makes use of the distribution of C_D with yaw angle, combined with a single mean terrestrial wind speed (U_{avg}) that represents long-term averaged conditions experienced on the road. The procedure involves averaging the vector combination of ground speed and wind speed for an equal probability of experiencing the mean wind speed from all directions. The general equation for the wind-averaged-drag coefficient is:

$$WAC_D(U_g) = \frac{1}{2\pi}\int_0^{2\pi} C_D(\psi)\left[1+\left(\frac{U_{avg}}{U_g}\right)^2+2\left(\frac{U_{avg}}{U_g}\right)\cos\theta\right]d\theta \tag{2.2}$$

where the yaw-angle of the wind relative to the direction of motion is

$$\psi = \tan^{-1}\left[\frac{(U_{avg}/U_g)\sin\theta}{1+(U_{avg}/U_g)\cos\theta}\right] \tag{2.3}$$

For Canada and the United States, a typical mean terrestrial wind speed (U_{avg}) used for these calculations is 11 km/h (7 mph, *SAE Wind Tunnel Test Procedure for Trucks and Busses*, 2012). Unless specified otherwise, the WAC_D values presented in this report represent those calculated for an 11 km/h mean terrestrial wind speed and a vehicle ground speed of 100 km/h. Depending on whether a full- or half-range yaw sweep was performed, the WAC_D was calculated for the positive yaw range, the negative yaw range, and the full yaw range. For each data plot in this report, the data presented will use an appropriate range for the wind-averaged-drag coefficient, and is defined on the plot by WAC_D^-, or $WAC_D^\pm$ for the negative yaw range and full yaw range, respectively.

Based on an analysis of the error sources for the current data set (McAuliffe and Kirchhefer, 2015), the uncertainty for the wind-averaged-drag coefficient (δWAC_D) is estimated to be on the order of 0.003. A large proportion of this uncertainty is associated with correlated bias errors, such that the uncertainty associated with the difference in wind-averaged-drag coefficient between different model configurations ($\delta\Delta WAC_D$) is on the order of 0.001.

The wind tunnel model was instrumented with surface pressure taps. Pressure coefficients were calculated according to:

$$C_P = \frac{P - P_{ref}}{1/2\rho U^2} \tag{2.4}$$

where P is the model surface pressure, P_{ref} if the local static pressure in the wind-tunnel test section, ρ is the air density, and U is the wind speed.

2.5 Fuel-Savings and Greenhouse-Gas-Reduction Analysis

Although an increase or decrease in vehicle drag provides an indication of a change in fuel consumption or greenhouse-gas emissions of a heavy-duty vehicle, estimates of these savings are important for quantifying economic factors that will influence the acquisition and use of particular technology.

The difference in wind-averaged-drag coefficient for a given vehicle configurations and a reference case is used to estimate the fuel-consumption savings, $\Delta\mu$, of the device when travelling at the specified speed, according to:

$$\Delta\mu(U_g)\left[\frac{l}{100km}\right] = 27.8 \times \frac{sfc\,1/2\,\rho\,U_g^2\Delta WAC_D\,A}{\eta} \tag{2.5}$$

where sfc is the specific fuel consumption of a modern diesel engine (taken here as 2.4×10^{-4} l/Whr), ρ is standard sea-level air density (taken here as 1.225 kg/m^3), U_g is the vehicle ground speed (taken here as 27.8 m/s, equivalent to 100 km/h), ΔWAC_D is the change in wind-averaged drag coefficient, A is the vehicle frontal area (taken here as vehicle height $\times$ vehicle width, 10.7 m^2), η is the transmission efficiency (taken here as 0.85), and 27.8 is a units scaling factor.

From the fuel-consumption-savings estimates of Equation 2.5, practical values of fuel savings and greenhouse-gas emission reductions for a typical vehicle can be developed. In a recent white paper on the adoption rates of fuel-savings technologies by Canadian fleets (Sharpe *et al.*, 2015), yearly travel distances for tractors and trailers for nine Canadian fleets are documented. Based on the numbers presented for tractors, an estimate of 156,000 km $\pm$ 45,000 km per tractor per year has been inferred. Not all of this distance is traveled at highway speed. Information regarding the speed profiles of the vehicles reported by Sharpe *et al.* (2015) are not available, however for the purpose of the current report, it has been assumed that these are long-haul operators and that the vehicles travel at highway speed 80% of their time. An evaluation of some unpublished raw data from the Canadian Vehicle Use Study (Transport Canada, 2015) indicates this to be a reasonable assumption. This 80%-highway duty cycle provides an estimate of 125,000 km $\pm$ 35,000 km traveled per tractor per year at highway speed. With such an estimate, the fuel savings (litres of diesel and fuel cost) and the reduction in CO_2 emissions for each vehicle every year can be calculated. As was used by Sharpe *et al.* (2015), the average 2014 price of diesel fuel is used in the analysis ($1.35/litre). Greenhouse-gas emission savings are calculated based on simple chemistry that shows 2.64 kg of CO_2 is emitted per litre of diesel burned. Based on the uncertainty estimate for the wind-averaged drag coefficient defined in the previous section ($\delta\Delta WAC_D \approx 0.001$), the uncertainty on the fuel savings and greenhouse-gas emissions are on the order of 50 litres/tractor/year and 130 kg CO_2/tractor/year.

3. Drag Characteristics of Tractor-Trailer Combinations

3.1 Truck Configurations

Although long-haul trucking is dominated by sleeper-cab tractors and dry-van trailers, numerous other vehicle configurations are found on the road. To assess adequately the fuel-savings potential of different aerodynamic treatments to heavy-duty vehicles, it was deemed important to use different vehicle configurations in the wind tunnel test program. This section of the report provides a brief discussion of the differences in drag characteristics that can be found between different vehicle combinations. Specific details on the differences, and why they are different, are deferred to later sections of the report that deal with the drag reduction technologies and how their influence differs between vehicle configurations. This section also provides an introduction to the manner in which the drag-coefficient data will be presented throughout the report.

3.2 Tractor Configurations

Two basic tractor configurations have been tested. Figure 3.1 shows the day-cab and sleeper-cab arrangements for the tractor model with their full-height roof fairings. Both variants of the model use the same fore-body surfaces. To convert from the day-cab to the sleeper, the wheelbase is extended, side-skirt extensions are added, a sleeper box structure and side panels are added, and the roof fairing is changed. The drag-coefficient performance of the two tractor variants, when paired with the 53 ft dry-van trailer, are compared in Figure 3.2. In the left-hand plot, the upper curves (with white-filled symbols) represent the variation of drag coefficient (C_D) with yaw angle. In Figure 3.2, the sleeper-cab is the reference case against which the day-cab data are measured. The curve with grey-filled symbols in the lower part of the left-hand plot shows the difference in drag coefficient between the day-cab and its reference case, the sleeper-cab (axis for this data set on right side of graph per the arrow). These data show that the greatest difference between the sleeper-cab and day-cab tractor variants is at low yaw angles. The bar graph on the right-hand plot represents the difference in wind-averaged-drag coefficient (WAC_D, evaluated at 100 km/h ground speed) between the sleeper-cab (reference case) and the day-cab. The tractor-trailer combination experiences higher drag with the day-cab tractor than with the sleeper-cab. This is an increase of approximately 7% (ΔWAC_D = +0.038) over the sleeper-cab value. The sleeper-cab shows a greater level of asymmetry in the variation of the drag-coefficient with yaw angle than does the day-cab. This



(a) Day-cab (b) Sleeper-cab

Figure 3.1: Day-cab and sleeper-cab tractor configurations.

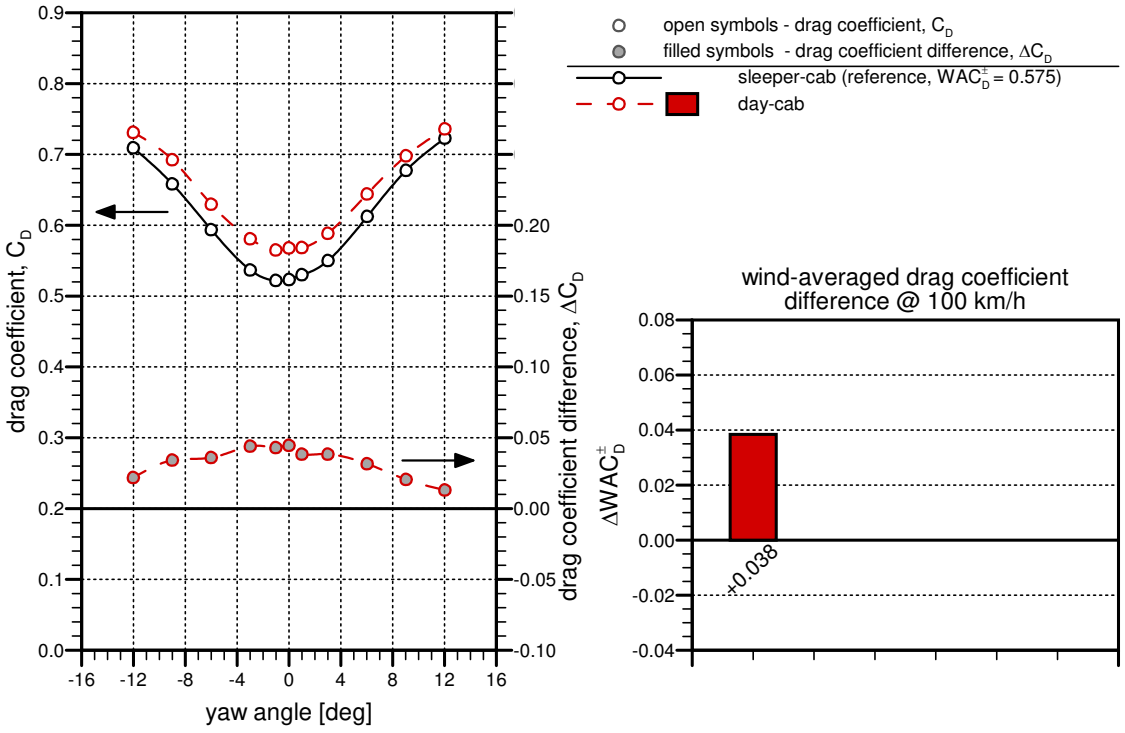
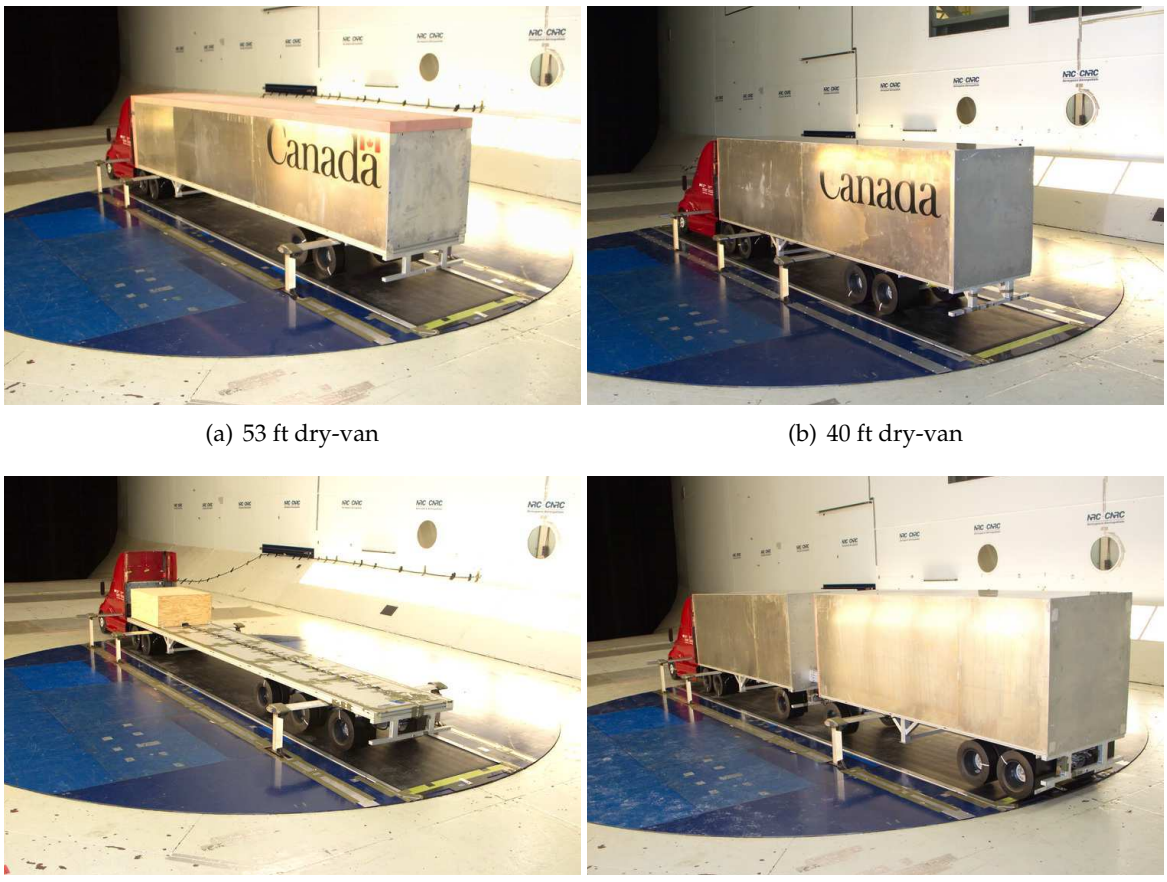


Figure 3.2: Comparison of the drag-coefficient performance of the sleeper and day-cab tractor variants with the 53 ft dry-van trailer.

is likely due to small asymmetries in the model build and configuration. For example, the sleeper-cab variant uses a vertical exhaust pipe in the gap region on the passenger side of the vehicle, whereas the day-cab variant uses a low exhaust pipe and therefore has greater symmetry in the tractor-trailer gap region.

3.3 Trailer Configurations

Several trailer configurations have been used throughout the current study. A sample set of four tested trailer configurations with the sleeper-cab tractor is shown in Figure 3.3, including the 53 ft dry-van, the 40 ft dry-van, the 53 ft flatbed, and the tandem 28 ft dry-van configurations. Note that the flatbed, although intended to be empty, required a small box to cover the on-board instrumentation that typically would reside inside the dry-van trailer. The drag-coefficient measurements for these four trailer configurations are shown in Figure 3.4, and are presented in the same manner as the tractor data, with the reference case for all others being



(a) 53 ft dry-van

(b) 40 ft dry-van

(c) 53 ft flatbed

(d) Tandem 28 ft dry-van

Figure 3.3: Sample of trailer configurations with sleeper-cab tractor.

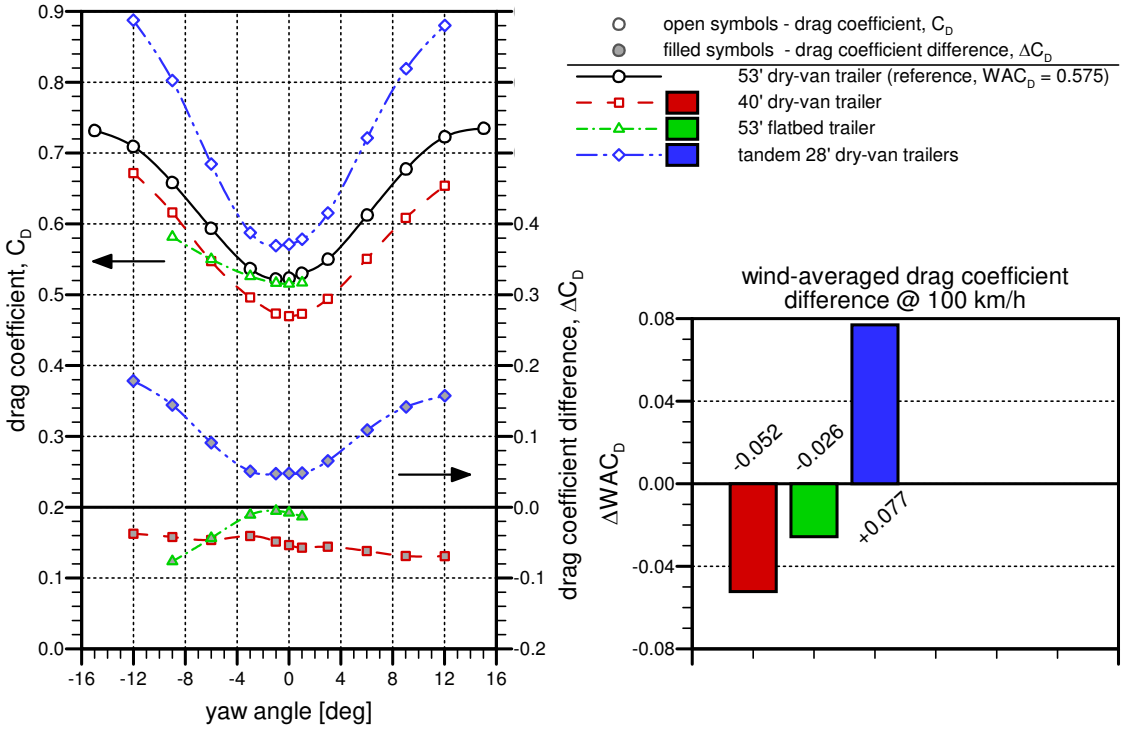


Figure 3.4: Comparison of the 53 ft dry-van, 40 ft dry-van, 53 ft flatbed (empty), and tandem 28 ft dry-van trailers with the sleeper-cab tractor.

the 53 ft dry-van configuration. A 9% decrease in drag is observed for the 40 ft dry-van trailer (ΔWAC_D = -0.052), compared to the 53 ft dry-van. Although not presented here, surface pressure measurements show that this lower drag is due to a combination of higher base pressure on the back face of the trailer and lower pressure on the front face of the trailer bogie. The latter effect is due to the bogie being closer to the tractor drive axles, providing less distance over which high-momentum air can be entrained and impinge on the front face of the bogie. The flatbed configuration shows little difference in drag from the 53 ft dry-van at low yaw angles. The influence of the low trailer is observed at higher yaw angles where the increase in C_D with yaw angle is not as great as for the dry-van. This results in a wind-average-drag coefficient approximately 5% lower for the 53 ft flatbed than for the same length dry-van. The drag-reduction study for the flatbed configuration is found in Section 5. The tandem 28 ft dry-van trailer shows a large increase in drag compared to the 53 ft dry-van (13% increase, ΔWAC_D = +0.077). This increase is due predominantly to drag associated with the trailer-trailer gap region, and due to the extra sets of trailer wheels. The drag-reduction study for the long-combination-vehicle configuration is found in Section 6.

3.4 Influence of Tractor and Trailer on Fuel Use and Greenhouse-Gas Emissions

The results presented in this section show a variability in the wind-averaged-drag coefficient on the order of $\pm$10% for the different tractor and trailer configurations using the sleeper-cab tractor and 53 ft dry-van trailer as the reference configuration. This does not consider any drag-reduction treatments. To demonstrate the difference in fuel use and greenhouse-gas emissions, Table 3.1 shows the fuel savings and reduction in CO_2 possible for the various tractor and trailer configurations discussed in this section, all relative to the sleeper-cab and 53 ft dry-van configuration. The use of the day-cab tractor configuration tested, instead of the sleeper-cab tractor, would provide an increase in fuel use and greenhouse-gas emissions of approximately 1,900$\pm$500 litres/tractor/year and 5,000$\pm$1,300 kg CO_2/tractor/year. Note that these estimates are based on the aerodynamic effects and do not include the influence of changes to the vehicle weight. Differences on the order of thousands of dollars and thousands of kg of CO_2 emissions are attributed to the various aerodynamic changes to the tractor-trailer. The remainder of the report will focus on ways to improve the drag characteristics of these various tractor-trailer combinations.

Table 3.1: Fuel savings and greenhouse-gas reduction estimates for changes in tractor and trailer configurations (for 125,000$\pm$35,000 km/tractor/year @ 100 km/hr), DV - dry-van, FB - flatbed. **Note: negative numbers imply increased fuel-use and emissions.**

Baseline Vehicle Configuration	**Modified Vehicle Configuration**	**Drag Change ΔWAC_D**	**Fuel Rate Savings [l/100km]**	**Fuel Saved [l]**	**Fuel Cost Savings [$ @ $1.35/l]**	**CO_2 Reduction [kg]**
sleeper-cab/53 ft DV	day-cab/53 ft DV	0.038	-1.5	-1,900 $\pm$ 500	$ -2,600 $\pm$ $ 700	-5,000 $\pm$ 1,300
sleeper-cab/53 ft DV	sleeper-cab/40 ft DV	-0.052	2.1	2,600 $\pm$ 700	$ 3,500 $\pm$ $ 900	6,900 $\pm$ 1,800
sleeper-cab/53 ft DV	sleeper-cab/53 ft FB	-0.026	1.0	1,300 $\pm$ 400	$ 1,800 $\pm$ $ 500	3,400 $\pm$ 1,100
sleeper-cab/53 ft DV	sleeper-cab/2x28 ft DV	0.077	-3.0	-3,800 $\pm$ 1,100	$ -5,100 $\pm$ $ 1,500	-10,000 $\pm$ 2,900

4. Drag Reduction Methods for Dry-Van Trailer

4.1 Approach

Aerodynamic improvements to tractor-trailer combinations have, until recently, focussed primarily on streamlining and modifying the tractor. Many low-drag aero-tractors are on the market and significant efforts have been expended by the tractor OEMs to develop and optimize these vehicles, pushed in part by regulatory efforts to reduce greenhouse-gas emissions (GHGs) and fuel consumption (Environment Canada, 2013; U.S. Environmental Protection Agency and U.S. Department of Transportation, 2011). Reducing the drag of tractor-trailer combinations through modifications to the trailer have been limited primarily to the use of side-skirts, although emissions regulations in some regions such as California have promoted a higher rate of adoption of other types of drag reducing trailer devices such as boat-tails. Except for California, regulations have not, to date, treated trailers.

To evaluate the performance of current and emerging drag reduction technologies for heavy-duty vehicles, a large part of the current study was directed towards reducing the drag associated with dry-van trailers. This section of the report evaluates the performance of technologies that treat several regions of the trailer:

1. The tractor-trailer gap (Sections 4.2 and 4.3);
2. The trailer underbody (Section 4.4);
3. The trailer base (Section 4.5); and
4. The trailer upper-body (Section 4.6).

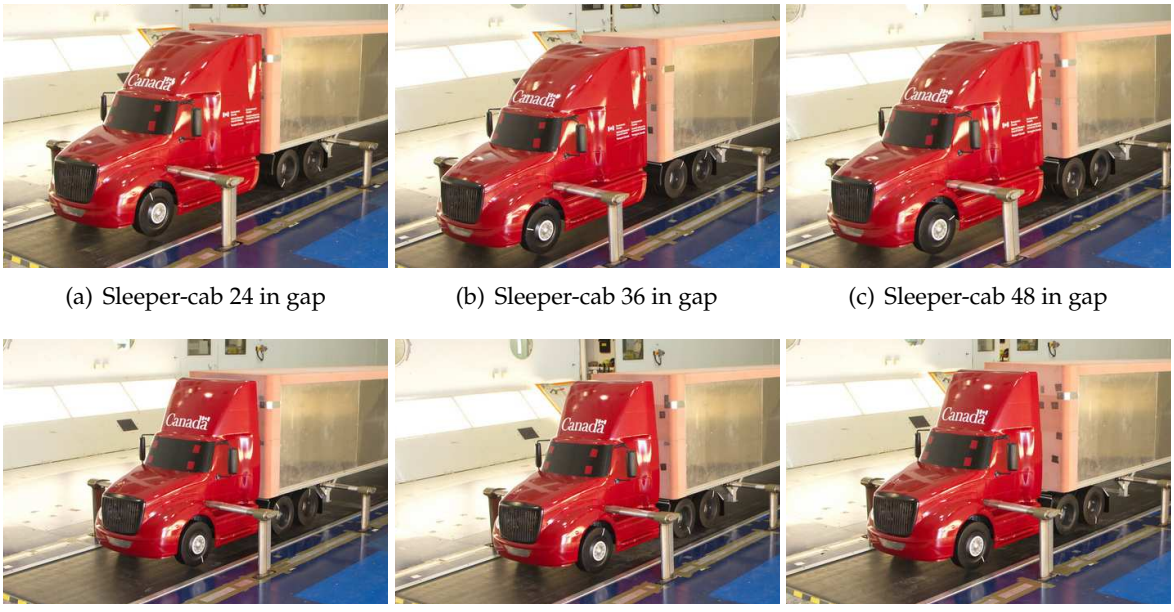
With the best-performing devices and configurations identified, combinations thereof were also tested to evaluate the interactions and influences between them. These aerodynamic interactions are discussed in Section 4.7. Furthermore, the differences in performance of some of these technologies and their combinations when applied to the day-cab and sleeper-cab variants have also been evaluated, and are discussed in Section 4.8.

The baseline configuration for most of the results presented in the following sections consisted of the sleeper-cab tractor with the 53 ft dry-van trailer and a 36 inch gap between them. Some of the tests were performed with the day-cab tractor variant, to evaluate any performance differences between the two tractor types.

4.2 Tractor-Trailer Gap Width

The tractor-trailer gap is one region of a tractor-trailer combination that has long been known to influence the drag of the vehicle. Wind flowing through the gap region has been recognized as a source of drag and changes to the distance between the tractor and trailer have been recognized to influence the vehicle drag (Leuschen and Cooper, 2006; National Academy of Sciences, 2010; Gelzer, 2011; Patten *et al.*, 2012). The results presented in this section provide guidance not only on optimum settings for the tractor-trailer gap but also on the potential benefit of active fifth-wheel technologies that may be useful to adjust the gap automatically while in motion.

To investigate the potential drag reduction from shortening the width of the tractor-trailer gap, the drag of the vehicle was measured for different positions of the tractor variants relative to a stationary trailer location. For this set of tests, full ground simulation was provided for the forward part of the vehicle such that the front of the tractor was located approximately 0.30 m from the front edge of the rolling road. The tractor struts were mounted in their forward-most locations on the model, immediately aft of the wheel wells, to minimize interactions of the strut wakes with the tractor-trailer gap region. Measurements were performed with five gap widths for the sleeper-cab tractor variant (equivalent to 24 in, 30 in, 36 in, 42 in, and 48 in full-scale) and three gap widths for the day-cab tractor variant (equivalent to 24 in, 36 in, and 48 in full-scale). Photographs of the two tractor variants with the 24 in, 36 in, and 48 in gap width are shown in Figure 4.1, in which the extent of the trailer front face visible in each photograph provides a representation of the change in gap width relative to the overall vehicle



(a) Sleeper-cab 24 in gap (b) Sleeper-cab 36 in gap (c) Sleeper-cab 48 in gap

(d) Day-cab 24 in gap (e) Day-cab 36 in gap (f) Day-cab 48 in gap

Figure 4.1: Tractor-trailer gap-width configurations

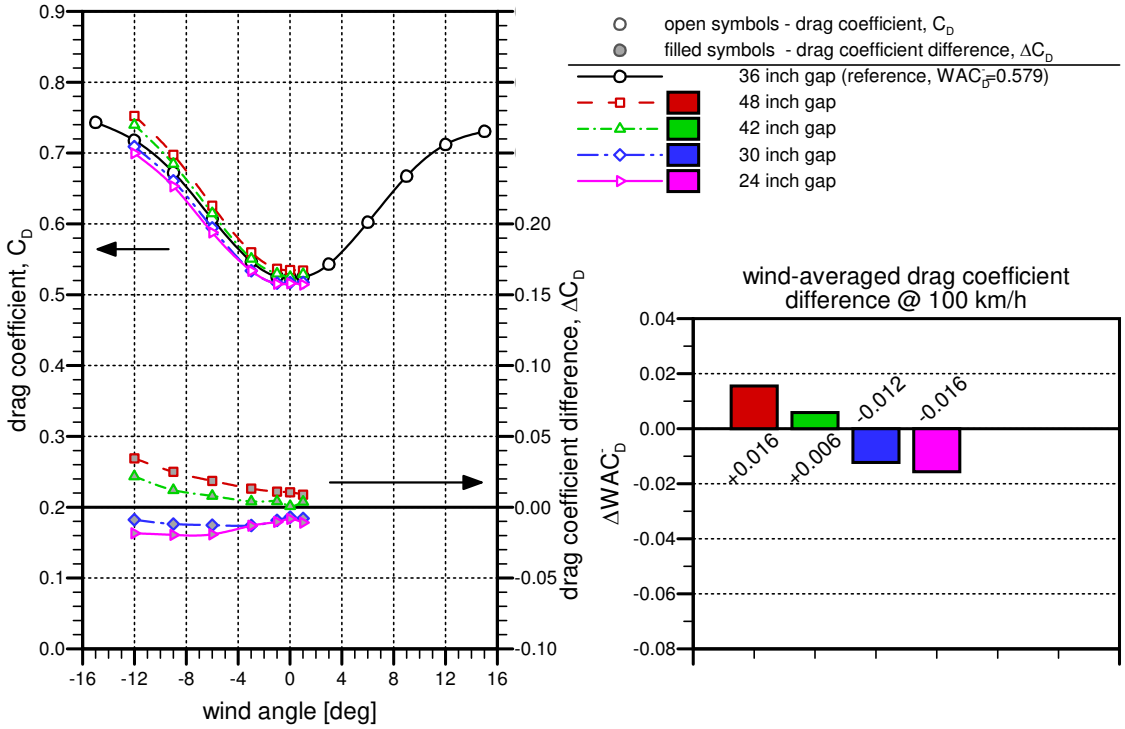


Figure 4.2: Influence of tractor-trailer-gap width for the sleeper-cab tractor with the 53 ft dry-van trailer.

dimensions. It is to be noted that the tractor-trailer gap width represents the distance from the aft surface of the tractor cab to the front face of the trailer. The tractor side-extenders provide a further reduction of 17 inches to the distance from the tractor back edge to the trailer front face, and therefore at the smallest gap width of 24 inches, the distance from the aft edge of the tractor side extenders to the trailer front face is only 7 inches. This distance is often referred to as the aerodynamic gap width.

Figure 4.2 shows the drag-measurement results for the sleeper-cab tractor. The results show that the drag increases with increased gap width, and that the magnitude of the increase varies with yaw angle, more so for the cases with increased gap width. The equivalent results for the day-cab tractor, with a 36 inch gap as the reference case, are shown in Figure 4.3 for which a similar trend as the sleeper-cab is observed. In general, the day-cab tractor exhibits higher drag than the sleeper. The trends in drag coefficient with changing gap width, most clearly observed in the ΔC_D plots, show some differences between the sleeper-cab and day-cab variants. For the day-cab, the largest gap width (48 in) shows a higher drag increase at small yaw angles, as compared to the sleeper cab.

To examine the overall influence of the gap on the two tractor variants, the change of wind-averaged-drag coefficient with gap width are plotted in Figure 4.4 for two ground speeds (80 km/h on the left and 100 km/h on the right). The results of Figure 4.4 show two important trends. First, due to increased C_D with yaw angle, the results at 80 km/h ground speed shows

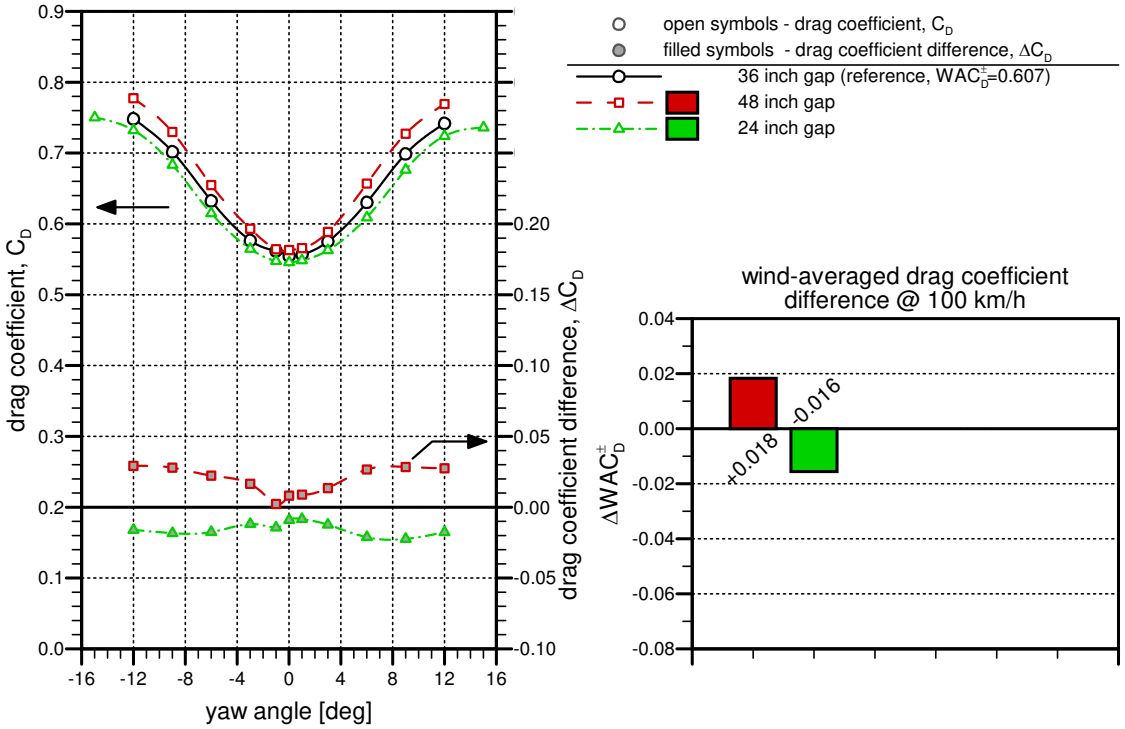


Figure 4.3: Influence of tractor-trailer-gap width for the day-cab tractor with the 53 ft dry-van trailer.

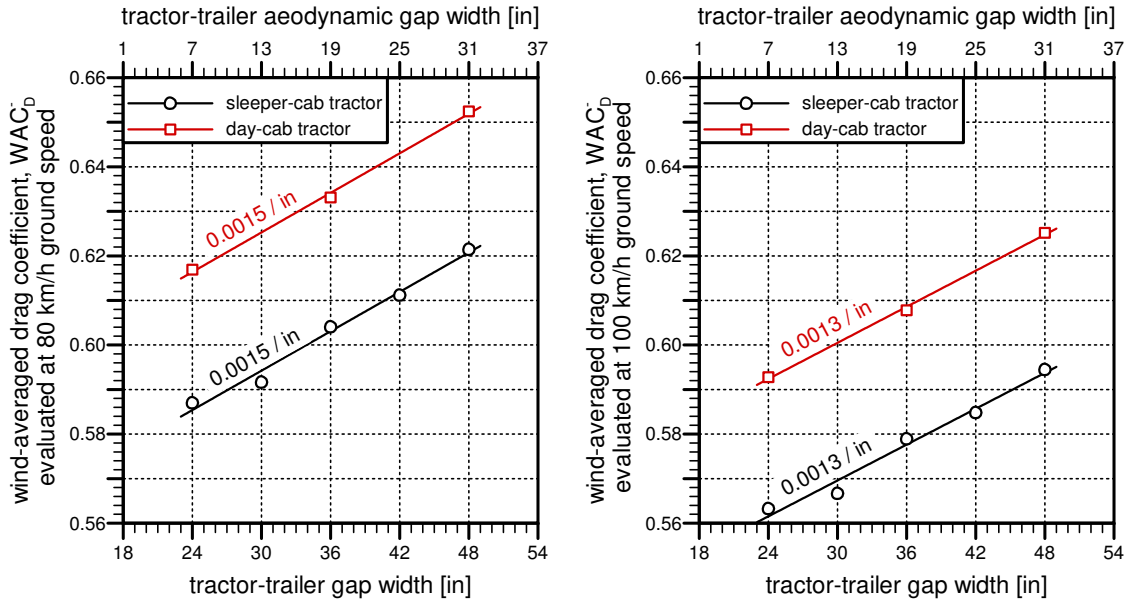


Figure 4.4: Sensitivity of wind-averaged drag coefficient to tractor-trailer-gap width for the sleeper-cab and day-cab tractors with the 53 ft dry-van trailer (left - 80 km/h ground, right - 100 km/h ground speed).

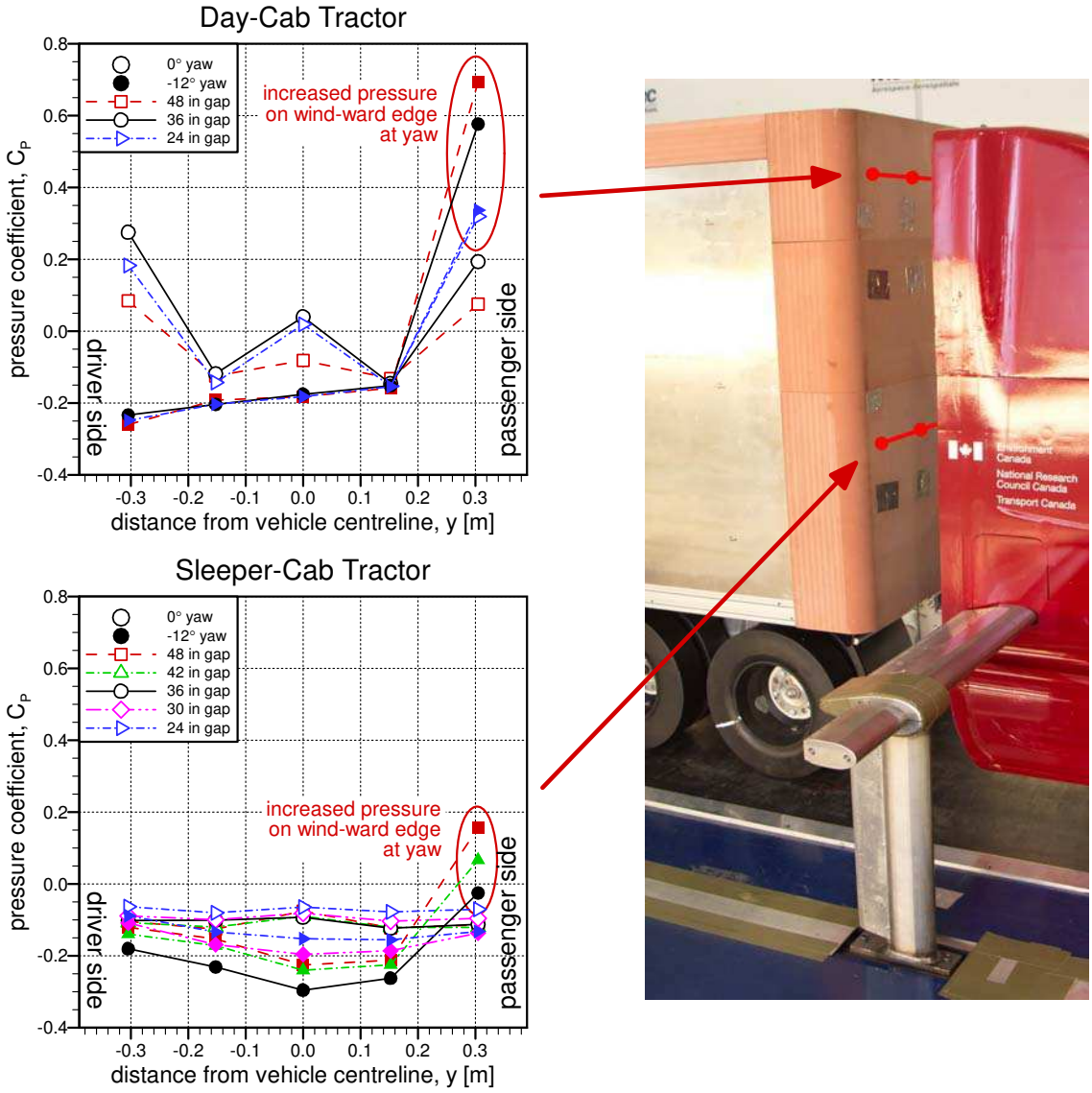


Figure 4.5: Influence of tractor-trailer-gap width on trailer front face pressures (open symbols for 0°yaw angle, filled symbols for -12°yaw angle).

higher WAC_D due to an increased weighting of higher yaw angles. Secondly, the rate of increase of WAC_D with gap width is higher at lower ground speeds (0.0015/inch compared to 0.0013/inch). Despite the differences in absolute drag coefficient between the day-cab and sleeper-cab tractors, these gap rates are consistent between the two for a given ground speed.

The increase in drag of the tractor-trailer combination as a result of increasing the tractor-trailer-gap width is attributed to two sources, as identified by surface-pressure measurements performed during the test campaign:

1. As yaw angle increases and an increased amount of air travels through the gap region

due to the effective cross-wind, a larger area of the wind-ward trailer vertical edge experiences high pressure from the air impinging on its surface. This is shown for both the day-cab and sleeper-cab in Figure 4.5, in which each subplot represents the horizontal row of pressure taps on the front face of the trailer that experiences the greatest increase in pressure as yaw angle increases. In both subplots, the wind-ward/passenger-side pressure tap shows increased pressure at -12° yaw, and this increase is higher for the larger gap widths. This increased surface pressure with gap width is the likely cause for the trend of increasing ΔC_D with yaw angle in Figures 4.2 and 4.3.

2. Over the range of yaw angles tested, pressure in the trailer-underbody region increases with increasing gap width. Figure 4.6 shows the change with yaw angle of the pressure coefficient measurements on the front-face of the trailer bogie, for the day-cab configuration. Both pressure taps show large changes in pressure coefficient with yaw angle. The pressure tap on the wind-ward side (passenger side for negative yaw and driver side for positive yaw) experiences its highest pressure around 9° as the effective cross-wind draws the air under the trailer. Both bogie pressure taps show increased pressure over the full yaw range with increasing gap width. No change with gap width is observed in the pressures at the base of the trailer bogie (not shown), and therefore the higher front-face pressure generates an increased rearward-directed force on the trailer bogie, and increased vehicle drag. Although not shown here, the same trends are observed for the sleeper-cab configuration. In examining other data collected for this test program (not shown here), the influence to the under-trailer pressure is not observed when the tractor drive-axles remain in the same location. Due to a miscommunication during the test program, two gap changes were initially performed by extending the tractor frame rail (designed to adjust between day-cab and sleeper-cab configurations), leaving

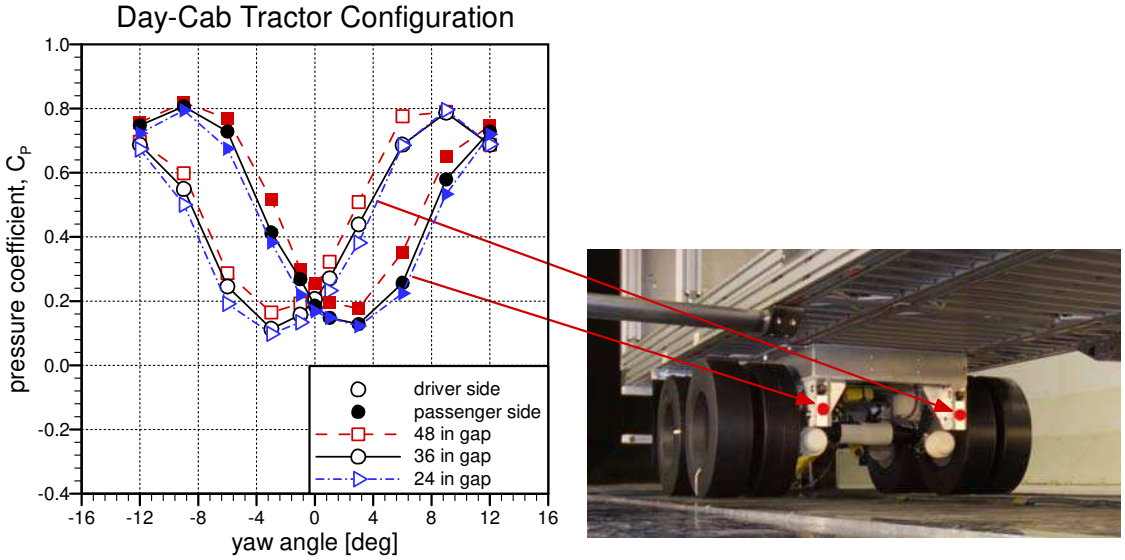


Figure 4.6: Influence of tractor-trailer-gap width on trailer bogie face pressures (open symbols for driver side tap, filled symbols for passenger side tap).

Table 4.1: Fuel savings and greenhouse-gas reduction estimates for changes in the tractor-trailer-gap width (for 125,000±35,000 km/tractor/year @ 100 km/hr).

Baseline Vehicle Configuration	Drag-Reduction Configuration	Drag Change ΔWAC_D	Fuel Rate Savings [l/100km]	Fuel Saved [l]	Fuel Cost Savings [$ @ $1.35/l]	CO_2 Reduction [kg]
sleeper-cab + 48" gap	24" gap	-0.032	1.3	1,600 ± 400	$ 2,200 ± $ 500	4,200 ± 1,100
sleeper-cab + 48" gap	36" gap	-0.016	0.6	800 ± 200	$ 1,100 ± $ 300	2,100 ± 500
day-cab + 48" gap	36" gap	-0.018	0.7	900 ± 200	$ 1,200 ± $ 300	2,400 ± 500

the tractor drive-axles in place relative to the trailer, rather than moving the entire tractor relative to the trailer. For these cases, no significant influence was observed on the trailer underbody pressures, and a lower rate of change of WAC_D with gap width was observed (0.0010/inch compared to 0.0013/inch). The same trend is observed for some gap-mounted devices that effectively reduce the gap width while retaining the tractor in position relative to the trailer (see next section), whereby negligible influence on the trailer underbody pressures was observed. It therefore appears that part of drag reduction associated with reducing the tractor-trailer gap width is a result of the aft position of the tractor drive-axles and their influence on the underbody pressures.

The results presented above show that reducing the tractor-trailer-gap width is a simple means to reduce the drag and fuel consumption of a tractor-trailer combination. Table 4.1 shows the fuel savings and reduction in CO_2 emissions possible for several configurations of tractor and gap width, according to the analysis defined in Section 2.5. If it is assumed that a 48 inch gap width is the current standard, reducing the gap width to 24 inches can provide a savings of 1,600±400 litres/tractor/year and 4,200±1,100 kg CO_2/tractor/year. A 24 inch gap is likely impractical due to interference between the tractor and trailer in low-speed turns. However, an active fifth wheel system that reduces the gap at highways speeds can lead to significant fuel savings. A standard 36 inch tractor-trailer gap is feasible and can provide a cost savings, over a 48 inch gap, of 800±200 litres/tractor/year and 2,100±500 kg CO_2/tractor/year, or possibly more for a day-cab configuration.

4.3 Tractor-Trailer Gap Devices

The previous section described the manner in which reducing the distance from the tractor to the trailer can reduce drag and save fuel. Simple gap-width changes may not always be possible due to operational considerations such as maneuverability and load distribution. Other techniques to reduce the flow in and through the tractor-trailer gap region are available and some technologies are currently on the market to do so. Several concepts for reducing drag from the gap regions have been described by others (for example Cooper and Leuschen, 2005; Leuschen and Cooper, 2006; Landman *et al.*, 2009; Burton *et al.*, 2013). The various techniques typically used to address the gap region have included tractor side extenders, devices mounted inside the gap, and full gap closure. The tractor model used in the current study is based on a modern aero tractor that has side-extenders, and therefore only devices that may be practically mounted in the gap have been studied here.

Three tractor-trailer-gap devices have been tested in the current campaign, all three of which are shown in Figure 4.7:

- Partial plate seal - a trailer-mounted vertical plate that partially spans the gap between the tractor and trailer;
- Full plate seal - a tractor- or trailer-mounted vertical plate that spans the full gap between the tractor and trailer; and
- Trailer fairing - a curved fairing that protrudes to covers the full front face of the trailer and reduce the size of the gap between the tractor and trailer.

These devices have been developed based on simple concepts and do not represent specific technologies on the market.

In addition to devices specifically designed to reduce drag, anecdotal evidence from drivers (and noted by Gelzer, 2011) has indicated that a refrigeration unit mounted to the front-face of a trailer can provide a fuel savings. These "Reefer" trailers are common for food distribution and it was therefore decided to evaluate the aerodynamic influence of a refrigeration unit mounted in the tractor-trailer gap. Conversely, heating units are often used in colder climates such as Canadian winters or year-round in the Canadian north, and may also provide some influence on the tractor-trailer-gap aerodynamics. The influence of these devices were evaluated in an attempt to identify dual uses or benefits. The simplified refrigeration and heater units tested are shown in Figure 4.8.

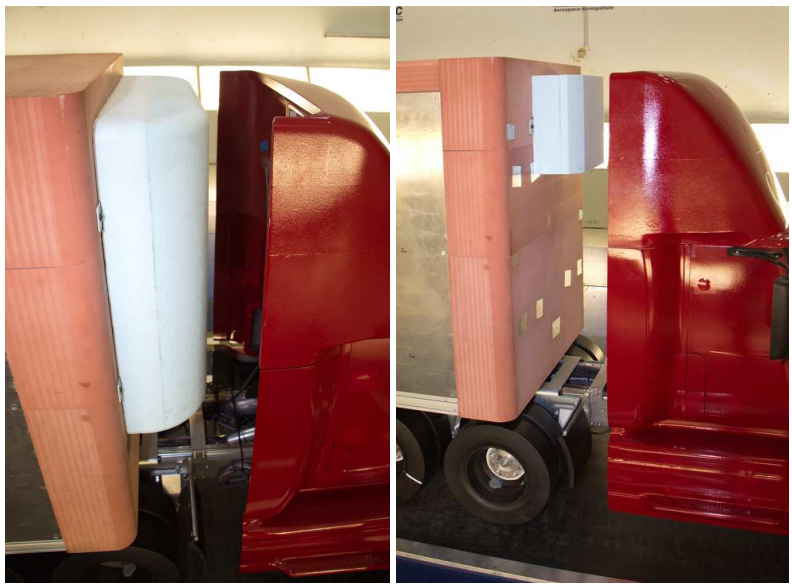
It was anticipated that the aerodynamic performance of the drag-reduction devices or the ancillary units would also be influenced by the size of the tractor-trailer-gap width in which they were mounted, and possibly influenced by the tractor style. The test program consisted of testing selective combinations of these above noted devices/units with the different tractor types and different gap widths.

All five gap-mounted devices/units were tested with the sleeper-cab tractor and a 36 inch tractor-trailer-gap width. The measurement results are shown in Figure 4.9. For this vehicle configuration, only two devices show any influence on the vehicle drag. The trailer fairing



(a) Partial plate seal (b) Full plate seal (c) Trailer fairing

Figure 4.7: Tractor-trailer-gap drag-reduction configurations.



(a) Refrigeration unit (b) Heating unit

Figure 4.8: Tractor-trailer-gap ancillary units.

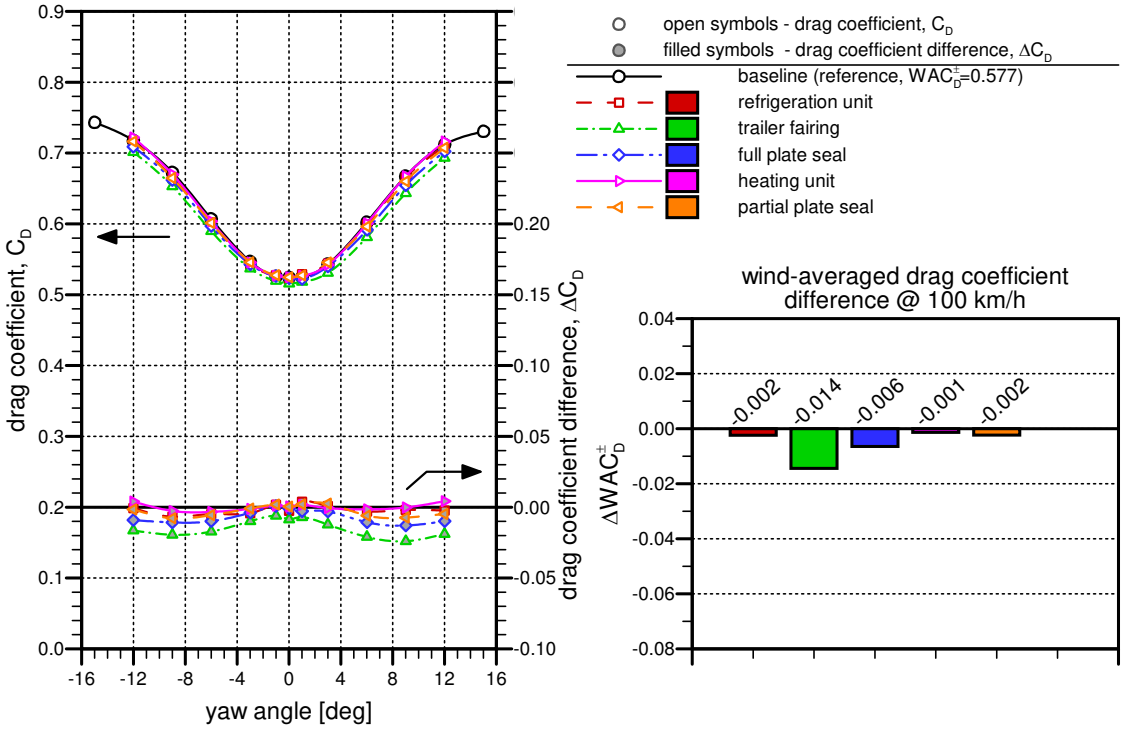


Figure 4.9: Influence of tractor-trailer-gap devices for the sleeper-cab tractor with the 53 ft dry-van trailer and a 36 inch gap.

and full plate seal provide reductions in wind-averaged-drag coefficient of 0.014 and 0.006, respectfully. The partial plate seal, refrigeration unit, and heating unit provide negligible change in vehicle drag. Of the two beneficial devices, only the trailer fairing provides a benefit at low yaw angles. The full plate seal is only effective at higher yaw angles. Although not shown here, the trailer fairing and full plate seal provide a small improvement in drag reduction when the gap-width is changed to 48 inches, with reductions in wind-averaged-drag coefficient of 0.015 and 0.009, respectfully, relative to the baseline 48 inch gap vehicle configuration. For this 48 in configuration, the refrigeration unit provided a small reduction in the wind-averaged-drag coefficient of 0.005, showing some benefit with a larger tractor-trailer gap.

With the day-cab tractor, the trends in drag reduction amongst the devices/units are different. Figure 4.10 shows the measurements for the refrigeration unit, trailer fairing, and full plate seal with the day-cab tractor and a 36 inch tractor-trailer gap. Here, the refrigeration unit and trailer fairing show much larger drag reductions than the equivalent sleeper-cab configuration, with the full plate seal showing negligible drag reduction. Also, in contrast to the sleeper-cab configuration, lower drag reductions are observed for the refrigeration unit and trailer fairing when the gap for the day-cab is increased to 48 inches (on the order of 0.006 lower, data not shown here). This provides strong evidence that the tractor has an influence on the performance of drag reduction technologies for heavy-duty vehicles. This issue will be addressed later in the report (Section 4.8). Of note here, the change in drag-coefficient difference with

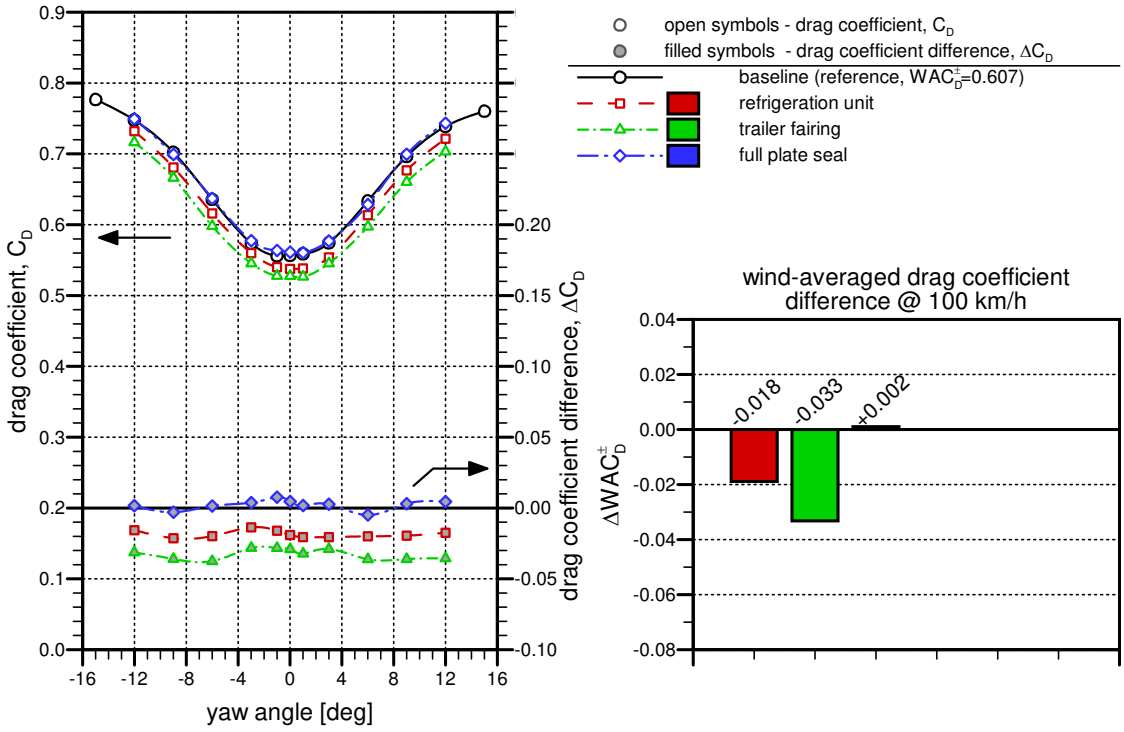


Figure 4.10: Influence of tractor-trailer-gap devices for the day-cab tractor with the 53 ft dry-van trailer and a 36 inch gap.

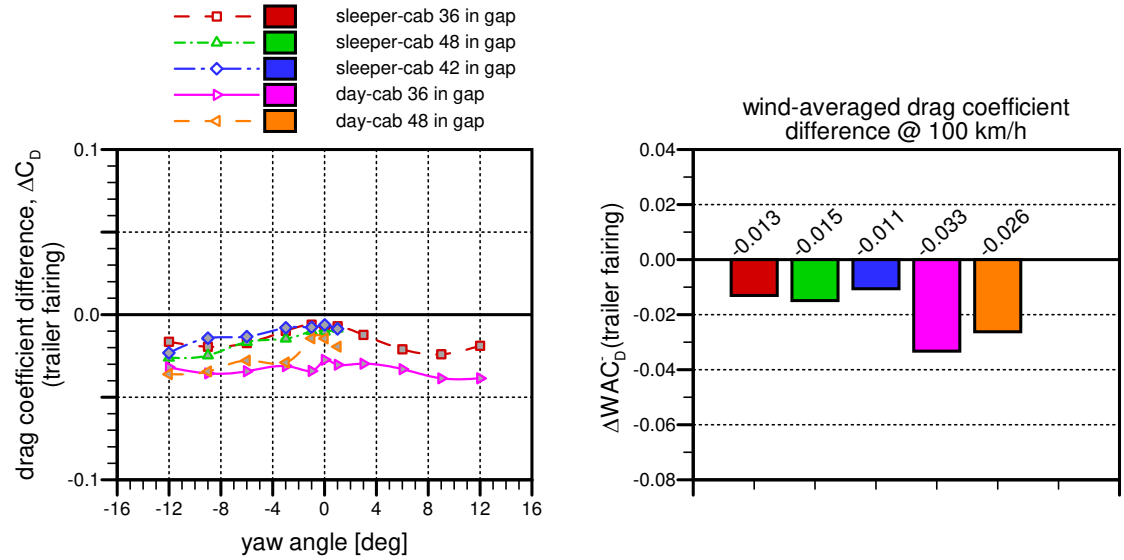


Figure 4.11: Drag reductions measurements for the trailer fairing with different tractor and gap-width combinations.

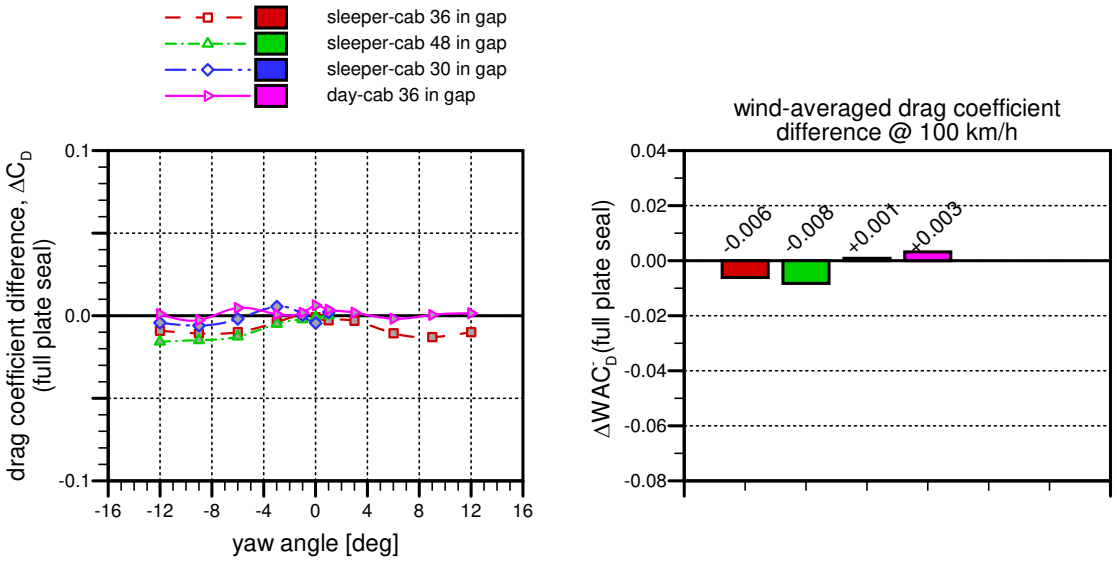


Figure 4.12: Drag reductions measurements for the full plate seal with different tractor and gap-width combinations.

yaw angle (ΔC_D measurements in Figure 4.10) shows a consistent variation with yaw angle, whereas the sleeper-cab data of Figure 4.9 shows increased benefit at higher yaw angles.

For all tractor and gap-width combinations for which gap devices were tested, the trailer fairing consistently provided the highest drag reduction. Figure 4.11 compiles the drag reduction measurements for the trailer fairing with the different tractor and gap-width configurations. It is evident from Figure 4.11 that the trailer fairing provides a greater benefit to the day-cab than the sleeper-cab tractor configuration.

The full plate seal and the refrigeration unit also provided measurable drag reduction for some tractor and gap-width combinations. Figures 4.12 and 4.13 show the drag reduction measurements for the full plate seal and refrigeration unit, respectively. As noted previously, the full plate seal only works for some of the sleeper-cab configurations. The refrigeration unit, however, provides a benefit under all configurations for which it was tested, with a higher drag reduction with the day-cab tractor.

An examination of the surface-pressure measurements has provided some insight into the manner in which the various devices influence the flow field and lead to changes in the drag of the vehicle. Unlike the tractor-trailer gap-width changes, the gap devices influence the flow-field near the aft end of the trailer. Figure 4.14 shows the difference in surface pressure coefficient along the roof of the trailer for various gap devices, relative to their baseline configuration of the sleeper-cab and 36 inch gap width. For both yaw angles represented in Figure 4.14, the trailer fairing exhibits higher pressure immediately downstream of the trailer leading edge as a result of a smoother transition over the edge. At 0° yaw, the roof pressure distributions show a deviation from the baseline configuration over the aft half of the trailer for most of the gap device configurations, with the plate seals and heating unit providing a distinct

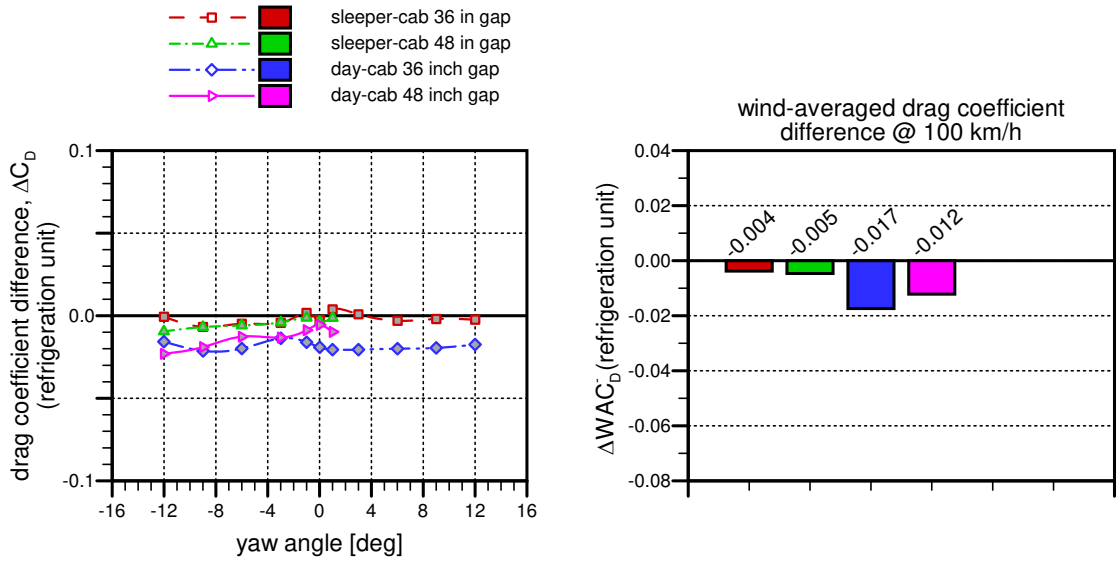


Figure 4.13: Drag reductions measurements for the refrigeration unit with different tractor and gap-width combinations.

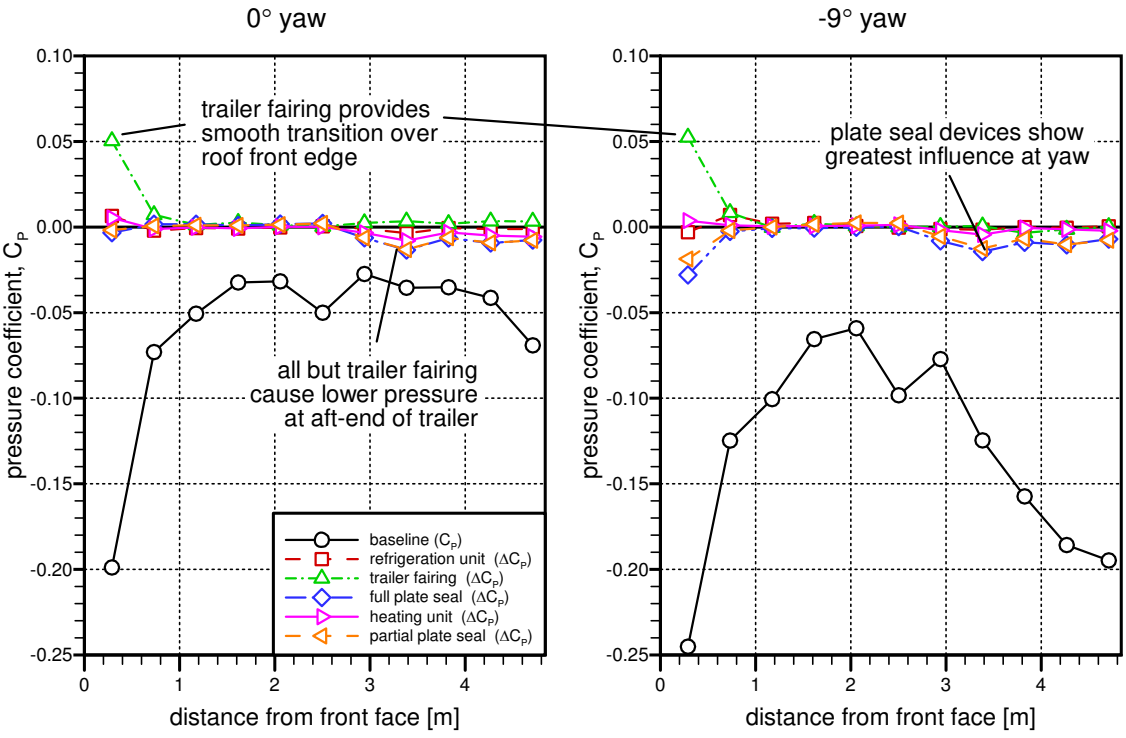


Figure 4.14: Influence of tractor-trailer-gap devices on the trailer roof centreline pressure distribution for the sleeper-cab tractor with the 53 ft dry-van trailer and a 36 inch gap (ΔC_P represents difference from configuration with no gap devices).

Table 4.2: Fuel savings and greenhouse-gas reduction estimates for tractor-trailer-gap devices (for 125,000±35,000 km/tractor/year @ 100 km/hr).

Baseline Vehicle Configuration	Drag-Reduction Configuration	Drag Change ΔWAC_D	Fuel Rate Savings [l/100km]	Fuel Saved [l]	Fuel Cost Savings [$ @ $1.35/l]	CO_2 Reduction [kg]
sleeper-cab + 36" gap	trailer fairing	-0.013	0.5	600 ± 200	$ 800 ± $ 300	1,600 ± 500
sleeper-cab + 42" gap	trailer fairing	-0.015	0.6	700 ± 200	$ 900 ± $ 300	1,800 ± 500
sleeper-cab + 48" gap	trailer fairing	-0.011	0.4	500 ± 200	$ 700 ± $ 300	1,300 ± 500
day-cab + 36" gap	trailer fairing	-0.033	1.3	1,600 ± 500	$ 2,200 ± $ 700	4,200 ± 1,300
day-cab + 48" gap	trailer fairing	-0.026	1.0	1,300 ± 400	$ 1,800 ± $ 500	3,400 ± 1,100
sleeper-cab + 30" gap	full plate seal	-0.006	0.2	300 ± 100	$ 400 ± $ 100	800 ± 300
sleeper-cab + 36" gap	full plate seal	-0.008	0.3	400 ± 100	$ 500 ± $ 100	1,100 ± 300
sleeper-cab + 36" gap	refrigeration unit	-0.004	0.2	200 ± 100	$ 300 ± $ 100	500 ± 300
sleeper-cab + 48" gap	refrigeration unit	-0.005	0.2	200 ± 100	$ 300 ± $ 100	500 ± 300
day-cab + 36" gap	refrigeration unit	-0.017	0.7	800 ± 200	$ 1,100 ± $ 300	2,100 ± 500
day-cab + 48" gap	refrigeration unit	-0.012	0.5	600 ± 200	$ 800 ± $ 300	1,600 ± 500

decrease in pressure in this region. This lower pressure is also observed over the base of the trailer (not shown here), which provides an increased drag force on the vehicle. At -9°, similar trends are observed with the plate seals providing lower pressure near the leading edge and over the aft half of the trailer. The modifications to the pressure field over the aft half of the trailer are also observed in the pressure measurements on the sides of the trailer, which are likely a result of changes to the boundary-layer growth on the sides of the tractor (not shown here).

The most effective tractor-trailer-gap device is the trailer fairing. The surface-pressure data suggest that it blocks the gap, reducing flow through the gap, but it does so in a manner that guides the flow smoothly from the tractor to the trailer, thus avoiding stagnating flow in the gap and minimizing any influence downstream due to adverse changes in the trailer-surface boundary layers. The plate seals appear to adequately block the flow through the gap but the flow that circulates and exits the gap region adversely influences the flow over the trailer and generates a reduced pressure at the base. This reduced base pressure then negates some of the beneficial influence of the device inside the gap. The refrigeration unit provides a similar benefit to the trailer fairing but not as great a change, and the heating unit provides a negligible influence on the vehicle drag. Table 4.2 shows the fuel savings and reduction in CO_2 emissions possible for several configurations of tractor, gap width, and gap device, according to the analysis defined in Section 2.5. Of the configurations tested, only those that provide a measurable drag reduction have been listed in the table. The heating unit and the partial plate seal have not been included, nor has the full plate seal for the day-cab configurations. The largest savings possible based on the gap devices tested is 1,600±500 litres/tractor/year and 4,200±1,300 kg CO_2/tractor/year for the trailer fairing with the day-cab tractor and a 36 inch tractor-trailer gap.

4.4 Trailer Underbody Devices

Over the past decade, trailer side-skirts have become the most common technology used to manage the flow underneath the trailer, however track testing has shown a wide range of beneficial results amongst various side skirt designs. Examples of studies or evaluations of side skirts for practical trailer lengths include Cooper and Leuschen (2005), Landman *et al.* (2009), Cooper (2012), Wood (2012b), Burton *et al.* (2013), and Surcel and Provencher (2013). It is unclear whether the differences observed between side-skirt designs are strictly due to the component design or other factors such as the opening between the skirt and the bogie wheels, or the bogie configuration (number of wheels), or the test methodology itself. Other trailer-underbody drag-reduction concepts have also been proposed (Cooper and Leuschen, 2005; Leuschen and Cooper, 2006; Ortega and Salari, 2008) including smoothing the underside and mounting other types of devices, and some technologies are currently on the market to do so. For the current study, the following underbody concepts have been evaluated, with photographs of the concepts shown in Figure 4.15:

- Standard side-skirts (Figure 4.15(a)) - The standard side-skirt for the current study consists of a flat panel flush with the side of the trailer and a tapered leading edge that starts at the landing gear location and ends approximately 2 inches (6 inches full-scale) ahead of the trailer tires. The total skirt length is 2.4 m/94 in (26 ft full-scale).
- Short side-skirts (Figure 4.15(b)) - A variant of the tractor-trailer combination was tested using a 45 inch tractor-trailer gap with the trailer bogie moved forward 2 ft (full-scale). With this configuration, a shorter side-skirt with a length of 2.0 m/79 in (22 ft full-scale) was tested, with its leading edge at the same location as the standard side-skirts, and leaving a 30 inch gap (full-scale) between the skirt and the tires.
- Split side-skirts (Figure 4.15(c)) - In an effort to minimize the skirt-to-tire distance when changing bogie locations, a split-skirt concept has been demonstrated (Wood, 2012b) that consists of a two part skirt. The aft part of the skirt moved with the bogie such that a gap in the skirt is present when the bogie is located further back. A gap of 0.37 m/14 in (4 ft full-scale) was introduced in the standard side-skirt for this test to evaluate the split-skirt concept.
- Extended side-skirts (Figure 4.15(d)) - Many concept trailers show full-length side-skirts that enclose the trailer wheels. This concept was evaluated by extending the standard side-skirt to the aft end of the vehicle with an equivalent taper at the rear as at the leading edge.
- Bogie fairing (Figure 4.15(e)) - Guiding the flow smoothly around the trailer bogie is a concept that has previously been shown to work (Cooper and Leuschen, 2005; Leuschen and Cooper, 2006).
- Belly box (Figure 4.15(f)) - Adding a storage compartment to the bottom of the trailer, similar to a low-bow trailer, may reduce drag by preventing air from being entrained in the underbody.
- Removing/retractible landing gear (Figure 4.15(g)) - The landing gear is a non-streamlined



(a) Standard side-skirts



(b) Short side-skirts (diff. bogie location)



(c) Split side-skirts



(d) Extended side-skirts



(e) Bogie Fairing



(f) Belly box



(g) Smoothed, no landing gear



(h) Diffuser fairing

Figure 4.15: Trailer-underbody drag-reduction configurations.



(a) Tridem axle (b) Tridem axle with short side-skirts

Figure 4.16: Tridem-axle dry-van trailer configurations.

structure protruding below the trailer that, if removed, may provide a drag reduction.

- Smoothed underbody, no landing gear (Figure 4.15(g)) - The supporting structure for the trailer floor provide a rough underbody environment, consisting of many cross-beams. Eliminating these sources of roughness may provide a drag reduction.
- Diffuser fairing (Figure 4.15(h)) - A concept to mitigate the influence of the drive-axle wake in the underbody region has been demonstrated through CFD to provide a significant drag reduction (Ortega and Salari, 2008). This concept introduces a tapered fairing immediately behind the tractor drive-axle wheels to smoothly guide air in the underbody region without generating a large wake from the wheels.

In addition to modifying the trailer underbody region, the influence of the number of trailer axles is expected to have an influence on the vehicle drag and on the benefit of side-skirts. During a road trip between Ottawa and Toronto in the summer of 2014, the author performed an informal survey over a period of approximately 20-30 minutes on a stretch of Highway 401 to identify the proportion of dry-van trailers with a tridem axle (three-axle) arrangement. 31 of 104 dry-van trailers observed were configured with a tridem axle arrangement, with the remaining having a tandem axle (two-axle) arrangement. For the current study, the trailer was configured with a tridem axle arrangement to evaluate the implications of the third axle and the overall layout (6 ft spacing instead of 4 ft used for tandem), as shown in Figure 4.16(a). The short side-skirt was also tested with this arrangement (Figure 4.16(b)), for which the same 6 inch full-scale gap between the skirt and first-axle tire was maintained, as with the standard side-skirt with tandem-axle configuration.

Figure 4.17 presents the measurement results for the various tandem-axle side-skirt concepts, the bogie fairing, and the belly box, with the associated pressure distribution over the centreline of the trailer base shown in Figure 4.18. The standard, short, and split side-skirt all provide nearly identical drag reduction trends and magnitudes, exceeding 10% drag reduction. Although the side-skirts demonstrate a large drag reduction at low yaw angles (order of 0.05), they show the greatest benefits at yaw angles exceeding 4°. The similarity of these results, despite some differences in skirt length, skirt-tire gap width, and solidity of the skirt, indicates that the location and shape of the leading edge of the skirt is a likely dominant con-

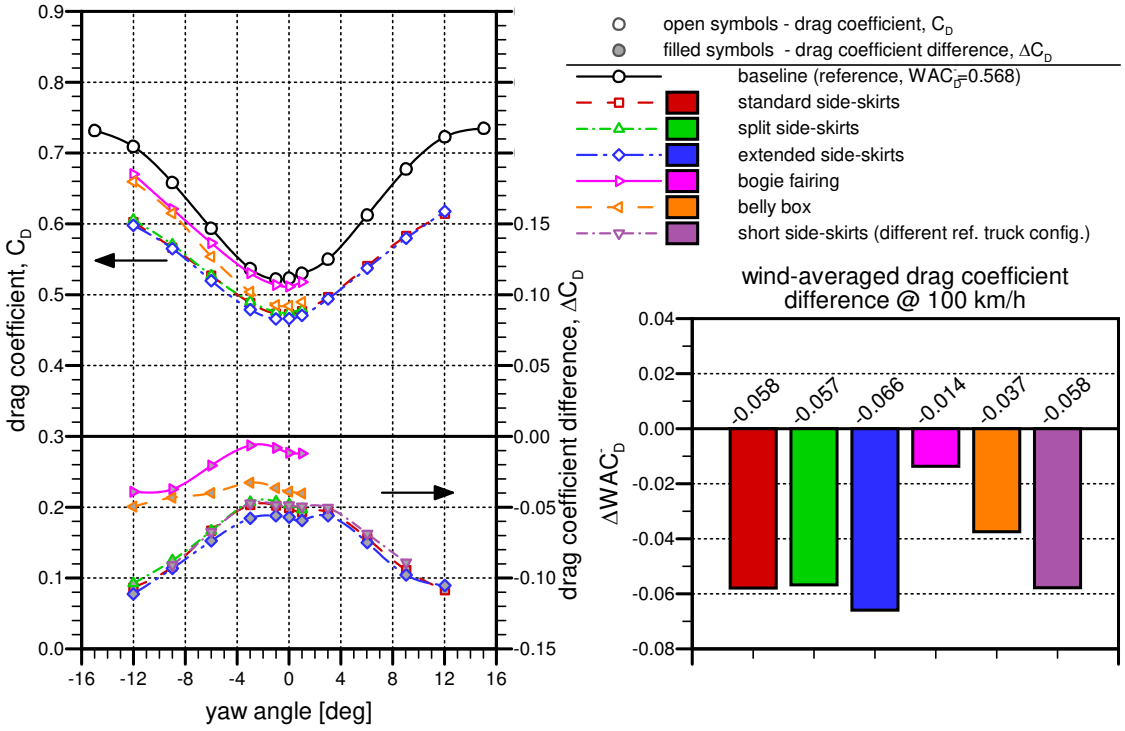


Figure 4.17: Influence of side-skirt configurations, bogie fairing, and belly box for the sleeper-cab tractor with the 53 ft dry-van trailer.

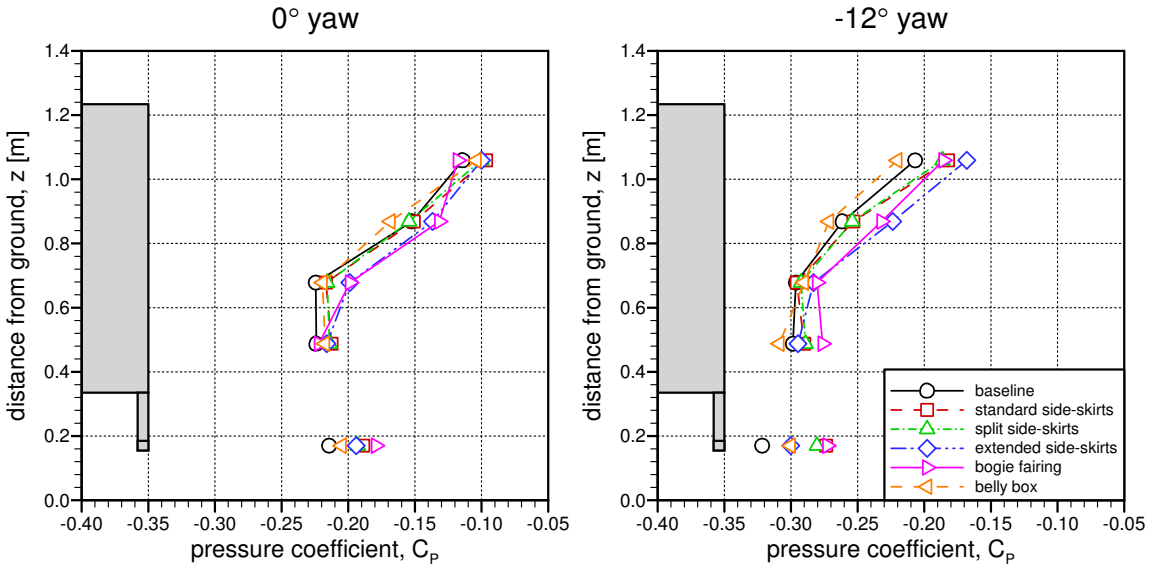


Figure 4.18: Influence of the side-skirts, bogie fairing, and belly box on the trailer centreline base-pressure distributions for the sleeper-cab tractor with the 53 ft dry-van trailer and a 36 inch gap (vertical location of trailer base and impact guard shown as grey outlines).

tribution to the performance of side-skirts. This implies that as long as the flow is redirected along the sides of the trailer, instead of underneath, the drag reduction is significant. It is likely that the leading edge contributes most to the flow split between what enters the underbody region and what is redirected around the trailer bogie. Extending the skirts over the trailer wheels provides an additional reduction in drag, as identified by the increased performance of the extended side-skirts over the standard side-skirts. The pressure measurements of Figure 4.18 show that the side-skirt configurations provide higher pressure at the base of the vehicle, which reduces the resistive force in the direction of motion, hence reducing vehicle drag. In addition to the increase in base pressure, the side-skirt configurations have significantly lower pressure on the front face of the trailer bogie (not shown here) as a result of the air being redirected around the underbody region.

The bogie fairing provides a reduction in drag primarily at higher yaw angles, as seen in Figure 4.17, which limits its benefit in a wind-averaged-drag sense. Although air is still entrained under the trailer, it impinges on the bogie faring which guides the air in a smoother manner around the bogie and wheels than without it. The pressure measurements of Figure 4.18 show, for the bogie fairing, that the pressure is increased over the base of the trailer as it is for the side-skirts configurations. The belly box, on the other hand, shows some regions of lower pressure over the base that would increase the drag force. The belly-box acts in a manner similar to the side-skirts by preventing air from being entrained in the underbody region and impinging on the trailer bogie. It provides a somewhat consistent level of drag reduction over a wide range of yaw angles. The flat and sharp-edged front face of the belly box, is likely a major contributor to why the belly box doesn't perform as well as the side skirts. Pressure measurements from the side of the trailer (not shown here) indicate that the belly box generates greater disturbance to the flow structure on the sides of the vehicle, which in turn influences the base pressure. The increase in base-pressure drag is outweighed by the reduced impingement of air on the trailer bogie, therefore a net benefit is achieved.

Results for the underbody modifications intended to reduce the drag of the underbody components, rather than redirecting flow around it, are shown in Figure 4.19. This includes removing the landing gear, smoothing the underbody, and installing the diffuser fairing. The standard side-skirt data is again shown in Figure 4.19. It is immediately evident that no drag reduction is observed for any of the three concepts, and that a slight increase in drag was measured for each. The diffuser fairing was also tested with the standard side-skirts, and no beneficial interaction was observed. Based on the expectation of a measurable drag reduction from the diffuser fairing, an initial thought was that it was located too far downstream of the aft tractor wheels to adequately guide the wake inwards. It was therefore moved forward approximately 6-7 inches to within 1 inch of the tractor mud flaps, represented by pos. 2 in Figure 4.19. However, this did not provide any improvement. Figure 4.20 shows the influence of these various configurations on the trailer-bogie front face pressures, which provides an indication to why these concepts do not provide any reduction in vehicle drag. For all but removing the landing gear, the modifications intended to reduce the drag on the underbody exhibit higher pressures on the front face of the trailer bogie. It appears that by reducing the resistance to flow in the underbody region, more air is entrained and impinges on the bogie creating an increased drag force on the vehicle. This is observed even for the case with the diffuser fairing and side-skirts, for which higher pressure are observed than with the side-skirts alone.

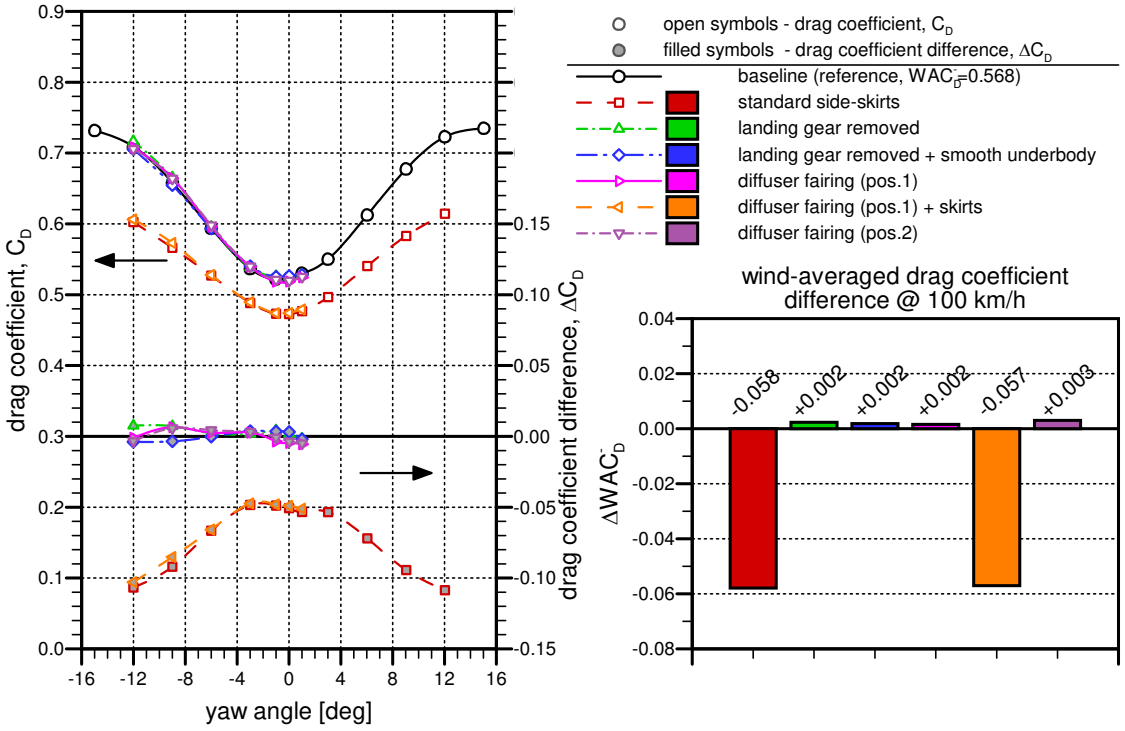


Figure 4.19: Influence of the standard side-skirts, removing the landing gear, smoothing the trailer underbody, and installing the diffuser fairing for the sleeper-cab tractor with the 53 ft dry-van trailer.

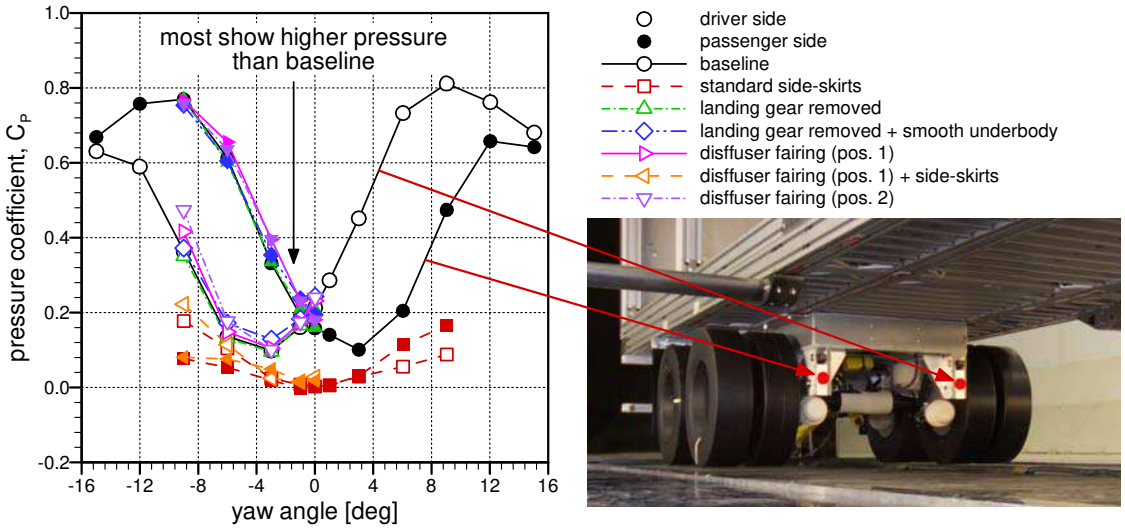


Figure 4.20: Influence of the standard side-skirts, removing the landing gear, smoothing the trailer underbody, and installing the diffuser fairing on trailer bogie face pressures.

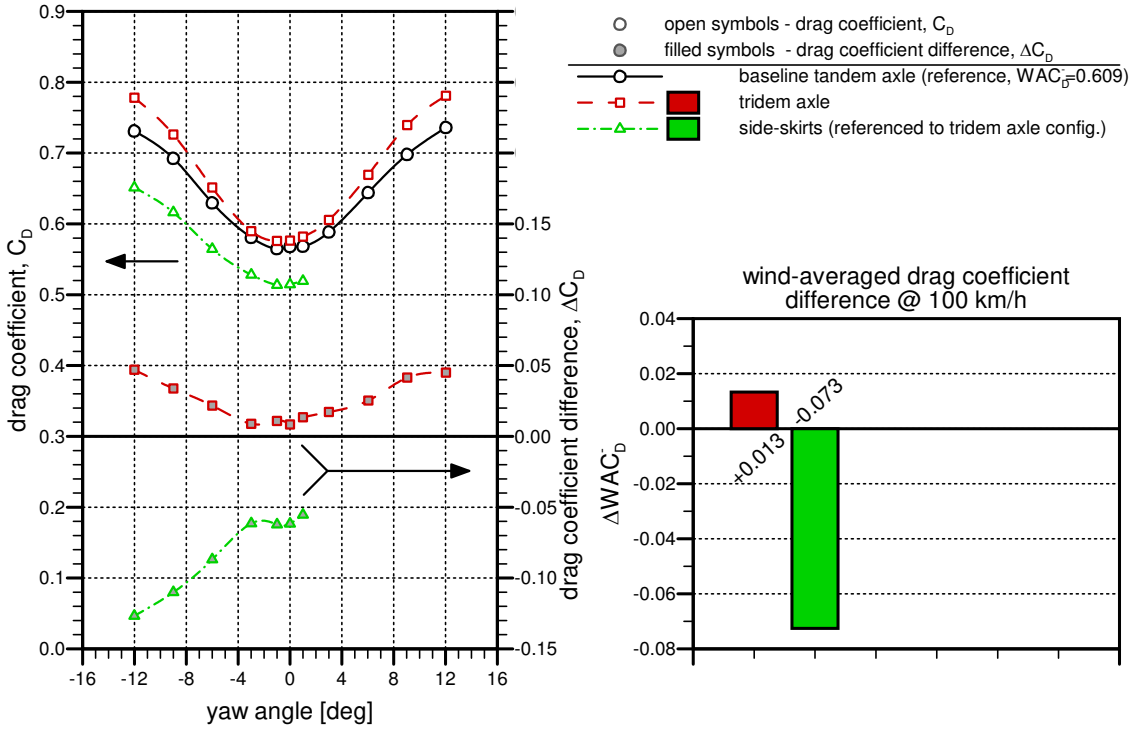


Figure 4.21: Influence of a tridem-axle arrangement and side-skirts for the day-cab tractor with the 53 ft dry-van trailer.

The last underbody concept evaluated was the influence of a tridem-axle arrangement over the more common tandem-axle arrangement for the trailer bogie. Figure 4.21 presents the measurements for the tridem-axle trailer bogie configuration relative to the tandem-axle (baseline), and the influence of side-skirts applied to the tridem-axle arrangement. Higher drag is observed for the tridem-axle arrangement (approximately 2% increase in WAC_D), more so at higher yaw angles, due to greater exposure of the extra wheels as the cross-wind component increases. More than a third of the increase is attributed to the aerodynamic torque of the added wheel set. When the short side-skirts are applied to the tridem-axle configuration, a much higher drag reduction is observed over that for the tandem-axle configuration (ΔWAC_D of -0.073 compared to -0.058).

Of the trailer underbody devices and concepts tested, the various side-skirt configurations provided the highest drag reductions observed. Table 4.3 shows the fuel savings and reduction in CO_2 emissions possible for the various underbody configurations that showed a measurable change in drag, according to the analysis defined in Section 2.5. Apart from the tridem-axle configuration, which is provided to illustrate the increased fuel use and greenhouse gas emissions for such trailers, all the configurations listed shield the trailer bogie and guide the air around this component of the trailer. Of the tandem-axle configurations, the standard side-skirts provide savings on the order of 2,900±800 /tractor/year and 7,700±2,100 kg CO_2/tractor/year. The split and short skirts provide similar levels of fuel savings and

Table 4.3: Fuel savings and greenhouse-gas reduction estimates for trailer underbody configurations (for 125,000±35,000 km/tractor/year @ 100 km/hr).

Baseline Vehicle Configuration	Drag-Reduction Configuration	Drag Change ΔWAC_D	Fuel Rate Savings [l/100km]	Fuel Saved [l]	Fuel Cost Savings [$ @ $1.35/l]	CO_2 Reduction [kg]
sleeper-cab + 36" gap	standard side-skirts	-0.058	2.3	2,900 ± 800	$ 3,900 ± $ 1,100	7,700 ± 2,100
sleeper-cab + 36" gap	split side-skirts	-0.057	2.3	2,800 ± 800	$ 3,800 ± $ 1,100	7,400 ± 2,100
sleeper-cab + 45" gap	short side-skirts	-0.058	2.3	2,900 ± 800	$ 3,900 ± $ 1,100	7,700 ± 2,100
sleeper-cab + 36" gap	extended side-skirts	-0.066	2.6	3,300 ± 900	$ 4,500 ± $ 1,200	8,700 ± 2,400
sleeper-cab + 36" gap	bogie fairing	-0.014	0.6	700 ± 200	$ 900 ± $ 300	1,800 ± 500
sleeper-cab + 36" gap	belly box	-0.037	1.5	1,800 ± 500	$ 2,400 ± $ 700	4,800 ± 1,300
day-cab + 36" gap	tridem-axle bogie	0.013	-0.5	-600 ± 200	$ -800 ± $ 300	-1,600 ± 500
day-cab + 36" gap (tri)	short side-skirts	-0.073	2.9	3,600 ± 1,000	$ 4,900 ± $ 1,400	9,500 ± 2,600

greenhouse-gas reductions. The extended side-skirts provided the greatest drag reduction for the tandem-axle arrangement with a savings of 3,300±900 litres/tractor/year and 8,700±2,400 kg CO_2/tractor/year. As identified in Table 4.3, a tridem-axle trailer requires greater fuel consumption, but the addition of side-skirts to a tridem-axle trailer can provide a savings of 3,600±1,000 litres/tractor/year and 9,500±2,600 kg CO_2/tractor/year.

4.5 Trailer Base Devices

Tapering the back end of a trailer, often referred to as boat-tailing, is a means of streamlining a tractor-trailer combination to reduce drag. Although the concept has been known and understood for decades (Gelzer, 2011), practical ways of implementing the concept have only been introduced over the past decade or so. From an operational standpoint, the base of the trailer is required to maintain the same size for access and loading of cargo. This limits what can be done to the aft end of the trailer. Sets of extension panels that can fold or flip out of the way have been the primary method used for commercial products, although other concepts such as inflatable structures have also been introduced (Leuschen and Cooper, 2006). In December 2013, Transport Canada amended the Canadian Motor Vehicle Safety Standards (CMVSS 223) to allow for greater variety of "boat tail" designs to be used by trucking companies once the provincial regulations are updated.

For the current study, variations on a simple boat-tail concept have been investigated. Figure 4.22 shows the five boat-tail configurations tested. All the concepts use panel angles of 13° which is lower than that used in previous studies by NRC for Transport Canada which was 15°(Patten *et al.*, 2010). A major difference in the concept design used here, compared to previous work performed at NRC, is the lowering of the top panel by 3 inches (full-scale) to leave clearance for trailer lights. This introduces a backward-facing step that, as noted by (Kehs *et al.*, 2013) induces a region of separated flow over the top panel that can influence the drag reduction of the boat-tail. The five concepts are:

- Long 4-panel boat-tail (Figure 4.22(a)) - This concept represents a 4 ft length boat-tail with a lower panel that is raised 1 ft from the bottom edge of the trailer box, similar to concepts on many vehicles in the US;
- Long 3-panel boat-tail (Figure 4.22(b)) - This concept has the same top and side panels as the long 4-panel, without the bottom panel;
- Short 4-panel boat-tail (Figure 4.22(c)) - This concept represents a shorter 2 ft length boat-tail with a lower panel that is mounted at the same location on the trailer base as the long 4-panel concept;
- Tapered 3-panel boat-tail (Figure 4.22(d)) - This concept is similar to the long 3-panel boat-tail, with the side panels tapered from 4 ft at the top to 1 ft at the bottom; and
- Long 4-panel covered boat-tail (Figure 4.22(e)) - This concept is the same as the long 4-panel boat-tail, with a cover to enclose the cavity, that represents an inflatable boat-tail concept.

All five concepts are compliant with the recent amendments to CMVSS 223.

Figure 4.23 shows the drag reduction performance of the five boat-tail concepts, with the sleeper tractor and 36 inch gap as the baseline configuration. The different variations provide a drag reduction between -0.033 and -0.039 (-5.7% to -6.8%), without a significant difference between all five concepts. However, the drag reduction is of a smaller magnitude than anticipated, based on previous work at NRC and by other (Leuschen and Cooper, 2006; Landman



(a) Long 4-panel boat-tail (b) Long 3-panel boat-tail)



(c) Short 4-panel boat-tail (d) Tapered 3-panel boat-tail



(e) Long covered 4-panel boat-tail

Figure 4.22: Trailer-base drag-reduction configurations

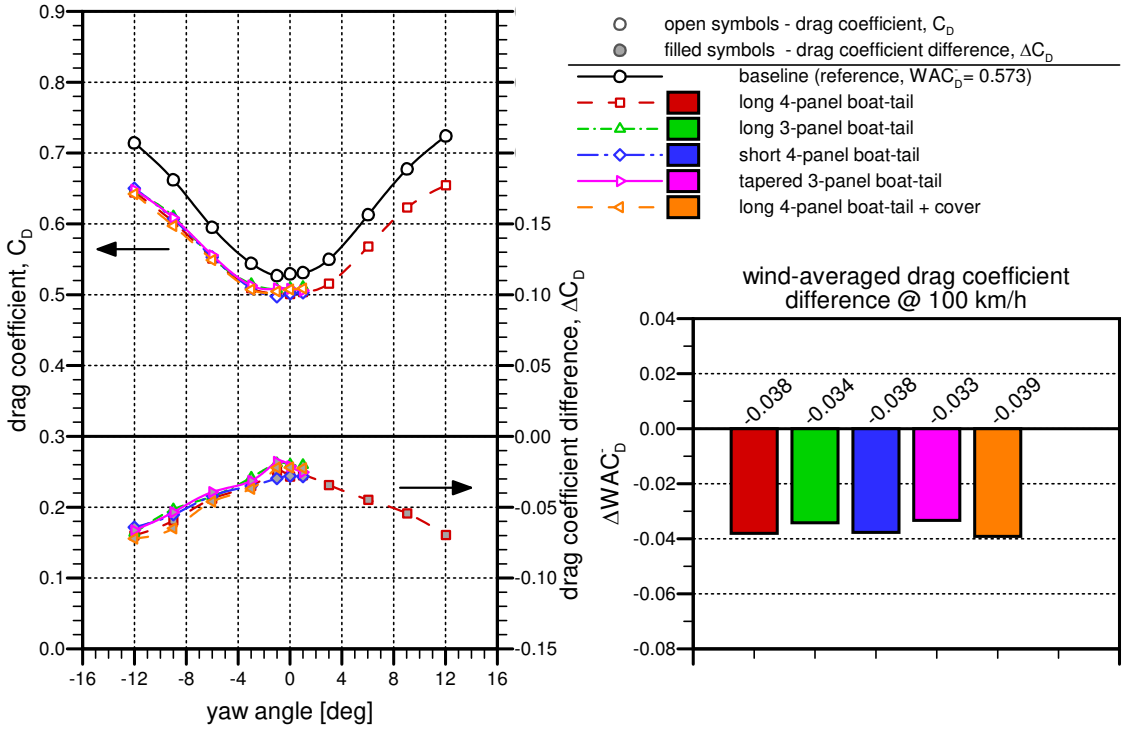


Figure 4.23: Influence of the boat-tails for the sleeper-cab tractor with the 53 ft dry-van trailer.

et al., 2009; Cooper, 2012; Patten *et al.*, 2010; Kehs *et al.*, 2013). Drag reductions on the order of -0.06 have been measured elsewhere. It is possible that the offset between the roof edge and the top panel of the boat-tail (3 inches full-scale in this case) negatively influences the drag-reduction potential of the boat-tails. The negative influence of such an offset has been demonstrated by Kehs *et al.* (2013) for a boat-tail with a smaller offset ($\approx$ 2 inches full-scale) than that used here, whereby the offset introduces a region of reversed flow over part of the top panel that may hinder the potential to draw the wake inwards.

Figure 4.24 shows the centreline pressure distribution over the aft face of the trailer, with and without several boat-tail configurations, for which an increase in the base pressure is observed when a boat-tail is installed. This increase in base pressure reduces the overall front-to-back pressure difference in the direction of motion, leading to a reduced vehicle drag. The long 4-panel boat-tail provides the greatest increase in base pressure, with the 3-panel and short 4-panel boat-tails providing a smaller difference from the baseline configuration. Despite the larger increase in base pressure for the long 4-panel boat-tail, pressurization inside the boat-tail cavity that acts on the inside surfaces of the inward-facing panels provides an added component of drag. This is likely a contributing factor towards the small difference in drag reduction between the short and long boat-tails. Little difference is observed for the drag reduction and the pressure distributions between the long 3-panel and the tapered 3-panel boat-tails, indicating that the size of the side panels do not have a major influence on the boat-tail performance. This correlates well to trends observed in CFD simulations of a

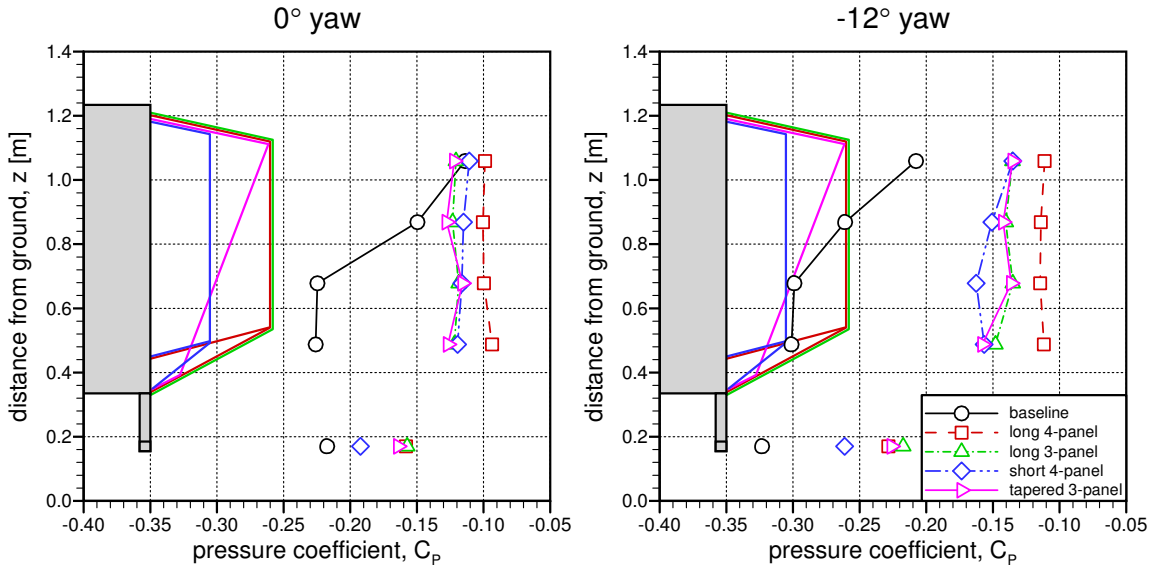


Figure 4.24: Influence of the boat-tails on the trailer centreline base-pressure distributions for the sleeper-cab tractor with the 53 ft dry-van trailer and a 36 inch gap (vertical location of trailer base, impact guard, and boat-tail variants outlined).

Table 4.4: Fuel savings and greenhouse-gas reduction estimates for trailer base configurations (for 125,000±35,000 km/tractor/year @ 100 km/hr).

Baseline Vehicle Configuration	Drag-Reduction Configuration	Drag Change ΔWAC_D	Fuel Rate Savings [l/100km]	Fuel Saved [l]	Fuel Cost Savings [$ @ $1.35/l]	CO_2 Reduction [kg]
sleeper-cab + 36" gap	long 4-panel boat-tail	-0.038	1.5	1,900 ± 500	$ 2,600 ± $ 700	5,000 ± 1,300
sleeper-cab + 36" gap	long 3-panel boat-tail	-0.034	1.3	1,700 ± 500	$ 2,300 ± $ 700	4,500 ± 1,300
sleeper-cab + 36" gap	short 4-panel boat-tail	-0.038	1.5	1,900 ± 500	$ 2,600 ± $ 700	5,000 ± 1,300
sleeper-cab + 36" gap	tapered 3-panel boat-tail	-0.033	1.3	1,600 ± 500	$ 2,200 ± $ 700	4,200 ± 1,300
sleeper-cab + 36" gap	covered long 4-p. boat-tail	-0.039	1.5	1,900 ± 500	$ 2,600 ± $ 700	5,000 ± 1,300

boat-tail-equipped tractor-trailer for another project under the ecoTECHNOLOGY for Vehicles program (McAuliffe, 2014d), where the wake of the truck with a boat-tail was shown to be directed downwards towards the road. This results in a wider wake at ground level than without a boat-tail, and the influence of top panel appeared to provide the greatest contribution to the change in the wake structure that resulted in reduced vehicle drag.

Table 4.4 shows the fuel savings and reduction in CO_2 emissions possible for the various boat-tail configurations, according to the analysis defined in Section 2.5. The 4-panel boat-tails all provide similar savings of 1,900±500 litres/tractor/year and 5,000±1,300 kg CO_2/tractor/year.

4.6 Trailer Upper-Body Shaping and Devices

One of the goals of the current project was to evaluate the drag reduction potential for a dry-van trailer without negatively impacting the cargo volume. The top edges of a typical dry-van trailer consists of sharp edges around which the air must negotiate a sharp turn if it is not adequately directed over the trailer by the tractor. It may be possible to adapt the internal structure in these regions to accommodate a rounded edge without limiting internal volume. In addition, it may be possible to taper the aft edge of the roof without changes to the cargo-carrying capacity. Front-edge rounding and aft-end tapering have been attempted (Surcel and Provencher, 2013) with success demonstrated in a wind tunnel (at 1/15 scale in smooth flow conditions) but not on the road. In cross-wind conditions, rounding the side edges might help guide the wind over the roof in a smoother manner. Commercial vortex generator concepts have also been proposed as a means to reduce the drag of a vehicle, particularly under cross wind conditions, by managing the flow over the upper surface of the trailer and reducing the size of the wake on the downwind side of the vehicle.

Four concepts for reducing the drag of a dry-van trailer through modifications to the roof are shown in Figure 4.25 and described as follows:

- Rounded front edge (Figure 4.25(a)) - The top 6 inches (full-scale) of the front edge was rounded using a 2:1 ellipse shape;
- Rounded side edges (Figure 4.25(b)) - The top 6 inches (full-scale) of the side edges were rounded using a 2:1 ellipse shape;
- Aft roof taper (Figure 4.25(c)) - The aft roof edge was dropped by 6 inches (full-scale) with the surface tapered over a distance of 120 inches (full-scale) with a slope of 2.9°; and
- Roof-mounted vortex generators (Figure 4.25(d)) - Small simple vortex generators were designed and added to the top edge of the trailer roof and were directed outward at an angle of 30°from the direction of vehicle motion. These vortex generators were designed to provide counter-rotating vortices that will allow the bulk flow over the trailer to negotiate better the edge on the downwind side of the trailer under yaw/cross-wind conditions. A series of 34 vortex generators were mounted to edges on each side of the trailer roof at a pitch of approximately 18 inches (full-scale).

In addition, the combination of the three edge treatments (rounded front and side with aft taper) was also tested, as shown in Figure 4.25(e).

The results for the roof modification tests are shown in Figure 4.26. Rounding the front and side edges show no significant difference in the wind-averaged drag coefficient, although the side-edge rounding appears to provide some benefit at the higher yaw angles. The ineffectiveness of the front edge rounded is likely a result of the wind being smoothly guided over the top of the trailer by the tractor fairing. A dry-van trailer paired with a lower tractor may see a benefit from this type of modification. Rounding the side edges modifies the pressure distribution over the aft part of the trailer roof (not shown here), particularly at the higher yaw angles, but does not translate to a significant reduction in vehicle drag. Of the three roof edge modifi-



(a) Rounded front edge



(b) Rounded side edges



(c) Aft roof taper



(d) Vortex generators



(e) Rounded front and side edges with aft taper

Figure 4.25: Trailer roof drag-reduction configurations.

cations, the aft taper is the only one to provide a measurable reduction in wind-averaged drag coefficient (ΔWAC_D = -0.014), and it is most effective for smaller yaw angles. When combining the aft taper with the front- and side-edge rounding, the roof modifications provide a reduction in wind-averaged drag coefficient of ΔWAC_D = -0.020 (3.5%), which is greater than the combination of the individual savings from each (ΔWAC_D = -0.017, 3.0%). This implies that the aft taper likely benefits from the flow modifications made by the rounded side edges.

As shown in Figure 4.26, the roof-mounted vortex generators increase the drag of the vehicle such that ΔWAC_D = +0.005 (+0.9%). The increased drag appears to be consistent at all yaw angles up to $\pm 9^\circ$, above which a small decrease is drag coefficient is observed. This provides ev-

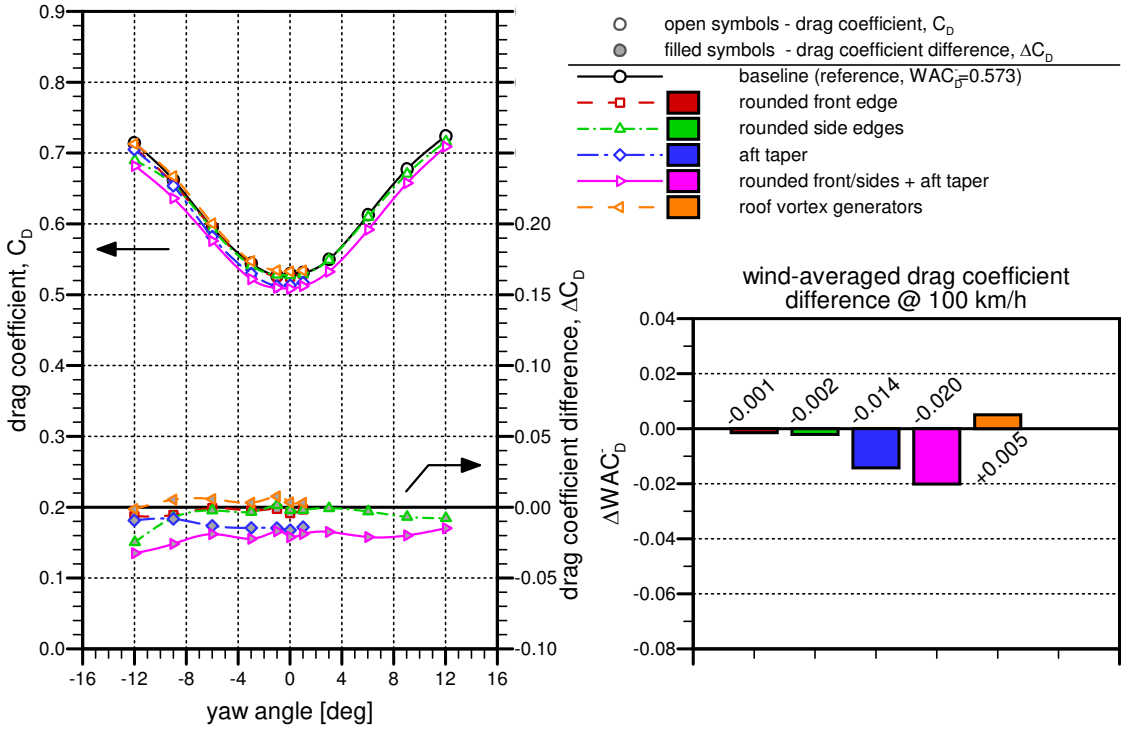


Figure 4.26: Influence of the trailer roof modifications for the sleeper-cab tractor with the 53 ft dry-van trailer.

idence that roof-mounted vortex generators may provide a benefit under strong cross-winds, but higher drag at low yaw angles may preclude their use as a fuel-savings technology.

Table 4.5 shows the fuel savings and reduction in CO_2 emissions possible for the various roof modifications and configurations, according to the analysis defined in Section 2.5. The full roof edge treatment (front and side edges with aft taper) can provide an estimated savings of 1,000±300 litres/tractor/year and 2,600±800 kg CO_2/tractor/year.

Table 4.5: Fuel savings and greenhouse-gas reduction estimates for trailer upper-body configurations (for 125,000±35,000 km/tractor/year @ 100 km/hr).

Baseline Vehicle Configuration	Drag-Reduction Configuration	Drag Change ΔWAC_D	Fuel Rate Savings [l/100km]	Fuel Saved [l]	Fuel Cost Savings [$ @ $1.35/l]	CO_2 Reduction [kg]
sleeper-cab + 36" gap	rounded front edge	-0.001	0.0	0 ± 0	$ 0 ± $ 0	0 ± 0
sleeper-cab + 36" gap	rounded side edges	-0.002	0.1	100 ± 0	$ 100 ± $ 0	300 ± 0
sleeper-cab + 36" gap	aft roof taper	-0.014	0.6	700 ± 200	$ 900 ± $ 300	1,800 ± 500
sleeper-cab + 36" gap	roof front + sides + taper	-0.020	0.8	1,000 ± 300	$ 1,400 ± $ 400	2,600 ± 800
sleeper-cab + 36" gap	roof vortex generators	0.005	-0.2	-200 ± 100	$ -300 ± $ 100	-500 ± 300

4.7 Device Combinations and Interactions

Significant fuel savings have been identified in preceding sections of this report for drag-reduction technologies and methods applied to different regions of a dry-van trailer. Another question addressed in this project was whether combinations of these technologies added to a trailer would yield additive savings, or whether the law of diminishing returns prevails and there are limits to the potential drag reduction. For each region of the trailer, some of the best performing devices have been selected and combinations of them were tested in order to identify whether the individual drag-reduction results are additive or not. For this study, the baseline vehicle consists of the sleeper-cab tractor with a 53 ft equivalent trailer and a 36 inch tractor-trailer gap width. The devices selected for this study were:

- Trailer fairing (Figure 4.7(c));
- Standard side-skirts (Figure 4.15(a));
- Extended side-skirts (Figure 4.15(d));
- Long 4-panel boat-tail (Figure 4.22(a)); and
- Profiled roof (Figure 4.25(e)).

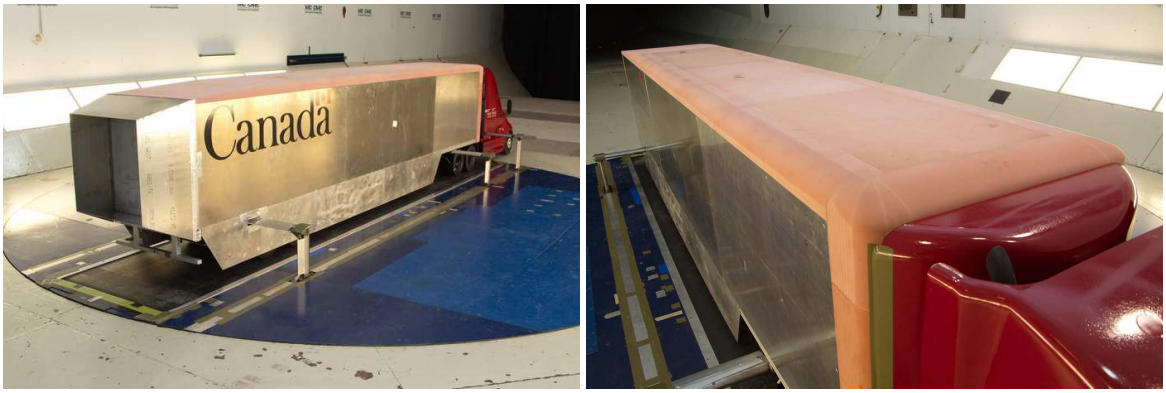
Figures 4.27 and 4.28 show two of the combinations of devices, including one with side-skirts and a boat-tail, and one with treatments to the tractor-trailer gap, the trailer underbody, the trailer base, and the trailer roof.

The drag-reduction results for the various combinations tested are shown in Figure 4.29. Significant drag reductions are observed for all of the combinations tested, all of which show increased benefit with increasing yaw angle. The combinations with three or more devices all have reductions of wind-averaged drag exceeding 20%, with the greatest reduction coming from the configuration with the extended side-skirts, the long 4-panel boat-tail, the trailer fairing, and the profiled roof, providing a ΔWAC_D = -0.153 (26.6% of the baseline drag).

Upon detailed inspection of the drag-reduction results from the various device combinations, it was recognized that some combinations provide a mutual benefit such that the measured drag reduction is greater than the sum of the individual-component measurements. This is similar to what was identified with the combined roof-shaping techniques in Section 4.6. Figure 4.30 illustrates this interaction effect between the different drag-reduction techniques, in which the individual wind-averaged-drag-coefficient reductions are shown as stacked coloured bars next to the grey bars that represent the measurement with the respective combinations. In Figure 4.30, the ΔWAC_D^{int} values represent the added drag-reduction due to the mutually-beneficial interaction between devices or configurations. Combinations of the side-skirts with the trailer fairing or the boat-tail with the trailer fairing appear to be additive, such that there is no measurable interactive benefit or detriment when combining the two respective devices. All the other configurations in Figure 4.30, which consist of some combination of side-skirts and a boat-tail, show a positive mutual interaction in the drag reduction. With the extended side-skirts instead of the standard side-skirts, this interaction effect is more than doubled, providing an interaction benefit of ΔWAC_D^{int} = 0.018 (3% of baseline). The influence of diminishing



Figure 4.27: Truck configuration with standard side-skirts and long 4-panel boat-tail.



(a) Rear view (b) Roof and gap view

Figure 4.28: Truck configuration with trailer fairing, extended side-skirts, long 4-panel boat-tail, and profiled roof.

returns is also seen in this data. For example, when adding the trailer fairing to the side-skirt and boat-tail combination, the interaction benefit is reduced to $\Delta WAC_D^{int} = 0.007$ from 0.010. Also, when adding the profiled roof, the interaction is reduced from $\Delta WAC_D^{int} = 0.018$ to 0.015. This latter effect is likely caused by the fact that the aft roof taper provides a similar change to the flow as does the boat-tail, and therefore the boat-tail does not provide as great an influence on the flow emanating from the roof of the trailer.

To understand better the interactive benefits between the side-skirts and boat-tail, Figures 4.31 and 4.32 show the drag reductions and base-pressure differences when adding side-skirts to various truck configurations. The results in Figure 4.31 clearly show the added benefit when side-skirts are added to a vehicle that has a boat-tail, and that this benefit is predominantly from an interaction at low yaw angles ($\pm 4^\circ$ range). It should be noted here that the skewed ΔC_D curve for the side-skirts with trailer-fairing combination is a result of the different truck locations in the wind tunnel between the gap-device study and the other studies. Figure 4.32 shows the manner in which the standard side-skirts influence the centreline base-pressure distributions for the same four truck configurations. Recall that a higher pressure on the base of

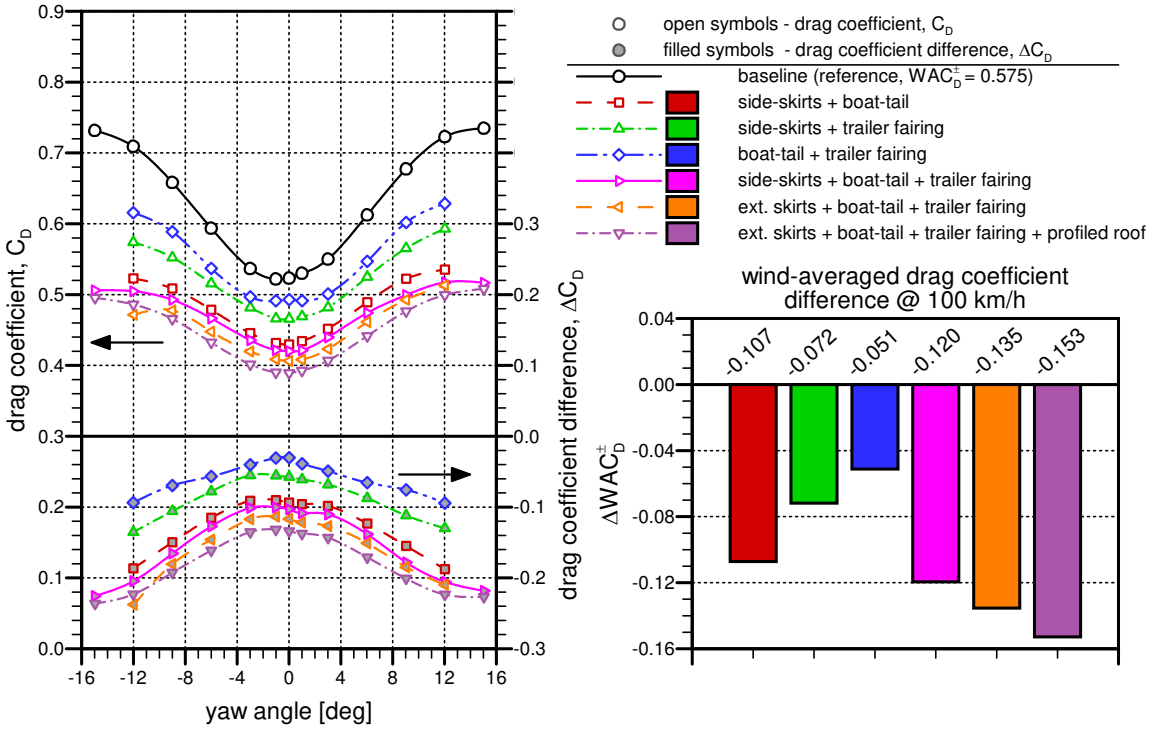


Figure 4.29: Influence of the drag-reduction combinations for the sleeper-cab tractor with the 53 ft dry-van trailer.

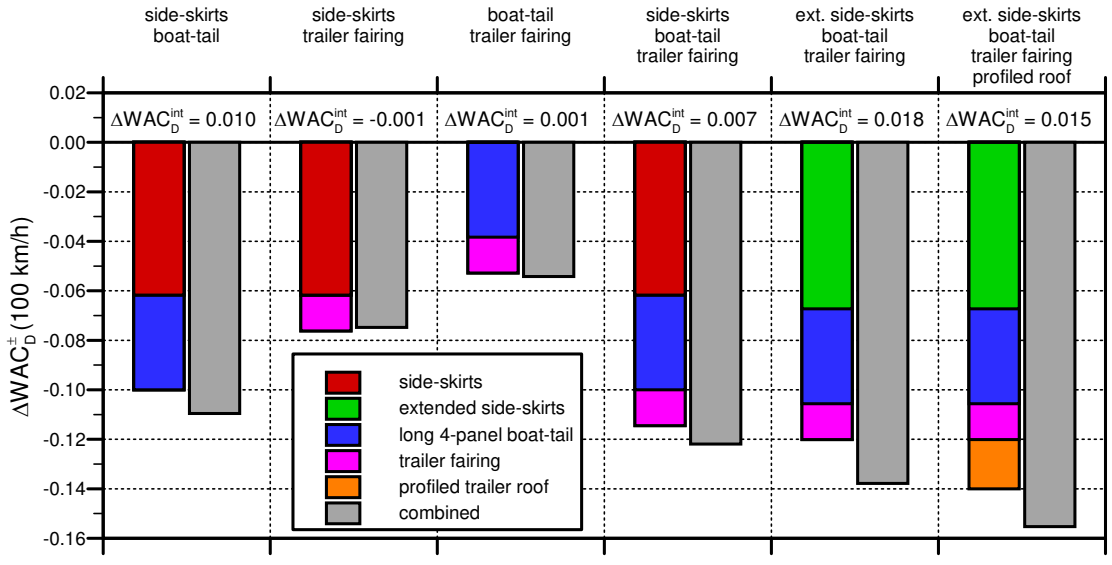


Figure 4.30: Mutual benefits from interactions between drag-reduction combinations.

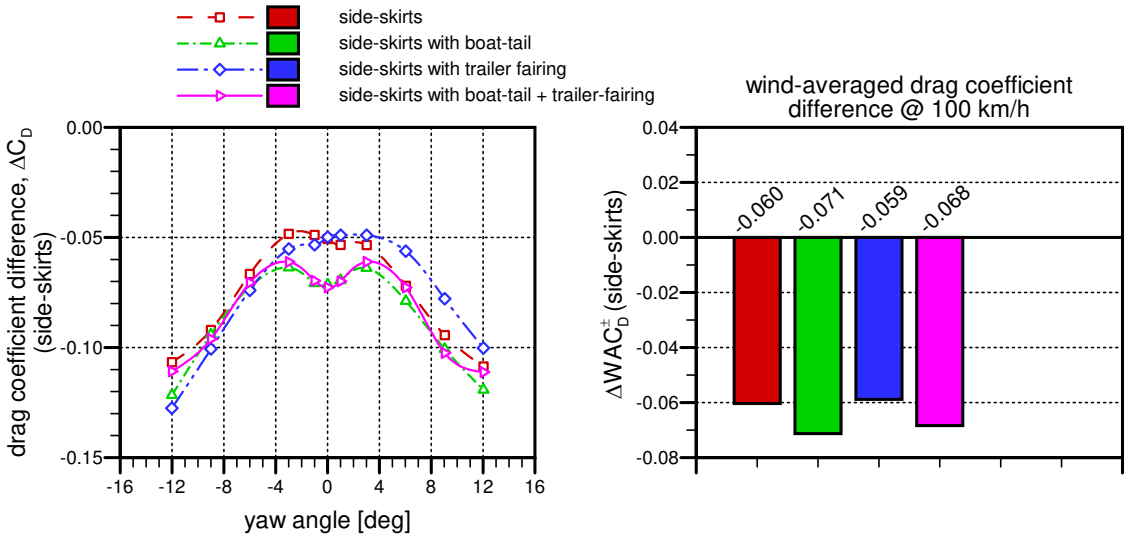


Figure 4.31: Drag-reduction trends for the standard side-skirts with different reference truck configurations.

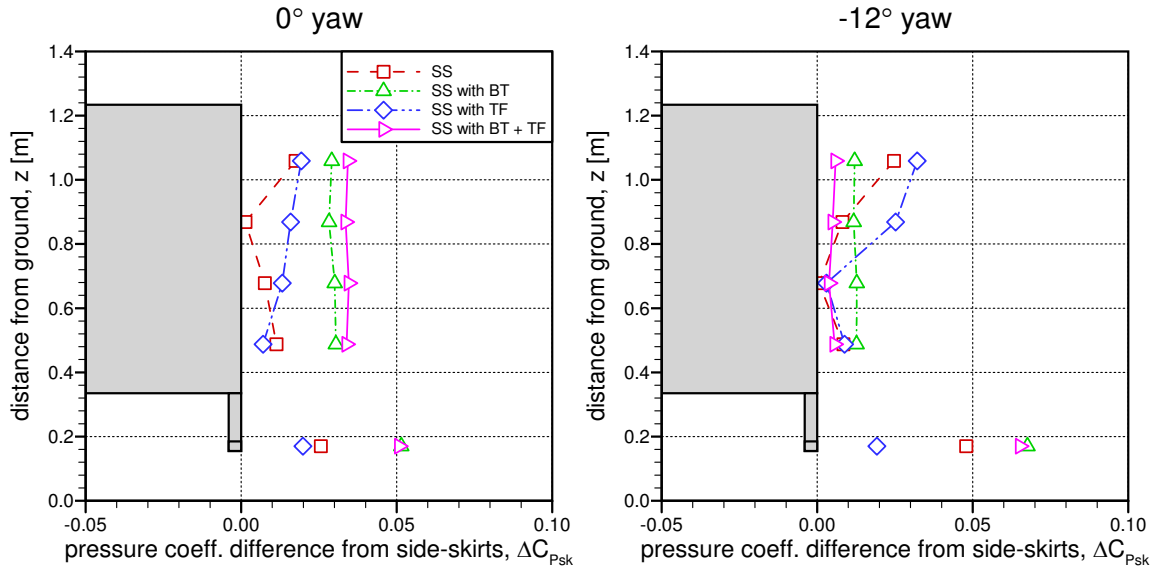


Figure 4.32: Differences in base pressure distribution from the standard side-skirts for different reference truck configurations (vertical location of trailer base and impact guard shown as grey outlines).

the vehicle results in a smaller front-to-back pressure distribution in the direction of motion, and is an indicator of reduced drag. The pressure coefficients presented in Figure 4.32 represent the difference from the respective configuration without the side-skirts. It is evident that at 0° yaw angle the centreline pressure coefficients change by a much greater level when the side-skirts are added to a boat-tail-configured truck. This is also seen to some extent at -12°yaw on the lower part of the trailer base, but the differences are not as distinct as at 0° yaw angle, which is consistent with the changes in drag coefficient shown in Figure 4.31. The greatest differences in the base pressure are observed on the base of the rear-impact guard (lowest data point in Figure 4.32), where the boat-tail configured trucks show a greater influence of side skirts than the non-boat-tail configurations. Although not shown here in graphical format, similar trends are observed in the drag-coefficient distributions and base-pressure distributions if evaluating the influence of the boat-tail added to the various truck configurations. The configurations that have a side-skirt show greater drag-coefficient reductions at low yaw angles that are associated with greater increases in the vehicle base pressure.

Returning to the low-performance of the boat-tail tests described in Section 4.5, many of the studies for which greater drag-reduction was observed from a boat-tail were performed with the boat-tail added to a side-skirt-equipped trailer. With the current data, re-evaluating the side-skirts + boat-tail case using the side-skirt-equipped trailer as reference provides a drag reduction of ΔWAC_D = -0.049 which is 9.5% relative to the side-skirt-based reference value of WAC_D = 0.515. This is in contrast to ΔWAC_D = -0.038 for the long 4-panel boat-tail in Section 4.5, that provides 6.6% reduction relative to the baseline (no-device) configuration. The interactive influence may therefore be a source of uncertainty and discrepancy for aerodynamic performance claims associated with individual components.

As described earlier in this section, significant drag reductions have been achieved with various combinations of techniques. Table 4.6 shows the fuel savings and reduction in CO_2 emissions possible for the various combinations tested with the sleeper-cab tractor and 53 ft-equivalent dry-van trailer, according to the analysis defined in Section 2.5. The standard side-skirt with the long 4-panel boat-tail, which are a common combination especially in California, can provide an estimated savings of 5,300±1,500 litres/tractor/year and 14,000±4,000 kg CO_2/tractor/year. The measurements provided in this section have been referenced to the 36 inch tractor-trailer gap configuration of the truck as tested. If considering a 48 inch gap as the reference, then the combination of a 12 inch reduction in gap width with the trailer fairing, the standard side-skirts, the long 4-panel boat-tail, and the profiled roof, a drag reduction of 29% provides an estimated savings of 8,300±2,300 litres/tractor/year and 21,900±6,100 kg CO_2/tractor/year can be achieved.

Table 4.6: Fuel savings and greenhouse-gas reduction estimates for dry-van drag-reduction combinations (for 125,000±35,000 km/tractor/year @ 100 km/hr), SS - standard side-skirts, ES - extended side-skirts, BT - long 4-panel boat-tail, TF - trailer fairing, PR - profiled roof, ALL = ES + BT + TF + PR.

Baseline Vehicle Configuration	Drag-Reduction Configuration	Drag Change ΔWAC_D	Fuel Rate Savings [l/100km]	Fuel Saved [l]	Fuel Cost Savings [$ @ $1.35/l]	CO_2 Reduction [kg]
sleeper-cab + 36" gap	SS + BT	-0.107	4.2	5,300 ± 1,500	$ 7,200 ± $ 2,000	14,000 ± 4,000
sleeper-cab + 36" gap	SS + TF	-0.072	2.8	3,600 ± 1,000	$ 4,900 ± $ 1,400	9,500 ± 2,600
sleeper-cab + 36" gap	BT + TF	-0.051	2.0	2,500 ± 700	$ 3,400 ± $ 900	6,600 ± 1,800
sleeper-cab + 36" gap	SS + BT + TF	-0.120	4.7	5,900 ± 1,700	$ 8,000 ± $ 2,300	15,600 ± 4,500
sleeper-cab + 36" gap	ES + BT + TF	-0.135	5.3	6,700 ± 1,900	$ 9,000 ± $ 2,600	17,700 ± 5,000
sleeper-cab + 36" gap	ES + BT + TF + PR	-0.153	6.0	7,600 ± 2,100	$ 10,300 ± $ 2,800	20,100 ± 5,500
sleeper-cab + 48" gap	36" gap + ALL	-0.169	6.7	8,300 ± 2,300	$ 11,200 ± $ 3,100	21,900 ± 6,100

4.8 Influence of Tractor Type on Dry-Van Trailer Drag Reduction

One objective of the current study was to examine whether the fuel savings and emissions reductions associated with dry-van-trailer aerodynamic improvements are influenced by the type of tractor. To accomplish this, several configurations of drag-reduction technologies were tested with both the day-cab and sleeper-cab tractor arrangements. The two tractor-model variants were shown in Figure 3.1 on Page 22.

As already highlighted in Section 4.3, some differences in the drag-reduction potential of tractor-trailer-gap devices have been identified for the two tractor configurations. These results are re-examined in Figure 4.33 which shows the data for different gap-width and gap-device combinations with the day-cab and sleeper-cab tractors. In Figure 4.33, each colour represents a different drag-reduction configuration, with the differences between sleeper-cab and day-cab identified by different line type or bar outline colour. The tractor type does not have an influence on tractor-trailer gap-width changes, but has an influence on the performance of the trailer fairing. The trailer fairing provides a greater drag reduction for the day-cab than for the sleeper-cab, but with varying levels of improvement depending on the gap width. This, along with data for other gap devices presented earlier in Section 4.3, provides strong evidence to suggest that the tractor-trailer-gap region is highly influenced by the tractor type.

Several combinations of side-skirts, a boat-tail, and the trailer fairing were tested with both tractor types. These measurements are shown in Figure 4.34, from which is it clear again that drag reductions are greater for the day-cab than the sleeper-cab. For the three combinations shown, the difference in drag reduction between the sleeper-cab and day-cab tractor types vary between ΔWAC_D = 0.006 and 0.023, with higher values measured for configurations with the trailer fairing. This greater drag-reduction for the day-cab tractor when the trailer fairing is installed is also reflected in the data of Figure 4.33. There appears to be a beneficial interac-

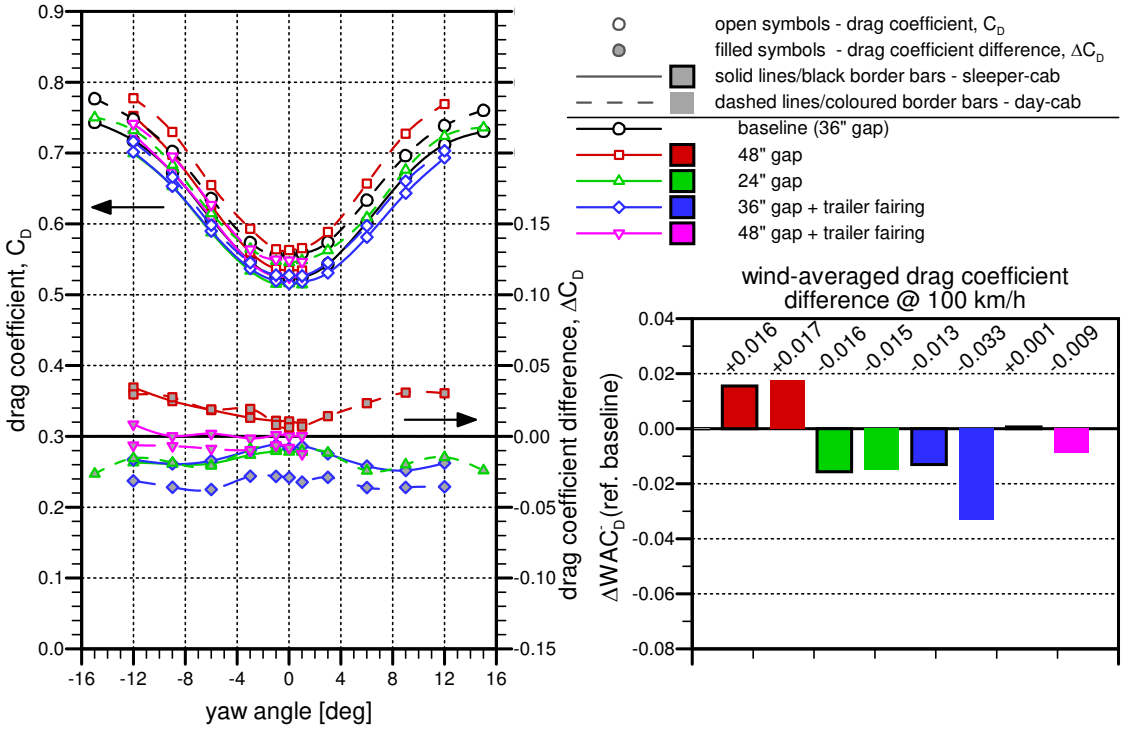


Figure 4.33: Drag reduction measurements for tractor-trailer gap-width and gap-device combinations for the different tractor types.

tion between the trailer fairing and the day-cab tractor that is not present for the sleeper-cab tractor. In examining the surface pressures over the trailer sides and top (not shown here), lower stream-wise pressure gradients are observed for the sleeper-cab near the front of the trailer. This implies that the sleeper-cab conditions and guides the flow over the the tractor-trailer-gap region in a smoother manner than the day-cab, which is a likely cause for the lower sensitivity of the sleeper-cab drag to gap devices.

To contrast the fuel savings and greenhouse-gas reductions possible between the two tractor-types tested, Table 4.7 provides these estimates for the two tractor types with three combinations of drag reduction methods. By reducing the gap width and adding a trailer fairing to the front of the trailer, the day-cab configuration receives an 80% greater benefit than the sleeper-cab (2,500 vs. 1,400 litres fuel savings). With the gap reduced, and with side-skirts and a boat-tail, the day-cab experiences a marginal benefit over the sleeper-cab of approximately 5% (6,400 vs. 6,100 litres fuel savings). For an advanced trailer configuration (extended skirts, boat-tail, trailer fairing) and a reduced gap width, a 15% benefit may be realized by the day-cab over the sleeper-cab tractor (8,600 vs. 7,500 litres fuel savings).

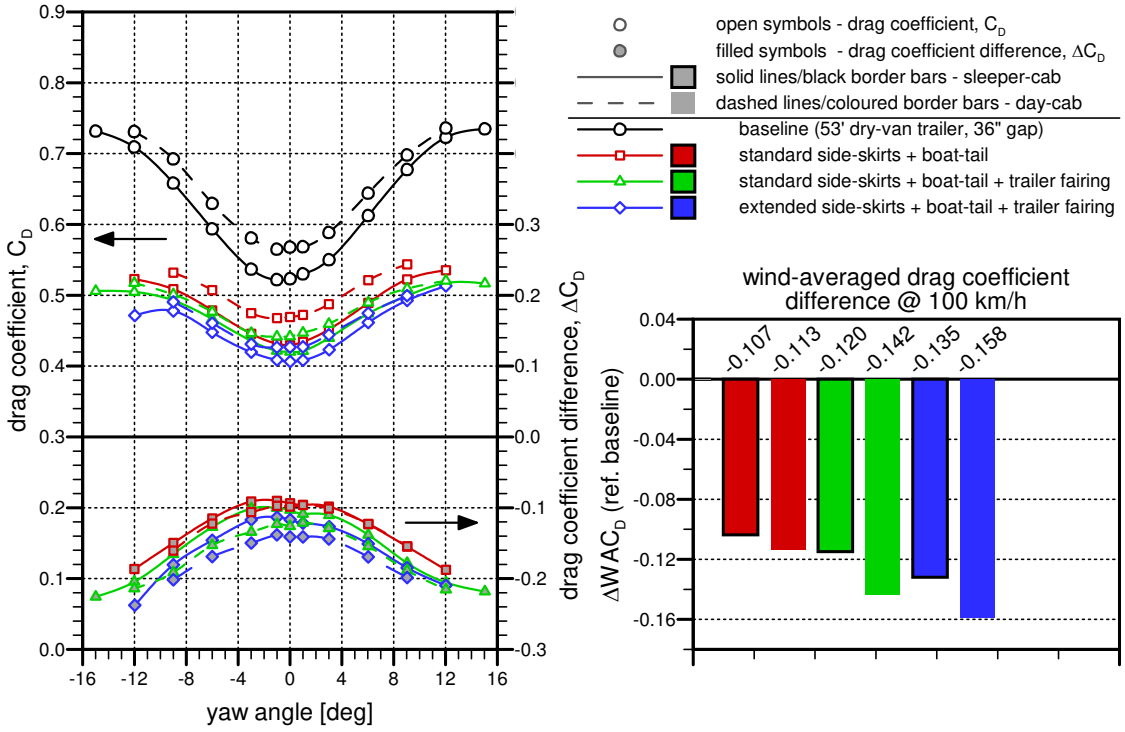


Figure 4.34: Drag reduction measurements for side-skirt, boat-tail, and trailer fairing combinations for the different tractor types.

Table 4.7: Fuel savings and greenhouse-gas reduction comparisons for the different tractor types (for 125,000±35,000 km/tractor/year @ 100 km/hr), SS - standard side-skirts, ES - extended side-skirts, BT - long 4-panel boat-tail, TF - trailer fairing.

Baseline Vehicle Configuration	Drag-Reduction Configuration	Drag Change ΔWAC_D	Fuel Rate Savings [l/100km]	Fuel Saved [l]	Fuel Cost Savings [$ @ $1.35/l]	CO_2 Reduction [kg]
sleeper-cab + 48" gap	36" gap + TF	-0.029	1.1	1,400 ± 400	$ 1,900 ± $ 500	3,700 ± 1,100
day-cab + 48" gap	36" gap + TF	-0.050	2.0	2,500 ± 700	$ 3,400 ± $ 900	6,600 ± 1,800
sleeper-cab + 48" gap	36" gap + SS + BT	-0.123	4.9	6,100 ± 1,700	$ 8,200 ± $ 2,300	16,100 ± 4,500
day-cab + 48" gap	36" gap + SS + BT	-0.130	5.1	6,400 ± 1,800	$ 8,600 ± $ 2,400	16,900 ± 4,800
sleeper-cab + 48" gap	36" gap + ES + BT + TF	-0.151	6.0	7,500 ± 2,100	$ 10,100 ± $ 2,800	19,800 ± 5,500
day-cab + 48" gap	36" gap + ES + BT + TF	-0.175	6.9	8,600 ± 2,400	**$ 11,600 ± $ 3,200**	**22,700 ± 6,300**

4.9 Summary of Dry-Van Trailer Drag-Reduction Results

Numerous drag-reduction technologies and techniques were applied to various regions of a tractor-trailer combination, for a 53 ft dry-van trailer, to evaluate the potential fuel savings and reduction in greenhouse gas emissions. Practical drag reductions exceeding 20% of the wind-averaged drag for 100 km/h ground speed have been identified, which translate to fuel savings on the order of 6,000 litres/tractor/year and reduction in CO_2 emissions on the order of 16,000 kg CO_2/tractor/year.

The key findings from the dry-van-trailer drag-reduction study are:

- Changes to the tractor-trailer-gap width showed a sensitivity of the wind-averaged-drag coefficient to this width of 0.0013/inch (approximately 0.2%/inch) for both the sleeper-cab and day-cab tractor variants. The drag reduction was enabled by a combination of reducing the exposed front surface of the trailer to the wind, particularly in cross-wind conditions, and by reducing the distance between the tractor drive axles and the trailer bogie in the underbody region.
- The trailer fairing was found to be the most beneficial tractor-trailer gap device, providing a drag reduction (ΔWAC_D) between -0.011 and -0.033 (2 to 6%) depending on the gap width and tractor type. The good performance from this device over others tested is attributed to its ability to reduce the drag associated with the gap region without adversely influencing the flow downstream.
- The presence of a refrigeration unit on the front face of the trailer can provide a drag reduction (ΔWAC_D) between -0.004 and -0.017 (0.7 to 3%) depending on the gap width and tractor type.
- A standard side-skirt configuration can provide a drag reduction of ΔWAC_D = -0.058 (10%) by limiting the entrainment of air in the trailer underbody region. Similar drag reductions were observed for the split-skirt and short-skirt concepts tested.
- Reducing the resistance of underbody region by removing the landing gear, smoothing the underbody, or by introducing a diffuser for the tractor-axle wake allows more air to be entrained in the trailer underbody region, causing a small increase in drag.
- The short (2 ft) and long (4 ft) boat-tails show similar drag reductions (ΔWAC_D = -0.033 to 0.039, 5.8 to 6.8%).
- The top panel of a boat-tail provides the most influence on the wake such that tapering the extension of the side panels (long at the top, short at bottom) does not provide a significant decrease in performance.
- A profiled trailer roof can provide drag reduction of ΔWAC_D = -0.020 (3.5%), with the most benefit from tapering the aft surface.
- Mutually beneficial interactions between side-skirts and boat-tails can provide an additional drag reduction beyond the individual component savings. In the current study, an additional 3% drag reduction was observed.

- The performance of some drag reduction technologies were shown to be influenced by the type of tractor, day-cab or sleeper-cab, used to pull a 53 ft dry-van trailer. Wind-averaged-drag measurements showed performance differences for some device combination of up to ΔWAC_D = 0.023 between day-cab and sleeper-cab configurations (>3% of total drag).
- The combination of reducing the gap width by 12 inches, installing a trailer fairing, installing extended side-skirts, installing a boat-tail, and profiling the trailer roof resulted in a drag reduction of ΔWAC_D = -0.169 (29%) that can provide estimated fuel savings of 8,300$\pm$2,300 litres/tractor/year and greenhouse-gas reductions of 21,900$\pm$6,100 kg CO_2/tractor/year.

5. Drag Reduction for Flatbed Trailers

Flatbed trailers are commonly used for hauling large or irregularly shaped cargo which makes the application of standard drag reduction technologies difficult. Changing the tractor-trailer gap may not provide a benefit if the cargo is loaded in a mid or aft location. Gap devices or boat-tails cannot be used due to a lack of surface on which to mount them. Underbody treatments appear to be the most appropriate means to reduce the drag of flatbed trailers with irregular cargo configurations. An added difficulty is the numerous tractor configurations that may be paired with a flatbed trailer.

To evaluate the potential fuel savings and greenhouse-gas reductions for flatbeds, two types of modifications were performed to a sleeper-cab tractor and 53 ft flatbed trailer combination:

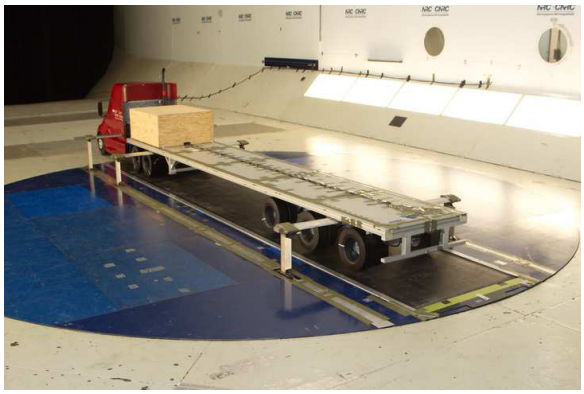
- A change to the tractor roof-fairing height was made to identify the sensitivity of different flatbed cargo configurations to tractor height. This analysis is deferred to Section 7 which deals with tractor-trailer height matching within the context of a broader data set.
- Side-skirts were added to the flatbed trailer for an evaluation of the potential drag reduction with different flatbed cargo configurations. This study was performed with a mid-height roof-fairing for the sleeper-cab tractor which, as will be discussed later in Section 7, provides a better aerodynamic match to the flatbed trailer configurations.

The flatbed model was configured using the tridem-axle wheel arrangement and tested with three cargo configurations that are shown in Figure 5.1:

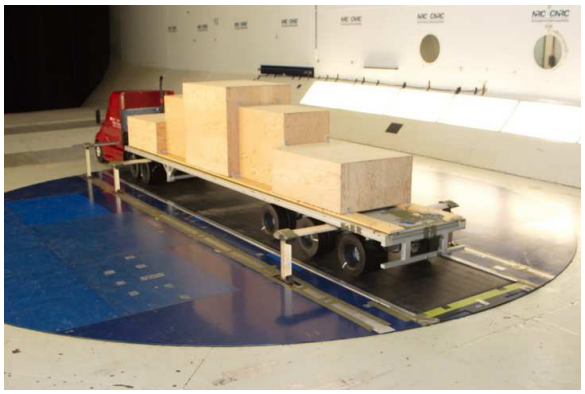
- Empty (Figure 5.1(a)) - only a small box is located at the front end of the tractor to shield on-board instrumentation and cables;
- Box cargo (Figure 5.1(b)) - A series of wooden boxes were built to represent an irregularly-shaped high-drag cargo configuration; and
- Tube cargo (Figure 5.1(c)) - As series of tubes were installed in a low arrangement that may represent large pipes, sewage ducts or rolls of wire/cable.

The same side-skirts tested for the tridem-axle dry-van trailer (Section 4.4) were installed and tested for the three cargo configurations, and are shown in Figure 5.1(d) with the box-cargo arrangement. In addition to using a tridem-axle arrangement that is typical of flatbed trailers, the large stiffeners found on the underbody of most flatbed trailers have been represented by installing two longitudinal I-beams on the trailer-model underbody (shown in Figure 5.2).

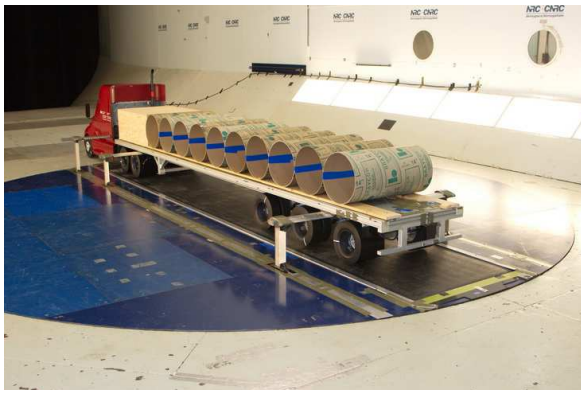
A comparison of the drag characteristics of the three flatbed cargo configurations is shown in Figure 5.3. Note that the mid-height sleeper-cab roof configurations is used for the flatbed data presented here, in contrast to the full-height tractor roof used for the dry-van trailer data set.



(a) Empty flatbed



(b) Box cargo



(c) Tube cargo



(d) Box cargo with side-skirts

Figure 5.1: Test configurations for flatbed-trailer study.



Figure 5.2: Flatbed underbody structure.

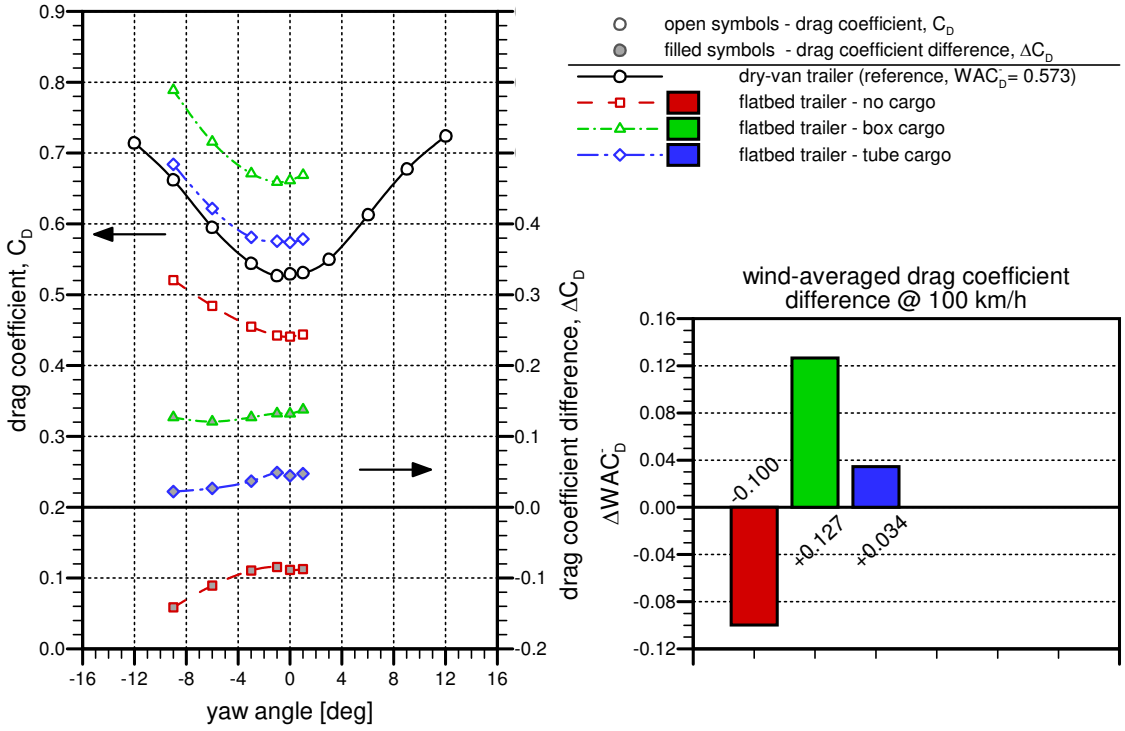


Figure 5.3: Drag characteristics of the flatbed cargo configurations compared to a dry-van trailer configuration (dry-van uses matched high roof sleeper-cab, flatbed uses matched mid-height roof sleeper-cab).

Compared to a standard sleeper-cab + dry-van configuration, the empty flatbed trailer shows significantly lower drag (17% lower), with the box and tube cargo configurations showing higher drag. The box-cargo configuration experiences 22% higher drag than the dry-van configuration as a result of the series of large sharp-edged faces of the boxes exposed to the wind. The tube-cargo configuration shows higher drag than the dry-van, despite it being half the height. The edges and cavities of the tubes provide a large source of drag, and were seen to deform and buffet a lot during the tests.

Adding side-skirts to the flatbed configurations is beneficial, but the magnitude of the drag reduction depends on the cargo configuration. This is shown in Figure 5.4, in which the drag reductions due to the side-skirts for each configuration is calculated with respect to the equivalent no-skirt configuration. The side-skirts provide a similar level of drag reduction for the empty and tube-cargo flatbeds, with ΔWAC_D = -0.036 and -0.032, respectively. The variation in ΔC_D with yaw angle is similar for these two configurations as well. Due to the different absolute drag values for each, these drag reductions represent percentage changes in drag of 8% and 5% for the empty and tube cargo configurations, respectively. The box cargo shows the largest reduction in drag due to the side-skirts with ΔWAC_D = -0.036 which translates to 8%. This configuration shows a greater change in ΔC_D with yaw angle than the empty and tube-cargo configurations, which is likely a result of the larger height of the box cargo that, in

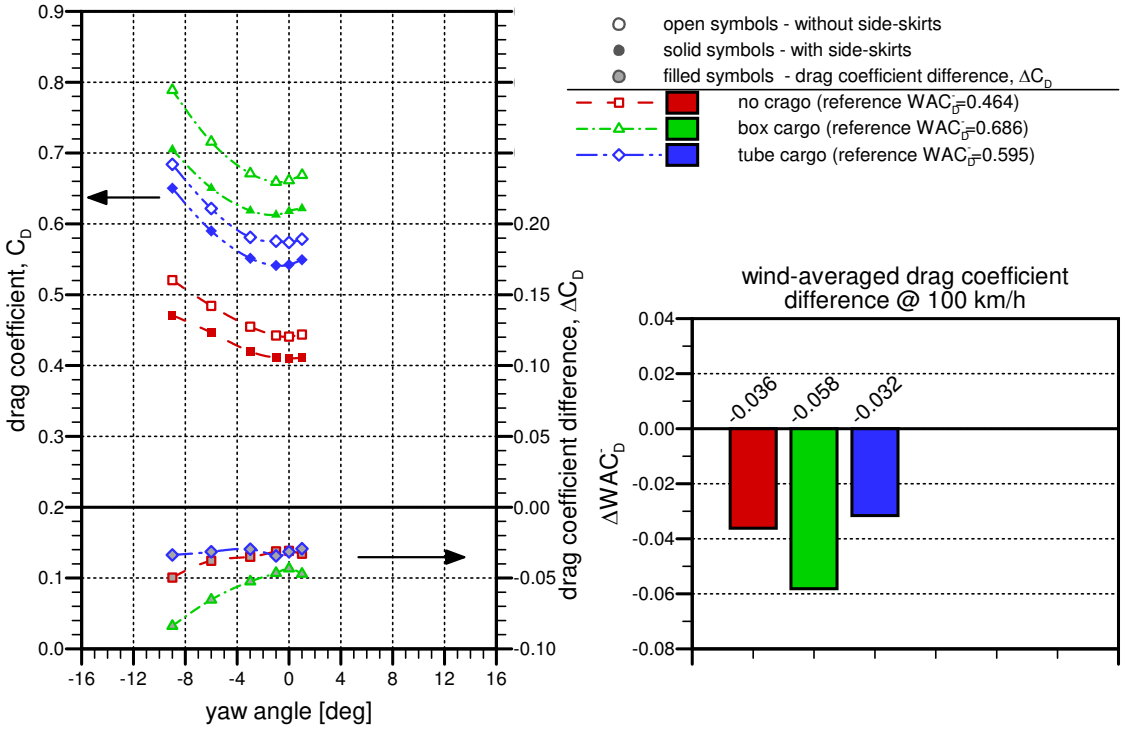


Figure 5.4: Influence of side-skirts on the drag characteristics of the flatbed trailer configurations.

the absence of skirts, would direct more air under the trailer than would the low cargo. The drag reductions observed with side-skirts for the three flatbed configurations do not provide the same benefit as they do for a dry-van trailer. For the equivalent tridem-axle dry-van trailer arrangement, the drag reduction from the side-skirts was ΔWAC_D = -0.077 (see Section 4.4).

Table 5.1 shows the fuel savings and reduction in CO_2 emissions possible for the three flatbed configurations, according to the analysis defined in Section 2.5. The maximum savings attained was for the box-cargo configuration for which side-skirts can provide an estimated savings of 2,900±800 litres/tractor/year and 7,700±2,100 kg CO_2/tractor/year.

Table 5.1: Fuel savings and greenhouse-gas reduction comparisons for the side-skirts applied to different flatbed-trailer configurations (for 125,000±35,000 km/tractor/year @ 100 km/hr).

Baseline Vehicle Configuration	Drag-Reduction Configuration	Drag Change ΔWAC_D	Fuel Rate Savings [l/100km]	Fuel Saved [l]	Fuel Cost Savings [$ @ $1.35/l]	CO_2 Reduction [kg]
empty flatbed	side-skirts	-0.036	1.4	1,800 ± 500	$ 2,400 ± $ 700	4,800 ± 1,300
box cargo on flatbed	side-skirts	-0.058	2.3	2,900 ± 800	$ 3,900 ± $ 1,100	7,700 ± 2,100
tube cargo on flatbed	side-skirts	-0.032	1.3	1,600 ± 400	$ 2,200 ± $ 500	4,200 ± 1,100

6. Drag Reduction for Long Combination Vehicles

With the prevalence of long combination vehicles (LCVs) such as tandem 53 ft trailers appearing on some Canadian roads, where permitted by provincial/territorial authorities, the trailer-trailer gap provides an additional source of aerodynamic drag that can be treated to reduce fuel consumption and greenhouse-gas emissions. Due to the inability to test a tandem 53 ft trailer combination because of its length relative to the turntable diameter, a tandem 28 ft configuration was tested to examine the influence of the best-performing concepts from the tractor-trailer-gap study, but applied to the trailer-trailer gap. The trailer connection is configured similar to an A-train arrangement that uses a converter dolly to link the two trailers, as shown in Figure 6.1, rather than the fifth-wheel arrangement of a B-train. However, here the rigid connection is made through the lower part of each trailer to ensure model rigidity. The results presented here are therefore representative of what might be attainable with a tandem trailer configuration, and provide guidance towards what may be appropriate for a real vehicle.

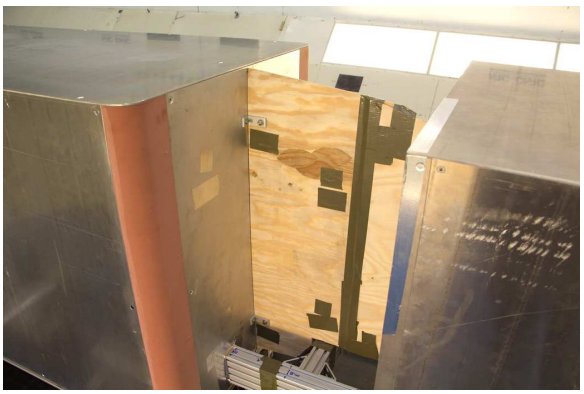
Figure 6.2 shows some of the LCV configurations and devices tested. As with the tractor-trailer gap, it was anticipated that reducing the width of the trailer-trailer gap would reduce the vehicle drag. The baseline gap width used was 5 ft, and this configuration is shown in Figure 6.2(a). A gap width of 3 ft was also tested. Based on the results of the gap-device tests



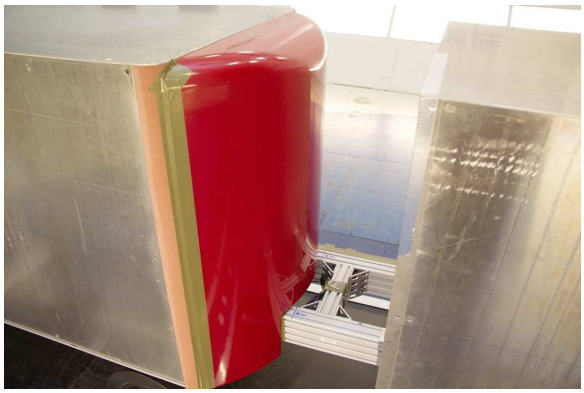
Figure 6.1: A-train type connection between tandem 28 ft trailers.



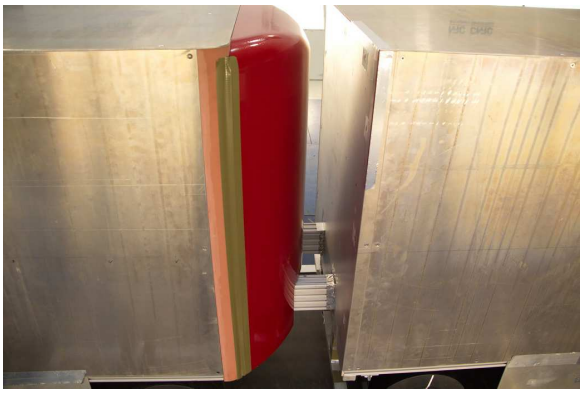
(a) Baseline LCV with 5 ft gap



(b) Plate seal in trailer-trailer gap



(c) trailer fairing in 5 ft trailer-trailer gap



(d) trailer fairing in 3 ft trailer-trailer gap



(e) LCV with Trailer Aero Package (TAP)

Figure 6.2: Test configurations and trailer-trailer-gap devices for long-combination vehicle study.

described in Section 4.3, the trailer fairing and the full plate seal were selected as concepts to test in the trailer-trailer gap. These are shown mounted in the trailer-trailer gap in Figures 6.2(b) and 6.2(c). The trailer fairing mounted in the shorter 3 ft gap is also shown, in Figure 6.2(d). The addition of an aerodynamic treatment package to the rest of the trailer combination was also examined, as shown in Figure 6.2(e). The Trailer Aero Package (TAP), as defined here, consists of a trailer fairing mounted in the forward tractor-trailer gap, side-skirts applied to both trailers, and the long 4-panel boat-tail installed on the aft face of the rear trailer.

In Section 3, the drag characteristics of the tandem 28 ft trailer combination with a 5 ft trailer-trailer gap width was shown to provide an increase in the wind-averaged-drag coefficient of 13% over that of the 53 ft dry-van trailer. The tandem 28 ft trailer combination is not much longer than the 53 ft dry-van trailer (8 ft longer), and therefore the majority of the drag difference likely results from the trailer-trailer gap and from the two extra wheel axles.

The drag-reduction potential for treatments to the trailer-trailer gap are shown in Figure 6.3. The three primary techniques chosen to reduce drag associated with the gap are the full plate seal, the trailer fairing, and reducing the gap width by 2 ft. The plate seal and the trailer fairing show the same magnitude of drag reduction (ΔWAC_D = -0.029) with same variation of ΔC_D with yaw angle. This is in contrast to what was observed for the tractor-trailer gap region (Section 4.3) for which the trailer fairing out-performed the full plate seal for both tractor

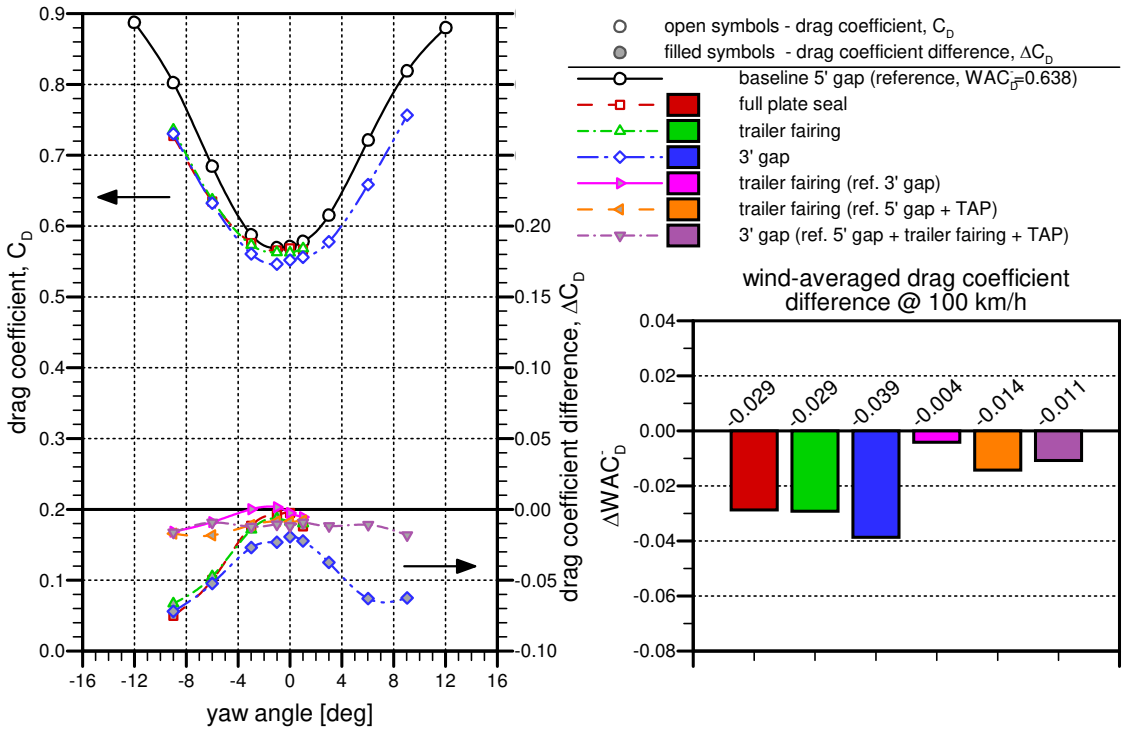


Figure 6.3: Drag characteristics of the tandem 28 ft trailer configuration with trailer-trailer gap changes and gap devices.

variants at different gap widths. In the trailer-trailer gap, these devices show no influence at zero yaw angle and their benefit is observed at higher yaw angles. Closing the gap from 5 ft to 3 ft provides the largest drag reduction (ΔWAC_D = -0.039), using the 5 ft gap as a baseline. To identify any limits or added benefits from combinations of techniques, the other three configurations for which data is presented in Figure 6.3 represent such combinations. The effect of the trailer fairing is shown when placed in the 3 ft trailer-trailer gap and when placed in the 5 ft gap when aerodynamic treatments have been applied elsewhere on the trailer (with the TAP). In both of these cases, the performance of the trailer fairing is lower than when placed in the baseline-vehicle 5 ft gap. This is similar for the influence of closing the gap from 5 ft to 3 ft when the trailer fairing is mounted in the gap and the TAP is installed on the full vehicle. These results show that there are limits to what can be combined to reduce drag associated with the trailer-trailer gap of a long combination vehicle.

To evaluate the potential benefits of full treatment to the trailer and the gap region, the TAP was installed and tested with different combinations of the trailer-trailer gap techniques. Figure 6.4 shows the drag reductions for three such combinations compared to the baseline vehicle with a 5 ft gap. The TAP provides a drag reduction of ΔWAC_D = -0.134 to the overall vehicle (21%). When adding the fairing to the gap the drag reduction is ΔWAC_D = -0.148 (23%) and further reducing the gap to 3 ft provides an overall drag reduction of ΔWAC_D = -0.159 (25%). As previously noted, the individual gains from these changes are not additive.

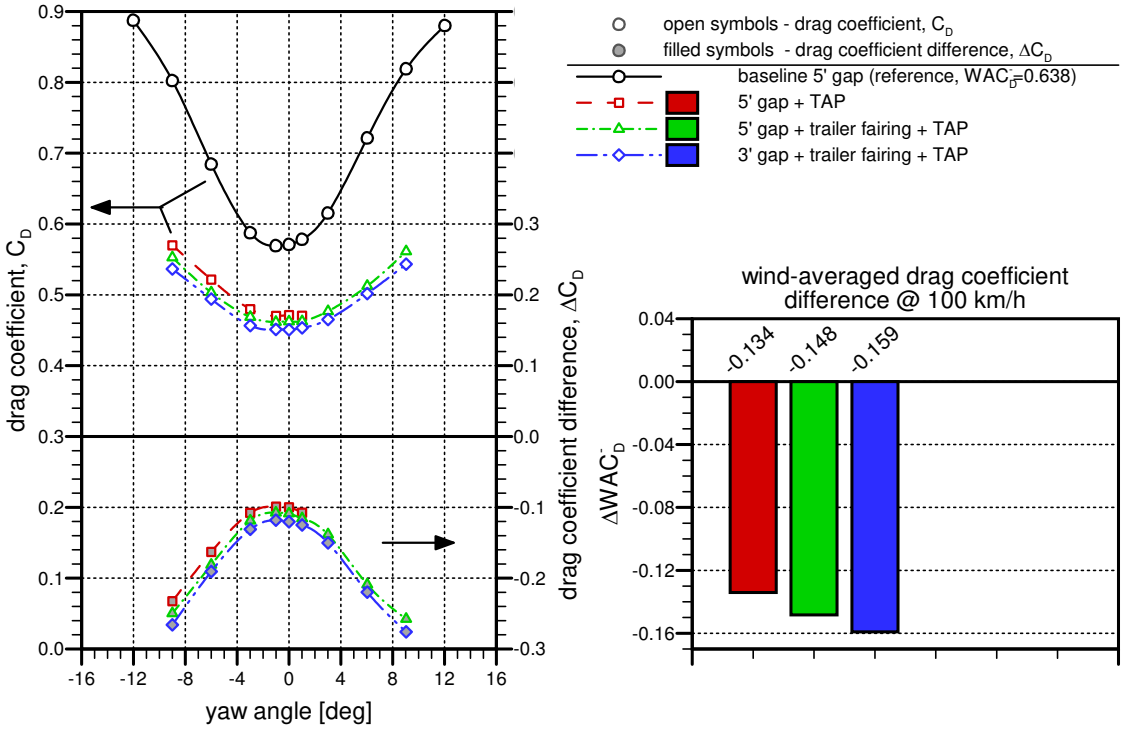


Figure 6.4: Influence of full-vehicle aerodynamic treatments to the tandem 28 ft trailers (TAP - Trailer Aero Package = front trailer fairing, side-skirts, rear trailer boat-tail).

Table 6.1: Fuel savings and greenhouse-gas reduction comparisons for the side-skirts applied to different flatbed-trailer configurations (for 125,000±35,000 km/tractor/year @ 100 km/hr).

Baseline Vehicle Configuration	**Drag-Reduction Configuration**	**Drag Change** ΔWAC_D	**Fuel Rate Savings [l/100km]**	**Fuel Saved [l]**	**Fuel Cost Savings [$ @ $1.35/l]**	**CO_2 Reduction [kg]**
5ft trailer gap	trailer fairing	-0.029	1.1	1,400 ± 400	$ 1,900 ± $ 500	3,700 ± 1,100
5ft trailer gap	full plate seal	-0.029	1.1	1,400 ± 400	$ 1,900 ± $ 500	3,700 ± 1,100
5ft trailer gap	3 ft gap	-0.039	1.5	1,900 ± 500	$ 2,600 ± $ 700	5,000 ± 1,300
5ft trailer gap	TAP	-0.134	5.3	6,600 ± 1,900	$ 8,900 ± $ 2,600	17,400 ± 5,000
5ft trailer gap	3 ft gap + faring + TAP	-0.159	6.3	7,900 ± 2,200	$ 10,700 ± $ 3,000	20,900 ± 5,800

An additive benefit would provide a drag reduction of ΔWAC_D = -0.202, which has not been demonstrated.

Table 6.1 shows the fuel savings and reduction in CO_2 emissions possible for some of the combinations of trailer-trailer-gap treatments and the TAP, according to the analysis defined in Section 2.5. The maximum savings attained was for the reduced gap width, the trailer fairing, and the TAP which can provide an estimated savings for an LCV of 7,900±2,200 litres/tractor/year and 20,900±5,800 kg CO_2/tractor/year.

7. Aerodynamic Matching of Tractor and Trailer Height

Tractor roof fairings, particularly those for sleeper tractors, are generally designed for matching with a standard dry-van trailer, however many other tractor and trailer types with different heights are found on the road. For example, low- or mid-height tractors are used with tanker trailers or flatbed trailers. Day-cab tractors often don't have roof fairings or sometimes simple deflectors are used. It is well known that a low tractor roof with a high trailer exhibits much higher drag than a properly paired fairing. This is what led to the roof fairing becoming one of the earliest drag reduction devices for heavy trucks. Questions are periodically posed regarding the usefulness of full-height tractor fairings with lower trailers, and whether there may be sufficient fuel savings associated with pairing a lower tractor with a lower trailer. To address this question, several tractor roof configurations were tested with various trailer configurations to identify the sensitivity of mismatching tractor and trailer heights. The configurations tested include:

- Three day-cab roofs with a full-height dry-van trailer;
- Three day-cab roofs with a half-height dry-van trailer;
- Two sleeper-cab roofs with a full-height dry-van trailer;
- Two sleeper-cab roofs with a half-height dry-van trailer; and
- Two sleeper-cab roofs with three flatbed configurations.

The half-height trailer is a shorter version of the 53 ft dry-van trailer model, and is shown in Figure 7.1. The height of this trailer was matched to the low-roof no-fairing day-cab tractor variant. In order to optimize the wind-tunnel test program, the full-height and half-height dry-



Figure 7.1: Half-height 53 ft dry-van trailer model with tridem-axle arrangement, paired with the day-cab tractor without a roof fairing.

van trailer tests presented here for the day-cab tractor were performed with the tridem-axle arrangement. The tandem-axle arrangement was used for the sleeper-cab roof-change tests with the full-height trailer, and the tridem-axle setup was used for the equivalent sleeper-cab + half-height dry-van trailer tests.

The three day-cab tractor configurations with the full-height 53 ft dry-van trailer are shown in Figure 7.2 and the corresponding test results are presented in Figure 7.3. As expected, the drag of the tractor-trailer combination increases as the roof deflector is simplified or removed, with an increase in wind-averaged-drag coefficient of ΔWAC_D = +0.110 (18%) when completely removed. The drag coefficient for the deflector-fairing configuration shows a greater sensitivity to yaw angle than the full-height or no-fairing cases. This is likely caused by an interaction of the wake of the deflector panel with the flow around the upper front face of the trailer. Despite this, the deflector fairing provides an improvement over the no-fairing case.

The three day-cab tractor configurations with the half-height 53 ft dry-van trailer are shown in Figure 7.4 and their corresponding test results are presented in Figure 7.5. It is to be noted that the reference vehicle configuration for this data set corresponds to the "well-matched" tractor-trailer combination, that being the low-roof/no-fairing tractor with the half-height trailer. Here, adding a roof fairing increases the drag of the vehicle. The deflector fairing causes the greater increase in drag of the two fairing shapes, resulting in an increase in wind-averaged-drag coefficient of ΔWAC_D = +0.204, which is 43% of the baseline drag level for the no-fairing case. The full-height fairing generates an increase of ΔWAC_D = +0.109 which is equivalent to the increase observed in Figure 7.3 when removing this fairing from the full-height trailer case.

Only two roof-fairing configurations were tested for the sleeper cab, one being the full-height fairing and the other being a mid-height fairing, and samples of them paired with different trailer configurations are shown in Figure 7.6. Although low-roof sleeper cabs are available, they are not as common as the variants represented here. To assess the implication of changing the sleeper-cab roof fairing, the data for all five trailer configurations with which these were paired are presented in Figure 7.7. In this figure, the drag differences represent the difference when changing from the full-height fairing to the mid-height fairing. For the full-height dry-van trailer, lowering the tractor roof increases the wind-averaged-drag coefficient by ΔWAC_D = +0.113 which is of similar magnitude to removing the fairing from the equivalent day-cab configuration. For the half-height trailer and the three flatbed cargo configurations, reducing the tractor roof height provides a decrease in drag, even for the box-cargo configuration that has the same maximum height as the full-height dry-van trailer, although this maximum height is positioned further back. This box-cargo configuration shows the benefit of the mid-height fairing is experienced at yaw angle exceeding about 3°, whereas the other low-height trailers show benefits at all yaw angles.

The data presented in this section shows that using a full-height fairing with a low dry-van trailer provide as great an increase in drag, over the properly-matched configuration, as does removing the same full-height fairing from a tractor paired with a full-height dry-van trailer. Improper matching of such configurations can generate much greater fuel waste than the best combinations of drag reduction technologies can provide. Table 7.1 shows the changes in fuel use/cost and changes in CO_2 emissions estimated for some of the combinations of tractor-



(a) Full-height fairing (b) Deflector fairing (c) No fairing

Figure 7.2: Day-cab roof-fairing configurations with the full-height dry-van trailer.

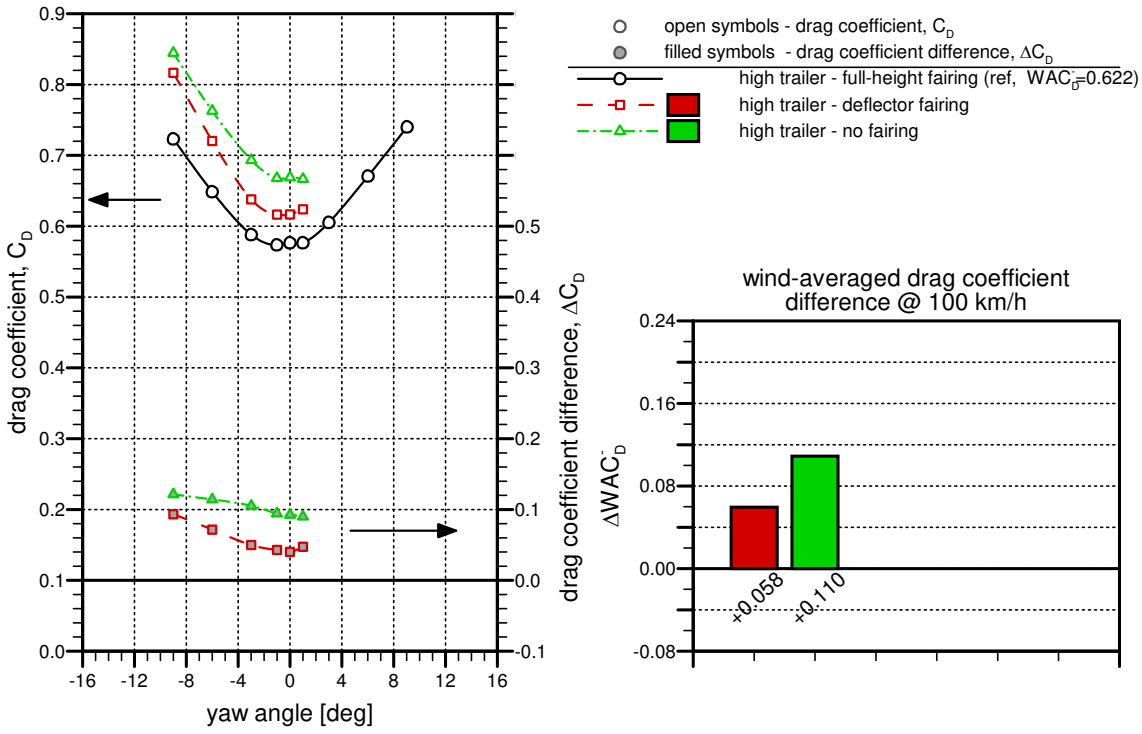


Figure 7.3: Drag characteristics of the day-cab roof-fairing configurations with the full-height dry-van trailer.



(a) Full-height fairing (b) Deflector fairing (c) No fairing

Figure 7.4: Day-cab roof-fairing configurations with the half-height dry-van trailer.

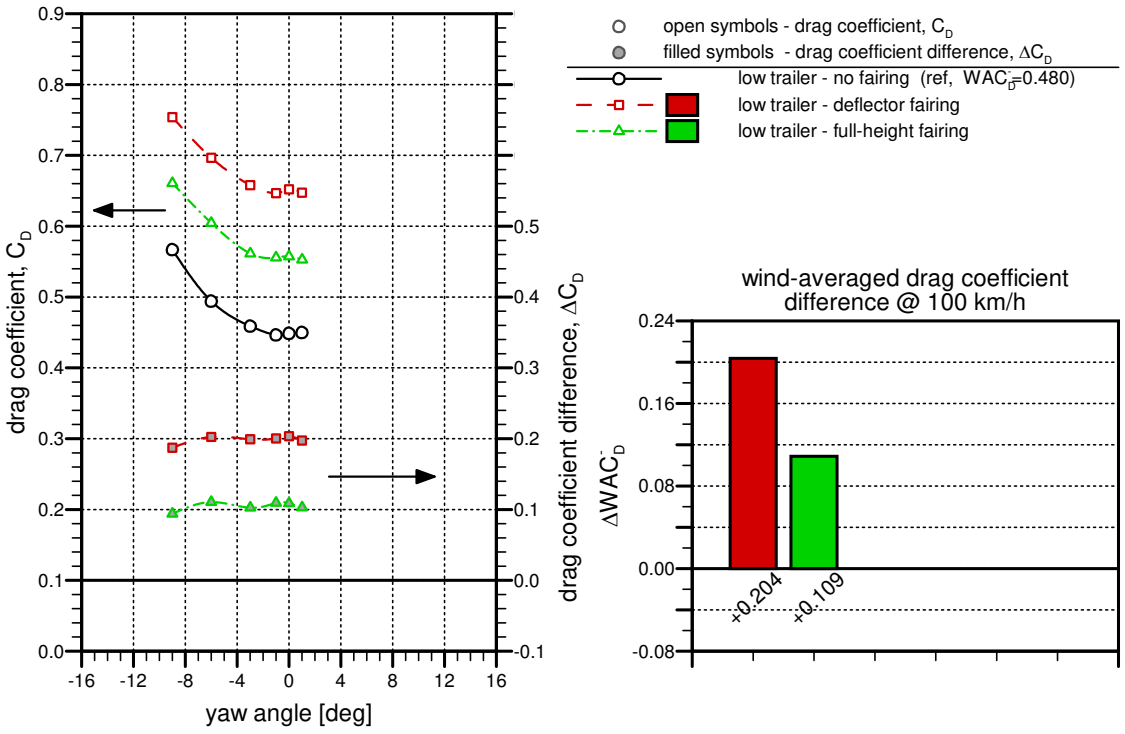


Figure 7.5: Drag characteristics of the day-cab roof-fairing configurations with the half-height dry-van trailer.



(a) Mid-height fairing with full-height dry-van (b) Full-height fairing with half-height dry-van (c) Full-height fairing with box-cargo flatbed

Figure 7.6: Sleeper roof-fairing configurations with various trailers.

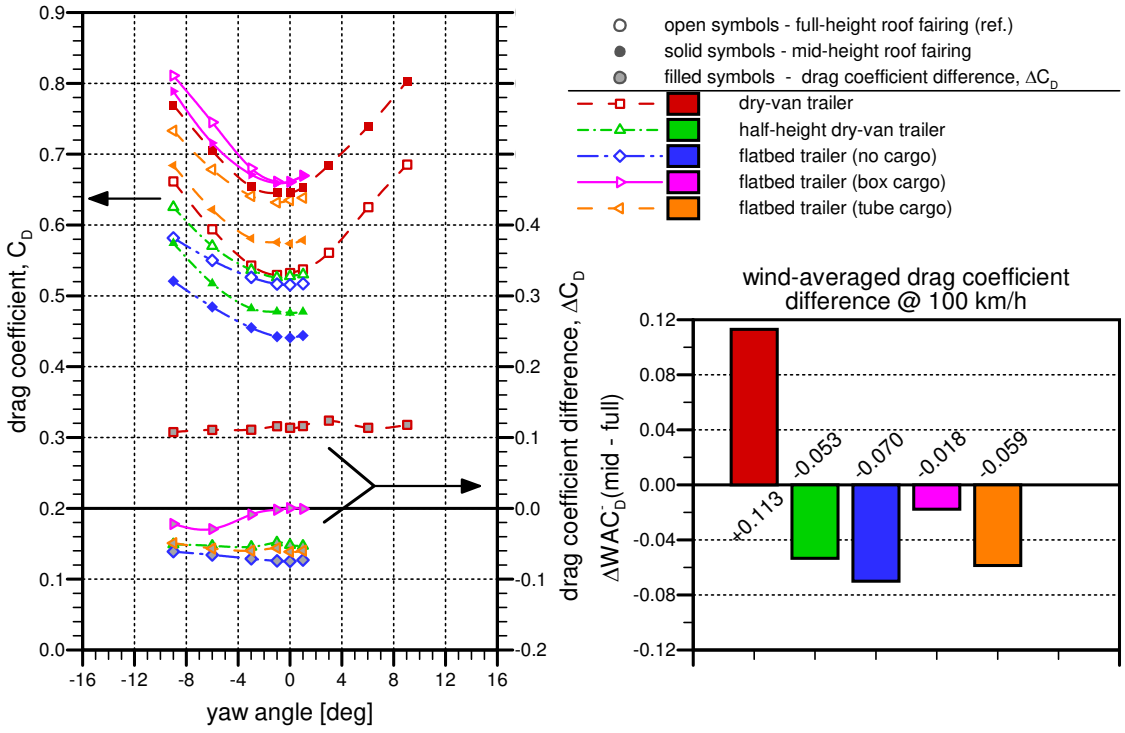


Figure 7.7: Drag characteristics of the sleeper-cab roof-fairing configurations with the full-height-dry-van and flatbed trailers.

Table 7.1: Fuel savings and greenhouse-gas reduction comparisons for different tractor- and trailer-height combinations (for 125,000±35,000 km/tractor/year @ 100 km/hr), DC - day-cab, SC - sleeper-cab.

Baseline Vehicle Configuration	**Drag-Reduction Configuration**	**Drag Change** ΔWAC_D	**Fuel Rate Savings [l/100km]**	**Fuel Saved [l]**	**Fuel Cost Savings [$ @ $1.35/l]**	**CO_2 Reduction [kg]**
DC + tall dry-van	remove full fairing	0.110	-4.3	-5,400 ± 1,500	$ -7,300 ± $ 2,000	-14,300 ± 4,000
DC + low dry-van	add full fairing	0.109	-4.3	-5,400 ± 1,500	$ -7,300 ± $ 2,000	-14,300 ± 4,000
DC + low dry-van	add deflector	0.204	-8.1	-10,100 ± 2,800	$ -13,600 ± $ 3,800	-26,700 ± 7,400
SC + tube-cargo	reduce fairing height	-0.059	2.3	2,900 ± 800	$ 3,900 ± $ 1,100	7,700 ± 2,100
tall DC & dry-van	low DC & dry-van	-0.142	5.6	7,000 ± 2,000	$ 9,500 ± $ 2,700	18,500 ± 5,300

trailer heights examined in the current study, according to the analysis defined in Section 2.5. The improper matching using a well-designed roof fairing can provide an estimated increase in fuel cost of 5,400±1,500 litres/tractor/year and increase in greenhouse-gas emissions by 14,300±4,000 kg CO_2/tractor/year. In addition, the use of a simple tractor-roof deflector for a low-cargo trailer setup can increase fuel costs by 10,100±2,800 litres/tractor/year and greenhouse-gas emissions by 26,700±7,400 kg CO_2/tractor/year.

Although not specifically compared by graphs in the current study, the use of a variable-height dry-van trailer that can be lowered for smaller-volume cargo loads or for empty return trips, and paired with a retractible tractor roof fairing, can provide a significant reduction in wind-averaged-drag coefficient of ΔWAC_D = +0.142 (based on the day-cab results presented herein). Although the respective data for this comparison in the lowest row of Table 7.1 estimates the full travel distance of 125,000±35,000 km/tractor/year @ 100 km/hr, even if a fraction of the travel is performed with a retractible-height tractor-trailer combination, thousands of dollars in fuel savings and significant emission reductions can be realized.

8. Summary and Conclusions

Through its ecoTECHNOLOGY for Vehicles program, Transport Canada commissioned the National Research Council Canada to investigate the aerodynamic improvements possible with new and emerging drag reduction technologies for heavy-duty vehicles. A wind-tunnel test campaign was undertaken in the NRC 9 m Wind Tunnel to evaluate the aerodynamic performance of various drag reduction concepts, with an emphasis on those for dry-van trailers, using a 30% scale model of modern tractor-trailer combinations. Testing technologies developed as part of the project have led to a wind-tunnel simulation that provides a high-fidelity representation of the real-world environment in which ground vehicles operate. This includes a modular model that can represent various tractor and trailer configurations, spinning wheels with appropriate ground-effect simulation using a moving ground plane, cooling-drag simulation, road-representative turbulent winds, negligible wind-tunnel wall-interference effects, and with the appropriate relative motions between the vehicle, the ground, and the wind.

The overall test program described herein included distinct sub-studies to address drag reduction techniques for various regions of the vehicle or for different vehicle types. For each vehicle configuration tested, the wind-tunnel drag-coefficient measurements were used to calculate a wind-averaged-drag-coefficient that represents a long-term average of the aerodynamic performance for typical North-American wind conditions, from which fuel savings and greenhouse-gas reductions have been estimated based on typical Canadian driving distances. These estimates are provided in Table 8.1 for a sample set of test cases, and are broken down by their respective sub-study.

Reducing the aerodynamic drag associated with dry-van trailers was the primary focus of the current effort, and several regions of a tractor-trailer combination were targeted with different drag reduction technologies. The vehicle model represents a modern aero tractor with a 53 ft dry-van trailer. The drag-reduction techniques tested do not represent specific commercial products, although some were inspired by technologies on the market.

The gap between the tractor and trailer is a region in which air can circulate and pass through, and is a dominant source of drag for a tractor-trailer combination. Many modern tractors are outfitted with side-extenders that reduce the effective air-gap between the two bodies, and provide a reduction in fuel use, however operational restrictions may prevent the ability to achieve such savings. To better understand the sensitivity of vehicle drag to the gap width, measurements were performed for several gap widths and it was found that the wind-averaged-drag was reduced by 2.6% for every foot the gap was reduced (8.5% per meter). A one foot reduction in gap with, which may be operationally feasible for many vehicles on the road, translates to a reduction in fuel consumption on the order of 800 litres per tractor per year, with CO_2 emissions reductions of 2,100 kg per tractor per year. An active fifth-wheel system can provide such benefits at highway speed without adversely affecting low-speed

Table 8.1: Sample of fuel savings and greenhouse-gas reductions estimated for different drag-reduction techniques (for 125,000±35,000 km/tractor/year @ 100 km/hr).

Drag-Reduction Technique	**Drag Change** ΔWAC_D	**Fuel Saved [l]**	**CO_2 Reduction [kg]**
Tractor-Trailer Gap (Sections 4.2 and 4.3):			
reduce tractor-trailer gap by 12"	-0.016	800 ± 200	2,100 ± 500
add trailer fairing for sleeper-cab w/ 36" gap	-0.013	600 ± 200	1,600 ± 500
add trailer fairing for day-cab w/ 36" gap	-0.033	1,600 ± 500	4,200 ± 1,300
Trailer Underbody (Section 4.4):			
add side-skirts to tandem axle trailer	-0.058	2,900 ± 800	7,700 ± 2,100
add extended side-skirts to tandem axle trailer	-0.066	3,300 ± 900	8,700 ± 2,400
add side-skirts to tridem axle trailer	-0.077	3,800 ± 1,100	10,000 ± 2,900
Trailer Base (Section 4.5):			
add long or short 4-panel boat-tail to trailer base	-0.038	1,900 ± 500	5,000 ± 1,300
add tapered-side 3-panel boat-tail to trailer base	-0.033	1,600 ± 500	4,200 ± 1,300
Trailer Upper-Body (Section 4.6):			
profile the trailer roof (top 6")	-0.020	1,000 ± 300	2,600 ± 800
Combinations (Section 4.7):			
48" to 36" gap, trailer fairing, side-skirts, boat-tail (sleeper)	-0.136	6,700 ± 1,900	17,700 ± 5,000
48" to 36" gap, trailer fairing, extended skirts, boat-tail, profile roof (sleeper)	-0.169	8,300 ± 2,300	21,900 ± 6,100
48" to 36" gap, trailer fairing, side-skirts, boat-tail (day-cab)	-0.160	7,900 ± 2,200	20,900 ± 5,800
48" to 36" gap, trailer fairing, extended side-skirts, boat-tail (day-cab)	-0.175	8,600 ± 2,400	22,700 ± 6,300
Flatbed Trailers (Section 5):			
add side-skirts to flatbed with high irregular cargo	-0.058	2,900 ± 800	7,700 ± 2,100
add side-skirts to flatbed with low irregular cargo	-0.032	1,600 ± 400	4,200 ± 1,100
Long Combination Vehicles - LCVs (Section 6):			
add trailer fairing to LCV trailer-trailer gap	-0.029	1,400 ± 400	3,700 ± 1,100
reduce LCV trailer-trailer gap from 5 ft to 3 ft	-0.039	1,900 ± 500	5,000 ± 1,300
add trailer fairing and reduce gap, and add full aero package to LCV	-0.159	7,900 ± 2,200	20,900 ± 5,800
Tractor-Trailer Height Matching (Section 7):			
remove full-height fairing from day-cab with low dry-van trailer	-0.109	5,400 ± 1,500	14,300 ± 4,000
remove full-height fairing from day-cab with full-height dry-van trailer	+0.110	-5,400 ± 1,500	-14,300 ± 4,000

manoeuvering and operations. Another technique to reduce drag associated with the tractor-trailer gap is to introduce a device that prevents air from flowing through the gap region. Of the concepts tested, a large trailer fairing was found to provide the greatest benefit, with drag reductions on the order of 2% for the sleeper-cab tractor variant tested, and 5% for the day-cab variant, providing associated fuel savings of 600 litres and 1,600 litres per tractor per year, respectively. Reducing the gap width and adding a trailer fairing can provide fuel savings in excess of 2,000 litres per tractor per year and greenhouse-gas reductions in excess of 4,000 kg CO_2 per tractor per year.

As would be expected based on their prevalent use on North-American highways, side-skirts provide the greatest drag reductions of the trailer-underbody concepts tested. By redirecting the wind around the trailer, they prevent high-momentum air from being entrained in the underbody region and from impinging on the trailer bogie. Drag reductions of 10% were measured for different side-skirt arrangements with a tandem-axle trailer bogie, and extending the skirts over the trailer wheels provided added benefit such that fuel savings exceeding 3,000 litres per tractor per year may be realized. An even greater reduction in drag was measured for side-skirts applied to a tridem-axle bogie arrangement, with fuel savings of nearly 4,000 litres per tractor per year and greenhouse-gas reductions of 10,000 kg CO_2 per tractor per year.

Recent federal regulatory amendments in Canada have opened up the possibility of applying aerodynamic fairings, commonly called boat-tails, to the aft end of dry-van trailers that are larger than previous regulations allowed. Several boat-tail concepts were tested to examine the influence of a lower panel, the sensitivity to length, and the relative potential for inflatable boat-tails. All showed similar results, with the greatest benefit realized from the four-panel configurations (6-7% drag reduction), providing an estimated fuel savings of 1,900 litres per tractor per year and greenhouse-gas reductions of 5,000 kg CO_2 per tractor per year. The short (2 ft full-scale) and long (4 ft full-scale) boat-tail concepts showed the same level of drag reduction. Removing the lower panel and reducing the surface area of the side panels showed only a small reduction in performance (5-6% drag reduction), providing further evidence to support the hypothesis that the manner in which the top panel guides the air downwards towards the ground is the dominant influence on boat-tail performance. Other studies have shown boat-tails to be as effective as side-skirts, reaching drag reductions of 10%. The vertical offset of the top panel tested here (3 inches full-scale), included to leave room for lights at the top edge of the trailer base, may be a reason why the boat-tail concepts tested here have not provided the same magnitude of drag reductions observed for other similar boat-tail concepts. This presents a clear challenge to developing effective boat-tails for real-world applications.

The intent of the current study was to evaluate ways of reducing the drag associated with dry-van trailers without changing cargo capacity. If an effort to modify the shape of the roof while minimizing any influence to the cargo volume, the top 6 inches of the trailer were modified in three ways: rounding the front edge, rounding the side edges, and tapering the aft edge. The aft taper provided the greatest benefit of the three, however the combined profiled roof provided a drag reduction of 3.5%, which translates to 1,000 litres per tractor per year in fuel savings and a reduction in greenhouse gas emissions of 2,600 kg CO_2.

Of the various technologies tested, some did not provide any measurable drag reductions and

some showed increased drag. A partial plate seal applied to the front face of the trailer and paired to the sleeper-cab with a 36 inch tractor-trailer gap showed no significant reduction in wind-averaged drag. Removing the landing gear, smoothing the trailer underbody, and adding an underbody diffuser fairing all showed a small increase in wind-averaged drag. Roof mounted vortex generators also showed increased wind-averaged drag. These poorly-performing concepts do not represent specific commercial products and the designs used have not been optimized. These test results should not be taken to mean such concepts will not work, only that they show much lower potential for fuel savings than the well-performing technologies.

The best performing techniques for each region of the dry-van trailer were combined to examine the additive properties of the various technologies, and similar combinations were paired with both the day-cab and sleeper-cab variants. Significant drag reductions of up to 29% have been observed for some combinations. Fuel savings in excess of 8,000 litres per tractor per year are predicted for some combinations (greater than $10,000 per year at current diesel rates). Greater reductions were observed for the day-cab than the sleeper-cab tractor, and have been attributed to the sleeper-cab guiding the wind over the gap region in a smoother manner as a result of its length, thus receiving less gains from the gap devices. Of particular note, it was found that side-skirts and boat-tails have a mutually beneficial interaction that provides a reduction in drag from their combined use that is greater than the sum of their individual drag reductions. An additional 3% drag reduction was observed in the current study when the extended side-skirts and boat-tail were paired. This interaction has been identified as a possible source of discrepancy for performance claims reported in literature of side-skirts and boat-tails when tested in a combined manner as opposed to when tested individually.

In addition to the full-height 53 ft single dry-van trailer, the current project examined other trailer types including a 53 ft flatbed trailer with different cargo configurations, a tandem 28 ft dry-van trailer, and a 53 ft half-height dry-van trailer. This was done in an attempt to identify fuel savings measures for a greater proportion of tractor-trailer combinations found on the road. Different tractor roof configurations were also tested for some trailer configurations to examine the sensitivity to proper matching of the tractor with the trailer.

Side-skirts were beneficial for all the flatbed configurations tested, but the magnitude of the drag reductions varied (5% to 8%). A mid-height tractor roof was shown to benefit all of the flatbed cargo configurations, even for a set of large boxes with a maximum height the same as a full-height dry-van trailer.

For the tandem 28 ft trailer, which was used to represent a long combination vehicle (LCV), reducing the trailer-trailer gap from 5 ft to 3 ft was most beneficial, but adding a trailer fairing or full-plate seal in the trailer-trailer gap provided measurable drag reductions. The same magnitudes of drag reductions were not realized when the rest of the trailer regions were treated with side-skirts, a boat-tail at the base of the aft trailer, and a fairing on the front of the forward trailer. A 25% drag reduction was measured for the full aerodynamic treatment of the LCV configuration.

Aerodynamic matching of the tractor and trailer was examined by testing different tractor-roof configurations with various trailers. The most interesting finding was that the drag increase

when adding a full-height roof fairing to a low-tractor/low-trailer configuration is as great as the drag increase when removing the fairing from a high-tractor/high-trailer (see lowest two rows of Table 8.1). The improperly-paired configurations can result in an increased fuel use in excess of 5,000 litres per tractor per year and increased greenhouse-gas emissions in excess of 14,000 kg CO_2 per tractor per year.

The results presented in this study are intended to provide guidance to Canadian regulators and Canada's transportation industry on effective ways to reduce the fuel consumption and emissions, through aerodynamic means, from the transportation of goods on Canadian roadways . Descriptions of the way in which the technologies affect the flow-field around a heavy-duty vehicle should also be helpful in providing guidance to technology developers, and in particular to trailer manufacturers that have the opportunity to design high-efficiency trailers for the next generation of heavy-duty vehicles.

References

Burton, D., McArthur, D., Sheridan, J. and Thompson, M. (2013), "Contribution of Add-On Components to the Aerodynamic Drag of a Cab-Over Truck-Trailer Combination Vehicle," SAE Int. J. Commer. Veh., **6(2)**, doi: 10.4271/2013-01-2428.

Cooper, K. R. (2012), "Wind Tunnel and Track Tests of Class 8 Tractors Pulling Single and Tandem Trailers Fitted with Side Skirts and Boat Tails," SAE Int. J. Commer. Veh., **5(1)**, doi:10.4271/2012-01-0104.

Cooper, K. R. and Leuschen, J. (2005), "Model and Full-Scale Wind Tunnel Tests of Second-Generation Aerodynamic Fuel Saving Devices for Tractor-Trailers," SAE Paper No. 2005-01-3512.

Environment Canada (2013), "Heavy-duty Vehicle and Engine Greenhouse Gas Emission Regulations," Canada Gazette Part II, **147(6)**, pp. 450–572.

Gelzer, C. (2011), "Fairing Well - From Shoebox to Bat Truck and Beyond: Aerodynamic Truck Research at NASA's Dryden Flight Research Center," NASA Report No. SP-2011-4546, *National Aeronautics and Space Administration*.

Kehs, J. P., Visser, K. D., Grossman, J., Niemiec, J., Smith, A. and Horrell, C. M. (2013), "A Comparison of Full Scale Aft Cavity Drag Reduction Concepts With Equivalent Wind Tunnel Test Results," SAE Int. J. Commer. Veh., **6(2)**, doi:10.4271/2013-01-2429.

Landman, D., Wood, R., Seay, W. and Bledsoe, J. (2009), "Understanding Practical Limits to Heavy Truck Drag Reduction," SAE Paper No. 2009-01-2890.

Leuschen, J. (2013), "Considerations for the Wind Tunnel Simulation of Tractor-Trailer Combinations: Correlation of Full- and Half-Scale Measurements," SAE Int. J. Commer. Veh., **6(2),** doi:10.4271/2013-01-2456.

Leuschen, J. and Cooper, K. R. (2006), "Full-Scale Wind Tunnel Tests of Production and Prototype, Second-Generation Aerodynamic Drag-Reduction Devices for Tractor-Trailers," SAE Paper No. 2006-01-3456.

McAuliffe, B. R. (2014b), "Aerodynamic Testing of Drag Reduction Technologies for HDVs: Progress Toward the Design of a Scale-Model HDV for Wind Tunnel Testing (Year 2)," NRC Report No. LTR-AL-2014-0015, *National Research Council Canada*.

McAuliffe, B. R. (2014d), "Progress Toward Assessing the Potential for the Accumulation and Shedding of Ice and Snow for a Boat-Tail Equipped HDV," NRC Report No. LTR-AL-2014-0012, *National Research Council Canada*.

McAuliffe, B. R., Belluz, L. and Belzile, M. (2014c), "Measurement of the On-Road Turbulence

Environment Experienced by Heavy Duty Vehicles," SAE Int. J. Commer. Veh., **7(2),** doi: 10.4271/2014-01-2451.

McAuliffe, B. R., D'Auteuil, A. and de Souza, F. (2014a), "Aerodynamic Testing of Drag Reduction Technologies for HDVs: Progress Toward the Development of a Flow Treatment System (Year 2)," NRC Report No. LTR-AL-2014-0014, *National Research Council Canada*.

McAuliffe, B. R., de Souza, F. and Leuschen, J. (2013a), "Aerodynamic Testing of Drag Reduction Technologies for HDVs: Progress Towards the Development of a Flow Treatment System," NRC Report No. LTR-AL-2013-0020, *National Research Council Canada*.

McAuliffe, B. R. and Kirchhefer, A. (2015), "Improving the Aerodynamic Efficiency of Heavy Duty Vehicles: Commissioning of the Road Turbulence System and the 30% Scale Tractor-Trailer Model," NRC Report No. LTR-AL-2015-0274, *National Research Council Canada*.

McAuliffe, B. R., Mamou, M., Desouza, F. and Leuschen, J. (2013b), "Aerodynamic Testing of Drag Reduction Technologies for HDVs: Progress Towards the Design of a Scale-Model HDV for Wind Tunnel Testing," NRC Report No. LTR-AL-2013-0021, *National Research Council Canada*.

National Academy of Sciences (2010), "Technologies and Approaches to Reducing the Fuel Consumption of Medium- and Heavy-Duty Vehicles," , *The National Academic Press*.

Ortega, J. M. and Salari, K. (2008), "Investigation of a Trailer Underbody Fairing for Heavy Vehicle Aerodynamic Drag Reduction," SAE Paper No. 2008-01-2601.

Patten, J., McAuliffe, B. R., Mayda, W. and Tanguay, B. (2012), "Review of Aerodynamic Drag Reduction Devices for Heavy Trucks and Buses," No. CSTT-HVC-TR-205, *National Research Council Canada*.

Patten, J., Poole, G., Mayda, W. and Wall, A. (2010), "Trailer Boat Tail Aerodynamic and Collision Study," No. CSTT-HVC-TR-169, *National Research Council Canada*.

SAE SP-1176 (1996), "Closed-Test-Section Wind Tunnel Blockage Corrections for Road Vehicles," SAE Special Publication No. SP-1176, *SAE International*.

SAE Wind Tunnel Test Procedure for Trucks and Busses (2012), "SAE Wind Tunnel Test Procedure for Trucks and Busses," 2012.

Sharpe, B., May, D., Oiver, B. and Mansour, H. (2015), "Costs and Adoption Rates of Fuel-Saving Technologies for Trailers in the Canadian On-Road Freight Sector," White Paper , *The International Council on Clean Transportation / Pollution Probe*.

Surcel, M. and Provencher, Y. (2013), "Trailer Aerodynamic Technologies Wind Tunnel Testing Compared to Track Test Results," SAE Paper No. 2013-01-2822.

Transport Canada (2015), "Canadian Vehicle Use Study," Online [Accessed February 2015] , *https://www.tc.gc.ca/eng/policy/aca-cvus-menu-2294.htm*.

U.S. Environmental Protection Agency and U.S. Department of Transportation (2011), "Greenhouse Gas Emissions Standards and Fuel Efficiency Standards for Medium- and Heavy-Duty Engines and Vehicles," US Federal Register, **76(179)**, pp. 57106–57513.

Watkins, S. and Cooper, K. R. (2007), "The Unsteady Wind Environment of Road Vehicle, Part Two: Effects on Vehicle Development and Simulation of Turbulence," SAE Paper No. 2007-01-1237.

Wood, R. (2012a), "A Review of Reynolds Number Effects on the Aerodynamics of Commercial Ground Vehicles," SAE International Journal of Commercial Vehicles, **5**, pp. 628–639.

Wood, R. (2012b), "EPA Smartway Verification of Trailer Undercarriage Advanced Aerodynamic Drag Reduction Technology," SAE Int. J. Commer. Veh., **5(2)**, doi:10.4271/2012-01-2043.

A. Test Log

This appendix contains the test log for all the data contained in this report. The data was collected in October and November of 2014 in the NRC 9 m Wind Tunnel as part of test number 6547. Table A.1 includes the following information:

- Study - the sub-study within the overall test program to which the run belongs (commissioning refers to the basic vehicle without any drag-reduction method applied to it);
- Run - the run number within test 6547;
- Tractor - the tractor type configuration used for the run;
- Trailer - the trailer model used for the run;
- T/T Gap - the tractor-trailer-gap width for the run (dwb refers to "different wheelbase" for tractor);
- Model Location - the position of the model with respect to the truntable/moving-ground-plane;
- Model Details - description of the model configuration (baseline refers to the basic vehicle for the given tractor, trailer, gap-width, and location setup);
- Run Conditions - identified the wind speed and yaw-angle range for the run;
- WAC_D^- - wind-averaged drag coefficient calculate for negative yaw-angle range, given a ground speed of 100 km/h;
- $WAC_D^\pm$ - wind-averaged drag coefficient calculate for total yaw-angle range, given a ground speed of 100 km/h; and
- WAC_D^+ - wind-averaged drag coefficient calculate for positive yaw-angle range, given a ground speed of 100 km/h.

Table A.1: Run Log for test program (WAC_D evaluated at 100 km/h ground speed).

Study	Run	Tractor	Trailer	T/T Gap	Model Location	Model Details	Run Conditions	WAC_D^-	$WAC_D^{\pm}$	WAC_D^+
Commissioning	96	Sleeper	40 ft	36 in	Mid	Baseline	50 m/s, $\pm$ 12°	0.523	0.523	0.524
Commissioning	164	Sleeper	53 ft	36 in	Aft	Baseline	50 m/s, $\pm$ 15°	0.579	0.577	0.575
Tractor-Trailer Gap	165	Sleeper	53 ft	36 in	Aft	cooling/reefer unit	50 m/s, $\pm$ 12°	0.575	0.575	0.574
Tractor-Trailer Gap	166	Sleeper	53 ft	36 in	Aft	heating unit	50 m/s, $\pm$ 12°	0.577	0.576	0.574
Tractor-Trailer Gap	167	Sleeper	53 ft	36 in	Aft	partial plate seal	50 m/s, $\pm$ 12°	0.576	0.575	0.573
Tractor-Trailer Gap	169	Sleeper	53 ft	36 in	Aft	full plate seal	50 m/s, $\pm$ 12°	0.573	0.571	0.568
Tractor-Trailer Gap	171	Sleeper	53 ft	36 in	Aft	trailer nose fairing	50 m/s, $\pm$ 12°	0.566	0.563	0.559
Tractor-Trailer Gap	176	Sleeper	53 ft	48 in dwb	Aft	trailer nose fairing	50 m/s, $\pm$ 12°	0.582	0.576	0.571
Tractor-Trailer Gap	178	Sleeper	53 ft	48 in dwb	Aft	Baseline	50 m/s, $\pm$ 12°	0.591	0.585	0.579
Tractor-Trailer Gap	179	Sleeper	53 ft	48 in dwb	Aft	cooling /reefer unit	50 m/s, $\pm$ 12°	0.588	0.582	0.577
Tractor-Trailer Gap	181	Sleeper	53 ft	48 in dwb	Aft	heating unit	50 m/s, $\pm$ 12°	0.592	0.588	0.583
Tractor-Trailer Gap	182	Sleeper	53 ft	48 in dwb	Aft	full plate seal	50 m/s, $\pm$ 12°	0.582	0.579	0.575
Tractor-Trailer Gap	185	Sleeper	53 ft	24 in dwb	Aft	baseline	50 m/s, $\pm$ 12°	0.566	0.565	0.564
Tractor-Trailer Gap	186	Sleeper	53 ft	24 in dwb	Aft	full plate seal	50 m/s, $\pm$ 12°	0.565	0.561	0.558
Tractor-Trailer Gap	191	Sleeper	53 ft	48 in	Aft	Baseline	50 m/s, -12 to 1 °	0.595	0.000	0.000
Tractor-Trailer Gap	192	Sleeper	53 ft	48 in	Aft	full plate seal	50 m/s, -12 to 1 °	0.586	0.000	0.000
Tractor-Trailer Gap	193	Sleeper	53 ft	48 in	Aft	cooling/reefer unit	50 m/s, -12 to 1 °	0.590	0.000	0.000
Tractor-Trailer Gap	195	Sleeper	53 ft	48 in	Aft	trailer nose fairing	50 m/s, -12 to 1 °	0.580	0.000	0.000
Tractor-Trailer Gap	197	Sleeper	53 ft	42 in	Aft	trailer nose fairing	50 m/s, -12 to 1 °	0.574	0.000	0.000
Tractor-Trailer Gap	202	Sleeper	53 ft	42 in	Aft	Baseline	50 m/s, -12 to 1 °	0.585	0.000	0.000
Tractor-Trailer Gap	204	Sleeper	53 ft	30 in	Aft	Baseline	50 m/s, -12 to 1 °	0.567	0.000	0.000
Tractor-Trailer Gap	206	Sleeper	53 ft	30 in	Aft	full plate seal	50 m/s, -12 to 1 °	0.568	0.000	0.000
Tractor-Trailer Gap	208	Sleeper	53 ft	24 in	Aft	Baseline	50 m/s, -12 to 1 °	0.563	0.000	0.000
Commissioning	213	Day-Cab	53 ft	36 in	Aft	Baseline	50 m/s, -15 to 15 °	0.608	0.607	0.607
Tractor-Trailer Gap	214	Day-Cab	53 ft	36 in	Aft	cooling/reefer unit	50 m/s, -12 to 12 °	0.590	0.589	0.587
Tractor-Trailer Gap	217	Day-Cab	53 ft	36 in	Aft	trailer nose fairing	50 m/s, -12 to 12 °	0.575	0.574	0.574
Tractor-Trailer Gap	218	Day-Cab	53 ft	36 in	Aft	full plate seal	50 m/s, -12 to 12 °	0.611	0.609	0.606
Commissioning	220	Day-Cab	53 ft	36 in	Aft	Baseline	50 m/s, -15 to 15 °	0.608	0.607	0.605
Tractor-Trailer Gap	222	Day-cab	53 ft	48 in	Aft	Baseline	50 m/s, -12 to 12 °	0.625	0.625	0.625
Tractor-Trailer Gap	223	Day-cab	53 ft	48 in	Aft	cooling/reefer unit	50 m/s, -12 to 1 °	0.613	0.000	0.000
Tractor-Trailer Gap	224	Day-cab	53 ft	48 in	Aft	heating unit	50 m/s, -12 to 1 °	0.628	0.000	0.000
Tractor-Trailer Gap	225	Day-cab	53 ft	48 in	Aft	trailer nose fairing	50 m/s, -12 to 1 °	0.599	0.000	0.000
Tractor-Trailer Gap	230	Day-cab	53 ft	24 in	Aft	Baseline	50 m/s, -12 to 12 °	0.593	0.591	0.589
Commissioning	239	Sleeper	53 ft	36 in	Forward	Baseline	50 m/s, -15 to 15 °	0.565	0.574	0.582
Height Matching	254	Sleeper	53 ft	36 in	Forward	mid-height roof	50 m/s, -12 to +12 °	0.685	0.699	0.713
Commissioning	256	Sleeper	53 ft	36 in	Forward	Baseline	50 m/s, -12 to +12 °	0.572	0.583	0.594
Trailer Underbody	257	Sleeper	53 ft	36 in	Forward	standard side-skirts	50 m/s, -12 to +12 °	0.510	0.515	0.520
Trailer Underbody	258	Sleeper	53 ft	36 in	Forward	split side-skirts	50 m/s, -12 to +1 °	0.512	0.000	0.000
Trailer Underbody	263	Sleeper	53 ft	36 in	Forward	extended side-skirts	50 m/s, -12 to +12 °	0.502	0.510	0.517
Trailer Underbody	264	Sleeper	53 ft	36 in	Forward	bogie fairing	50 m/s, -12 to +1 °	0.555	0.000	0.000
Trailer Underbody	266	Sleeper	53 ft	36 in	Forward	landing gear removed	50 m/s, -12 to +1 °	0.571	0.000	0.000
Trailer Underbody	267	Sleeper	53 ft	36 in	Forward	landing gear removed smooth underbody	50 m/s, -12 to +1 °	0.570	0.000	0.000
Trailer Underbody	268	Sleeper	53 ft	36 in	Forward	diffuser fairing (position 1)	50 m/s, -12 to +1 °	0.570	0.000	0.000
Trailer Underbody	269	Sleeper	53 ft	36 in	Forward	diffuser fairing (position 1) + standard side-skirts	50 m/s, -12 to +1 °	0.511	0.000	0.000
Commissioning	271	Sleeper	53 ft	36 in	Forward	Baseline	50 m/s, -15 to 15 °	0.568	0.576	0.583
Commissioning	272	Sleeper	53 ft	36 in	Forward	Baseline (readjusted tractor surfaces and taped skirt gap)	50 m/s, -9 to 9 °	0.570	0.576	0.582
Trailer Underbody	273	Sleeper	53 ft	36 in	Forward	diffuser fairing (position 2)	50 m/s, -12 to +1 °	0.571	0.000	0.000
Trailer Underbody	274	Sleeper	53 ft	36 in	Forward	belly box	50 m/s, -12 to +1 °	0.531	0.000	0.000
Trailer Base	279	Sleeper	53 ft	36 in	Forward	long 4-panel boat-tail	50 m/s, -12 to +12 °	0.535	0.540	0.545
Commissioning	281	Sleeper	53 ft	36 in	Forward	Baseline	50 m/s, -12 to +12 °	0.573	0.578	0.583
Trailer Base	282	Sleeper	53 ft	36 in	Forward	long 3-panel boat-tail	50 m/s, -12 to +1 °	0.538	0.000	0.000
Trailer Base	283	Sleeper	53 ft	36 in	Forward	short 4-panel boat-tail	50 m/s, -12 to +1 °	0.535	0.000	0.000
Trailer Base	284	Sleeper	53 ft	36 in	Forward	tapered 3-panel boat-tail	50 m/s, -12 to +1 °	0.539	0.000	0.000
Trailer Base	285	Sleeper	53 ft	36 in	Forward	long 4-panel boat-tail + cavity cover	50 m/s, -12 to +1 °	0.533	0.000	0.000
Interactions	287	Sleeper	53 ft	36 in	Forward	long 4-panel boat-tail + standard skirts	50 m/s, -12 to +12 °	0.465	0.468	0.472
Interactions	288	Sleeper	53 ft	36 in	Forward	long 4-panel boat-tail + standard skirts + trailer fairing	50 m/s, -15 to +15 °	0.454	0.456	0.458
Interactions	290	Sleeper	53 ft	36 in	Forward	long 4-panel boat-tail + extended skirts + trailer fairing	50 m/s, -12 to +12 °	0.436	0.440	0.444
Interactions	293	Sleeper	53 ft	36 in	Forward	long 4-panel boat-tail + extended skirts + trailer fairing + full roof	50 m/s, -15 to +15 °	0.420	0.423	0.426

Table A.1: Run Log for test program, continued (WAC_D evaluated at 100 km/h ground speed).

Study	Run	Tractor	Trailer	T/T Gap	Model Location	Model Details	Run Conditions	WAC_D^-	$WAC_D^\pm$	WAC_D^+
Trailer Upperbody	295	Sleeper	53 ft	36 in	Forward	full roof (rounded LE & SE tapered aft)	50 m/s, -12 to +12 °	0.552	0.558	0.564
Trailer Upperbody	296	Sleeper	53 ft	36 in	Forward	roof - rounded side edges	50 m/s, -12 to +12 °	0.570	0.576	0.581
Trailer Upperbody	301	Sleeper	53 ft	36 in	Forward	roof - aft taper	50 m/s, -12 to +1 °	0.558	0.000	0.000
Trailer Upperbody	302	Sleeper	53 ft	36 in	Forward	roof - round leading edge	50 m/s, -12 to +1 °	0.571	0.000	0.000
Trailer Upperbody	303	Sleeper	53 ft	36 in	Forward	roof - vortex generators	50 m/s, -12 to +1 °	0.578	0.000	0.000
Commissioning	305	Sleeper	53 ft	36 in	Forward	Baseline	50 m/s, -9 to 9 °	0.574	0.579	0.584
Interactions	307	Sleeper	53 ft	36 in	Forward	long 4-panel boat-tail + trailer fairing	50 m/s, -12 to +12 °	0.521	0.524	0.527
Interactions	308	Sleeper	53 ft	36 in	Forward	standard side-skirts + trailer fairing	50 m/s, -12 to +12 °	0.501	0.504	0.506
Interactions	310	Day-cab	53 ft	36 in	Forward	long 4-panel boat-tail + extended skirts + trailer fairing	50 m/s, -9 to 9 °	0.450	0.456	0.461
Interactions	314	Day-cab	53 ft	36 in	Forward	long 4-panel boat-tail + standard skirts + trailer fairing	50 m/s, -12 to +12 °	0.466	0.472	0.477
Interactions	315	Day-cab	53 ft	36 in	Forward	long 4-panel boat-tail + standard side-skirts	50 m/s, -9 °+9 °	0.495	0.501	0.507
Commissioning	317	Day-cab	53 ft	36 in	Forward	Baseline	50 m/s, -12 to +12 °	0.609	0.614	0.619
Trailer Underbody	319	Day-cab	53 ft	36 in	Forward	tridem wheels	50 m/s, -12 to +1 °	0.624	0.000	0.000
Trailer Underbody	321	Day-cab	53 ft	36 in	Forward	standard side-skirts + tridem wheels	50 m/s, -12 to +1 °	0.550	0.000	0.000
Interactions	323	Day-cab	53 ft	36 in	Forward	standard side-skirts + long 4-panel boat-tail + tridem wheels	50 m/s, -12 to +12 °	0.517	0.522	0.527
Height Matching	324	Day-cab	53 ft	36 in	Forward	tridem wheels	50 m/s, -9 to +9 °	0.622	0.631	0.639
Height Matching	330	Day-cab	53 ft	36 in	Forward	low roof + tridem wheels	50 m/s, -9 to +1 °	0.731	0.000	0.000
Height Matching	332	Day-cab	53 ft	36 in	Forward	roof deflector + tridem wheels	50 m/s, -9 to +1 °	0.682	0.000	0.000
Height Matching	344	Day-cab	53 ft short	36 in	Forward	roof deflector + tridem wheels	50 m/s, -9 to +1 °	0.683	0.000	0.000
Height Matching	345	Day-cab	53 ft short	36 in	Forward	low roof + tridem wheels	50 m/s, -9 to +1 °	0.480	0.000	0.000
Height Matching	346	Day-cab	53 ft short	36 in	Forward	tridem wheels	50 m/s, -9 to +1 °	0.589	0.000	0.000
Height Matching	348	Sleeper	53 ft short	36 in	Forward	mid-height roof + tridem wheels	50 m/s, -9 to +1 °	0.505	0.000	0.000
Height Matching	349	Sleeper	53 ft short	36 in	Forward	tridem wheels	50 m/s, -9 to +1 °	0.558	0.000	0.000
Flatbed	351	Sleeper	53 ft flat	36 in	Forward	tridem wheels + no cargo	50 m/s, -9 to +1 °	0.543	0.000	0.000
Flatbed	352	Sleeper	53 ft flat	36 in	Forward	mid-height roof + tridem wheels + no cargo	50 m/s, -9 to +1 °	0.473	0.000	0.000
Flatbed	353	Sleeper	53 ft flat	36 in	Forward	mid-height roof + standard skirts + tridem wheels + no cargo	50 m/s, -9 to +1 °	0.437	0.000	0.000
Flatbed	354	Sleeper	53 ft flat	36 in	Forward	mid-height roof + standard skirts + tridem wheels + cargo A (boxes)	50 m/s, -9 to +1 °	0.641	0.000	0.000
Flatbed	358	Sleeper	53 ft flat	36 in	Forward	mid-height roof + tridem wheels + cargo A (boxes)	50 m/s, -9 to +1 °	0.699	0.000	0.000
Flatbed	359	Sleeper	53 ft flat	36 in	Forward	tridem wheels + cargo A (boxes)	50 m/s, -9 to +1 °	0.717	0.000	0.000
Flatbed	361	Sleeper	53 ft flat	36 in	Forward	tridem wheels + cargo B (tubes)	50 m/s, -9 to +1 °	0.666	0.000	0.000
Flatbed	363	Sleeper	53 ft flat	36 in	Forward	mid-height roof + tridem wheels + cargo B (tubes)	50 m/s, -9 to +1 °	0.607	0.000	0.000
Flatbed	364	Sleeper	53 ft flat	36 in	Forward	mid-height roof + standard skirts + tridem wheels + cargo B (tubes)	50 m/s, -9 to +1 °	0.575	0.000	0.000
LCV	369	Sleeper	Tandem 28 ft	36 in	Forward	Baseline - long gap	50 m/s, -12 to +12 °	0.638	0.652	0.667
LCV	370	Sleeper	Tandem 28 ft	36 in	Forward	full plate seal - long gap	50 m/s, -9 to +1 °	0.610	0.000	0.000
LCV	371	Sleeper	Tandem 28 ft	36 in	Forward	rear trailer fairing - long gap	50 m/s, -9 to +1 °	0.609	0.000	0.000
LCV	372	Sleeper	Tandem 28 ft	36 in	Forward	rear + forward trailer fairing + side-skirts + long 4-panel boat tail - long gap	50 m/s, -9 to 9 °	0.490	0.494	0.497
LCV	374	Sleeper	Tandem 28 ft	36 in	Forward	forward trailer fairing + side-skirts + long 4-panel boat tail - long gap	50 m/s, -9 to +1 °	0.504	0.000	0.000
LCV	378	Sleeper	Tandem 28 ft	36 in	Forward	rear + forward trailer fairing + side-skirts + long 4-panel boat tail - short gap	50 m/s, -9 to 9 °	0.479	0.483	0.486
LCV	379	Sleeper	Tandem 28 ft	36 in	Forward	rear trailer fairing - short gap	50 m/s, -9 to 9 °	0.596	0.000	0.000
LCV	380	Sleeper	Tandem 28 ft	36 in	Forward	Baseline - short gap	50 m/s, -9 to 9 °	0.600	0.610	0.619
Commissioning	403	Sleeper	53 ft	36 in	Forward	Baseline	50 m/s, -15 to 15 °	0.575	0.577	0.580